

1988

Statistically constrained decimation of a turbulence model

Timothy Joe Williams

College of William & Mary - Arts & Sciences

Follow this and additional works at: <https://scholarworks.wm.edu/etd>



Part of the [Plasma and Beam Physics Commons](#)

Recommended Citation

Williams, Timothy Joe, "Statistically constrained decimation of a turbulence model" (1988). *Dissertations, Theses, and Masters Projects*. Paper 1539623778.

<https://dx.doi.org/doi:10.21220/s2-fsr6-9r96>

This Dissertation is brought to you for free and open access by the Theses, Dissertations, & Master Projects at W&M ScholarWorks. It has been accepted for inclusion in Dissertations, Theses, and Masters Projects by an authorized administrator of W&M ScholarWorks. For more information, please contact scholarworks@wm.edu.

INFORMATION TO USERS

The most advanced technology has been used to photograph and reproduce this manuscript from the microfilm master. UMI films the text directly from the original or copy submitted. Thus, some thesis and dissertation copies are in typewriter face, while others may be from any type of computer printer.

The quality of this reproduction is dependent upon the quality of the copy submitted. Broken or indistinct print, colored or poor quality illustrations and photographs, print bleedthrough, substandard margins, and improper alignment can adversely affect reproduction.

In the unlikely event that the author did not send UMI a complete manuscript and there are missing pages, these will be noted. Also, if unauthorized copyright material had to be removed, a note will indicate the deletion.

Oversize materials (e.g., maps, drawings, charts) are reproduced by sectioning the original, beginning at the upper left-hand corner and continuing from left to right in equal sections with small overlaps. Each original is also photographed in one exposure and is included in reduced form at the back of the book. These are also available as one exposure on a standard 35mm slide or as a 17" x 23" black and white photographic print for an additional charge.

Photographs included in the original manuscript have been reproduced xerographically in this copy. Higher quality 6" x 9" black and white photographic prints are available for any photographs or illustrations appearing in this copy for an additional charge. Contact UMI directly to order.

U·M·I

University Microfilms International
A Bell & Howell Information Company
300 North Zeeb Road, Ann Arbor, MI 48106-1346 USA
313/761-4700 800/521-0600



Order Number 8916118

Statistically constrained decimation of a turbulence model

Williams, Timothy Joe, Ph.D.

The College of William and Mary, 1988

U·M·I

**300 N. Zeeb Rd.
Ann Arbor, MI 48106**



**STATISTICALLY CONSTRAINED DECIMATION
OF A TURBULENCE MODEL**

A Dissertation

Presented to

**The Faculty of the Department of Physics
The College of William and Mary in Virginia**

In Partial Fulfillment

**Of the Requirements for the Degree of
Doctor of Philosophy**

by

Timothy J. Williams

1988

APPROVAL SHEET

This dissertation is submitted in partial fulfillment of
the requirements for the degree of

Doctor of Philosophy

Timothy J. Williams

Timothy J. Williams

Approved, November 1988

G.V.L.G.

George M. Vahala

Eugene R. Tracy

Eugene R. Tracy

Allen H. Boozer

Allen H. Boozer

John B. Delos

John B. Delos

Raymond W. Southworth

Raymond W. Southworth
Department of Mathematics

TABLE OF CONTENTS

	Page
ABSTRACT	vi
I. MOTIVATION: STATISTICAL TURBULENCE THEORY	2
A. Strong homogeneous turbulence	2
1. <i>Fourier modes</i>	3
2. <i>Statistical approaches to the problem of strong turbulence</i>	4
(a) <i>Cumulant-discard (quasinormal) approximation</i>	4
(b) <i>Renormalization group methods</i>	5
(c) <i>Direct interaction approximation</i>	6
II. THE CONSTRAINED DECIMATION SCHEME (CDS)	7
A. Statistical similarity	7
B. Decimation	7
C. Constrained stochastic forces	8
III. APPLICATION OF THE CDS TO A SYSTEM OF ODE'S	10
A. Generic system	10
B. The ensemble	10
C. Decimated system	12
1. <i>Sample set</i>	12
2. <i>Stochastic forces</i>	13
(a) <i>Statistical interpolation: q^*</i>	13
D. Statistical constraints	15
1. <i>Formulation of constraints</i>	15
2. <i>Choice of constraints</i>	16
3. <i>Enforcing the constraints</i>	17
(a) <i>Stochastic Newton-Raphson procedure</i>	17
(b) <i>Algebraic reduction to a determined matrix problem</i>	19
E. Strong decimation limit	21
F. Outline of numerical procedure	21
IV. THE BETCHOV SYSTEM	23
A. The system	23
1. <i>ODE's</i>	23

2. <i>Statistical properties</i>	25
3. <i>Numerical solution</i>	27
B. Reasons to choose this system for CDS analysis	28
C. Results from solving the full Betchov system	30
1. <i>General parameters in the numerical studies</i>	30
2. <i>General results</i>	31
3. <i>Estimate of statistical fluctuations</i>	35
4. <i>Estimate of numerical operations</i>	40
V. APPLICATION OF THE CDS TO THE BETCHOV SYSTEM	41
A. The decimated system	41
1. <i>Sample set</i>	41
2. <i>Stochastic forces</i>	42
(a) <i>Statistical interpolation: q^*</i>	43
3. <i>Statistical constraints</i>	44
(a) <i>Constraint set I</i>	45
(b) <i>Constraint set II</i>	48
(c) <i>General remarks about sets of constraints</i>	48
4. <i>General parameters in numerical studies</i>	49
5. <i>Estimate of statistical fluctuations</i>	50
6. <i>Estimate of numerical operations</i>	50
B. Results using constraint set I	55
1. <i>General results</i>	55
2. <i>Effects of the constraints</i>	64
(a) <i>Mean stochastic force constraint</i>	64
(b) <i>Mean energy constraint</i>	65
(c) <i>Force variance constraint</i>	65
(d) <i>Unequal-time constraints</i>	66
C. Results using constraint set II	73
1. <i>General results</i>	73
2. <i>Effects of the constraints</i>	83
(a) <i>Mean stochastic force constraint</i>	83
(b) <i>Equal-time force-variable constraint</i>	85
(c) <i>Unequal-time force-variable constraints</i>	85

VI. RELATION BETWEEN THE CDS AND THE DIA	90
A. DIA via CDS	90
B. Constraint set Π as "DIA constraints"	100
VII. CONCLUSIONS AND NEXT STEPS	101
A. Works with one symmetry group	101
B. Ideas behind derivation of DIA via CDS supported	104
C. Works where cumulant-discard approximation fails	105
APPENDIX A: CUMULANT-DISCARD APPROXIMATION SOLUTIONS OF THE BETCHOV SYSTEM	106
APPENDIX B: DIA SOLUTION OF THE BETCHOV SYSTEM	116
A. Derivation of $H_{\text{DIA}}(\tau)$	116
B. Numerical solution: code	137
APPENDIX C: CODE FOR CDS SOLUTION OF THE BETCHOV SYSTEM	139
APPENDIX D: MULTIDIMENSIONAL NEWTON-RAPHSON PROCEDURE	153
REFERENCES	156
VITA	158

ABSTRACT

The constrained decimation scheme (CDS) is applied to a turbulence model. The CDS is a statistical turbulence theory formulated in 1985 by Robert Kraichnan; it seeks to correctly describe the statistical behavior of a system using only a small sample of the actual dynamics. The full set of dynamical quantities is partitioned into groups, within each of which the statistical properties must be uniform. Each statistical symmetry group is then decimated down to a small sample set of explicit dynamics. The statistical effects of the implicit dynamics outside the sample set are modelled by stochastic forces.

These forces are not totally random; they must satisfy statistical constraints in the following way: Full-system statistical moments are calculated by interpolation among sample-set moments; the stochastic forces are adjusted by an iterative process until decimated-system moments match these calculated full-system moments. Formally, the entire infinite hierarchy of moments describing the system statistics should be constrained. In practice, a small number of low-order moment constraints are enforced; these moments are chosen on the basis of physical insights and known properties of the system.

The system studied in this work is the Betchov model — a large set of coupled, quadratically nonlinear ordinary differential equations with random coupling coefficients. This turbulence model was originally devised to study another statistical theory, the direct interaction approximation (DIA). By design of the Betchov system, the DIA solution for statistical autocorrelation is easy to obtain numerically. This permits comparison of CDS results with DIA results for Betchov systems too large to be solved in full.

The Betchov system is decimated and solved under two sets of statistical constraints. Under the first set, basic statistical properties of the full Betchov system are reproduced for modest decimation strengths (ratios of full-system size to decimated-system size); however, problems arise at stronger decimation. These problems are solved by the second set of constraints. The second constraint set is intimately related to the DIA; that relationship is shown, and results from the CDS under those constraints are shown to approach the DIA results as the decimation strength increases.

**STATISTICALLY CONSTRAINED DECIMATION
OF A TURBULENCE MODEL**

I. MOTIVATION: STATISTICAL TURBULENCE THEORY

A. Strong homogeneous turbulence	2
1. <i>Fourier modes</i>	3
2. <i>Statistical moment hierarchy</i>	4
3. <i>Statistical approaches to the problem of strong turbulence</i>	4
(a) <i>Cumulant-discard (quasinormal) approximation</i>	4
(b) <i>Renormalization group methods</i>	5
(c) <i>Direct interaction approximation</i>	6

A. Strong homogeneous turbulence

The ideas behind this dissertation come from the field of statistical turbulence theory. Work in this field has concentrated on finding a simple description of the average properties of turbulent flows, specifically *strongly* turbulent flows. Strong turbulence is characterized by very complicated flow patterns involving many degrees of freedom.

A common measure of the strength of the turbulence is the *Reynolds number*, Re , which is the ratio of inertial (nonlinear) to viscous (linear) forces.¹ When the inertial forces on fluid elements are sufficient to overcome the tendency of the viscosity to "stick" their motion to neighboring elements, the flow changes from *laminar* flow to *turbulent* flow. The transition to turbulence commonly occurs at a Reynolds number which is highly system-dependent; for example, water flowing in a straight pipe becomes turbulent around $Re = 2000$.² Atmospheric turbulence typically has a much higher Reynolds number than water turbulence because of the much lower viscosity of air. In strong turbulence, Re is well above the transition value.

The equations most commonly used to describe fluid flows are the Navier-Stokes equations, which are nonlinear partial differential equations involving the flow velocity field, the pressure field, and the equation of state. There is an unpleasant lack of knowledge about general solutions for these equations, as is the case for most nonlinear partial differential equations. Much of the current study of flows using these equations is done with numerical solution methods. Unfortunately, for common methods, the number of numerical operations required to resolve all the important aspects of a flow scales like Re^3 .³ The number of degrees of freedom (amount of computer storage) required scales like $Re^{9/4}$.⁴ Direct numerical solution becomes impossible long before the regime of strong turbulence.

1. Fourier modes

A direct numerical approach to solving for turbulent flows favored by statistical turbulence theorists involves spectral decomposition of the flow velocity field. The fluid flow velocity field $u(x,t)$ is expressed as an infinite series of Fourier modes

$$u(x,t) = \sum_k u(k,t) e^{i(k \cdot x)} .$$

The sum is over all wave vectors k , and the $u(k,t)$ are the mode amplitudes. Higher $|k|$ corresponds to smaller spatial scales; the complicated spatial evolution of strongly turbulent flows requires a large contribution from high- k modes.

Substitute this series for $u(x,t)$ into the Navier-Stokes equations; the PDE's become an infinite set of coupled, quadratically nonlinear

ODE's. This set of equations can be truncated and solved numerically as a finite set of coupled ODE's.

In order to resolve the important scales in a turbulent flow with Reynolds number Re , the Fourier-mode ODE formulation of the Navier-Stokes equations must be truncated not lower than a wavenumber level of $O(Re^{9/4})$.⁵ For strongly turbulent flows with $Re \sim 10^5$ - 10^8 , this yields an intractably large set of equations. The largest claimed Reynolds numbers for this and other direct numerical solution methods are $O(10^2)$ for three-dimensional flows (see references 5 and 6).

2. *Statistical approaches to the problem of strong turbulence*

(a) *Cumulant-discard (quasinormal) approximation*

Like many statistical turbulence theories, this one begins by taking statistical moments of the basic equations (i.e., the Navier-Stokes equations). Formally, the complete equations can be expressed as an infinite hierarchy of moment equations of increasing order. The equations are not closed because each moment equation contains higher-order moments in it. It is generally true that statistical theories seek to truncate the moment hierarchy by making some approximation which closes the system at a finite level.

The quasinormal approximation assumes that fourth-order statistical moments can be replaced by products of second-order moments. A Gaussian, or normal, distribution has this property; this approximation assumes that the distribution of flow-variable moments is "quasinormal." When applied to Navier-Stokes flows, this approximation has been shown to predict unphysical results such as the development of negative values

for positive-definite physical quantities.⁷

(b) Renormalization group methods

These methods^{3,8,9,10,11,12} have had some success in calculating some basic generally-accepted statistical properties of turbulent flows, but they are not without serious drawbacks (as are all existing statistical turbulence theories, with the possible exception of the CDS, which has yet to calculate any flows at all). A typical renormalization-group approach begins by splitting the Fourier-mode k -space into those modes above and below the cutoff for explicitly-followed modes. These two sets of modes are called, respectively, the *subgrid* and *supergrid* modes.

Beginning with some final high- k cutoff (such as the maximum k needed to describe the desired Reynolds number flow), peel away shells of wave vectors and calculate their effect on the remaining modes in the Navier-Stokes equations. This is done using some approximation equivalent to a moment-hierarchy closure approximation to incorporate the effects of "peeled-off" subgrid shell as a renormalized eddy viscosity and extra nonlinear terms.

Iterate this procedure until all the modes between the maximum cutoff and the boundary of the supergrid modes to be explicitly solved for are eliminated. The final renormalized equations are solved explicitly with some numerical method. The RNG theories have trouble with closure which are not resolved either in the ε -expansion method,^{3,8,9} which requires setting the "small" parameter $\varepsilon = 4$ to recover accepted physical properties or in the recursion method^{10,11}.

(c) *Direct interaction approximation*

The direct interaction approximation (DIA) was invented in the late 1950's by Robert Kraichnan.^{13,14,15,16} As the name implies, this method treats as dominant the direct interactions of the modes--that is, the interactions of modes directly coupled in the differential equations. For each mode, these direct interactions are treated *independently* as a continuous train of perturbations on a solution in which the direct interactions are absent.

The effects of each "perturbing" direct interaction on a mode are modelled using the *regression function*. The regression function is defined as the future effects of perturbing one mode with an impulse in its amplitude at some time; the function describes how the system regresses back to its unperturbed statistical properties after it loses memory of the impulse. It is vital for the validity of this theory that the regression function decays rapidly with time after the perturbation.

This decay is vital because it allows the fundamental statistical approximation of the DIA: Quadruple moments are replaced by products of double moments in the regression-function-weighted integral expression relating triple moments and quadruple moments. This is the same closure approximation made in the quasinormal approximation; but here, the approximation need only hold valid for short time displacements because of the rapid decay of the regression function which weights the moment integrands. A description of the application of the DIA to the model system of this dissertation is given in Appendix B.

II. THE CONSTRAINED DECIMATION SCHEME (CDS)

A. Statistical similarity	7
B. Decimation	7
C. Constrained stochastic forces	8

A. Statistical similarity

Experimental data has demonstrated small-scale isotropy in turbulent flows.⁷ Theoretical considerations also give reason to believe that modes having approximately equal wave number magnitudes have similar contributions to the flow.⁷ Modes in a group are *dynamically similar* if their couplings to other modes can be interchanged without changing the flow. Modes in a group are *statistically similar* if their average contributions to the flow are the same; this means that their couplings to other modes can be interchanged without changing the average flow. Here "average flow" means an average over an ensemble of flows evolved from different initial conditions but with the same boundary conditions and Reynolds number.

B. Decimation

If one is interested in calculating only statistical properties of turbulent flows, statistically similar modes are redundant. One could replace a whole group of statistically similar modes with a small, representative *sample set* of modes whose contribution to the flow is the average contribution of the entire group. This reduction of the number of explicitly-followed modes is called *decimation*.

C. Constrained stochastic forces

In order to mimic the couplings to modes which are lost in this decimation, the sample-set modes are driven with random forces which have the same statistical properties as the lost couplings. Because the sample-set modes and couplings are statistically similar to the lost modes, the observed statistical properties of the sample-set-mode couplings could then be interpolated, scaled, and used to dynamically construct the random force as the ensemble of systems evolves.

This is the basis of the *constrained decimation scheme* (CDS),¹⁷ which aims to reduce a large set of dynamical equations to a much smaller set which has the same statistical properties. With this method, one could study the statistical properties of strongly turbulent flows using a tractably small set of equations. It is the statistical properties of such flows which can best be quantitatively compared with experimental results.

An important requirement of the CDS is that the entire ensemble of these systems must be solved simultaneously. The realizations cannot be solved individually because statistical constraints on the ensemble of systems determine the time dependence of the stochastic forces. Various full-system, ensemble-average, moments are calculated via statistical interpolation among the evolving sample-set variables; the decimated-system moments are constrained to match these by adjusting the ensemble of stochastic forces.

This dissertation presents an application of the CDS to a model system of equations designed to mimic some properties of the Fourier mode equations derived from the Navier-Stokes equations. This work demonstrates an achievement of the formal goal of the CDS — the

reproduction of key statistical properties of a large system of equations by a much smaller system driven by constrained stochastic forces.

III. APPLICATION OF THE CDS TO A SYSTEM OF ODE'S

A. Generic system	10
B. The ensemble	10
C. Decimated system	12
1. Sample set	12
2. Stochastic forces	13
(a) Statistical interpolation: q^*	13
D. Statistical constraints	15
1. Formulation of constraints	15
2. Choice of constraints	16
3. Enforcing the constraints	17
(a) Stochastic Newton-Raphson procedure	17
(b) Algebraic reduction to a determined matrix problem	19
E. Strong decimation limit	21
F. Outline of numerical procedure	21

A. Generic system

Consider a system of N coupled, quadratically-nonlinear ODE's:

$$\frac{dx_i(t)}{dt} = \sum_{j,k=1}^N C_{ijk} x_j(t) x_k(t) \quad ; \quad i = 1,2,\dots,N \quad (N \gg 1) \quad (1)$$

The C_{ijk} are constant coupling coefficients. The dynamics of this system are determined by integrating from the initial condition $\{x_i(0) \mid i=1,2,\dots,N\}$ to solve for $\{x_i(t) \mid i=1,2,\dots,N\}$.

B. The ensemble

Now consider an ensemble made up of R realizations of the system integrated from R different initial conditions

$\{\{x_i^{(v)}(0) \mid i=1,2,\dots,N\} \mid v=1,2,\dots,R\}$. It is important to understand that the realizations differ only in their initial conditions; each realization is a system of N ODE's for N variables obeying Eq. (1), and all realizations have the same set of constant coupling coefficients.

Statistical properties of the system are calculated from simple ensemble averages of the form

$$\langle f(x_1(t), x_2(t), \dots) \rangle \equiv \frac{1}{R} \sum_{v=1}^R f[x_1^{(v)}(t), x_2^{(v)}(t), \dots] ,$$

where f is any function of the system variables. The notation $\langle \rangle$ denotes the ensemble average. For example, the mean (ensemble average) of variable x_i is

$$\langle x_i(t) \rangle = \frac{1}{R} \sum_{v=1}^R x_i^{(v)}(t) .$$

If two variables are statistically similar, *all* of their statistical properties are the same. This implies an infinite hierarchy of moment equalities:

$$\langle x_i(t) \rangle = \langle x_j(t) \rangle$$

$$\langle x_i^2(t) \rangle = \langle x_j^2(t) \rangle$$

$$\vdots$$

This relationship is denoted as follows:

$$x_i \leftrightarrow x_j .$$

If one is only interested in calculating statistical (reproducible) properties of the system (and not dynamical properties), the two variables x_i and x_j are redundant. The purpose of the CDS is to exploit that redundancy in calculating the statistical properties of the system.

C. Decimated system

1. Sample set

The first step in applying the CDS is the *decimation* of the system. The full set of variables $\{x_i | i=1,2,\dots,N\}$ is replaced by a much smaller *sample set* of selected variables $\{x_i | i=1,2,\dots,S\}$ (where $S \ll N$). For the sake of simplicity, suppose that all variables in the full system are statistically similar. Then the choice of sample set variables is completely arbitrary.

The next step is the modification of the system of ODE's to reflect its reduction from a set of N equations to a set of S equations. The original full-system ODE's (Eq. (1)) are replaced by the decimated-system equations

$$\frac{dx_i(t)}{dt} = \sum_{j,k=1}^S C_{ijk} x_j(t) x_k(t) + q_i(t) \quad i=1,2,\dots,S. \quad (2)$$

The *stochastic force* $q_i(t)$ in each equation is there to replace the statistical effects of the couplings to the variables outside the sample set (the variables lost in the decimation).

2. Stochastic forces

The stochastic forces must be statistically similar to the terms in the sum in Eq. (1) which are missing in Eq. (2). That is,

$$q_i(t) \leftrightarrow \sum_{j,k}^N ' C_{ijk} x_j(t) x_k(t) ,$$

where Σ' denotes the summation over all terms in which j and/or k is outside the sample set.

(a) Statistical interpolation: q^*

Clearly if $\{x_{S+1}, x_{S+2}, \dots, x_N\}$ have been decimated,

$$\sum_{j,k}^N ' C_{ijk} x_j(t) x_k(t) \quad (3)$$

cannot be computed directly. For the purpose of statistical calculations, however, the exact value of the sum in Eq. (3) is not needed; only its statistical properties are needed. Now the statistical similarity of the sample-set variables with those lost in the decimation is exploited to calculate the statistical properties of Eq. (3).

Because

$$x_i \leftrightarrow x_j \quad \text{for } i = 1, 2, \dots, S \text{ and } j = S+1, \dots, N ,$$

one knows that

$$\sum_{j,k}^N C_{ijk} x_j(t) x_k(t) \leftrightarrow w_i \sum_{j,k=1}^S C_{ijk} x_j(t) x_k(t) , \quad (4)$$

where w_i is a weighting factor to account for the different number of terms in the two sums in Eq. (4). This process of describing full-system statistics using combinations of decimated-system statistics is called *statistical interpolation*; $\{w_i | i=1,2,\dots,S\}$ are weights for that interpolation. A useful quantity to define is the righthand side of Eq. (4); denote this by $q_i^*(t)$:

$$q_i^*(t) \equiv w_i \sum_{j,k=1}^S C_{ijk} x_j(t) x_k(t) . \quad (5)$$

For systems with more than one group of statistically similar modes, such as the Fourier-decomposed Navier-Stokes equations, the statistical interpolation is more complicated. One must consider not only interpolation among the modes in a statistically-similar group, but also the modes in other groups which have different statistics. In this case there are sample-set modes from each group of statistically-similar modes. This is discussed briefly in §VIIA.

D. Statistical constraints

1. Formulation of constraints

Each stochastic force must be statistically similar to Eq. (5). That is, denoting statistical similarity by the symbol \leftrightarrow ,

$$q_i(t) \leftrightarrow q_i^*(t) . \quad (6)$$

To insure statistical similarity, all possible moments of $q_i(t)$ must be equal to the corresponding moments of the righthand side of Eq. (6).

That is,

$$\begin{aligned}
 \langle q_i(t) \rangle &= \langle q_i^*(t) \rangle \\
 \langle q_i^2(t) \rangle &= \langle q_i^{*2}(t) \rangle \\
 \langle q_i(t) q_j(t') \rangle &= \langle q_i^*(t) q_j^*(t') \rangle \\
 \langle q_i(t) x_j(t') \rangle &= \langle q_i^*(t) x_j(t') \rangle \\
 &\vdots
 \end{aligned} \tag{7}$$

In the CDS, this infinite hierarchy of equations is viewed as a set of *statistical constraints* on the random forces.

All statistical constraints can be written in the form of a function whose ensemble average is zero,

$$\langle F[q_1(t), q_1(t'), \dots, q_S(t), q_S(t'), x_1(t), x_1(t'), \dots, x_S(t), \dots] \rangle = 0 ; \tag{8}$$

F is a general function of all the variables and all the forces at some set of time values $\{t, t', t'', \dots\}$. For example, the first equation in Eq. (7):

$$\begin{aligned}
 F[q_1(t), \dots] &= q_1(t) - q_1^*(t) \\
 &= q_1(t) - w_i \sum_{j,k=1}^S C_{ijk} x_j(t) x_k(t) .
 \end{aligned}$$

The central assumption of the CDS is that the system given by Eq. (2) will have the same average properties as the original system given by Eq. (1) if the stochastic forces satisfy the full hierarchy of constraints.

2. Choice of constraints

The next step of the CDS is to replace the infinite set of constraints in the full hierarchy with a small subset of chosen constraints. This subset determines the time dependence of the stochastic forces, which are generated randomly then forced to satisfy the statistical constraints as the ensemble of systems is integrated.

Choosing an appropriate set of statistical constraints is the key to the success of the CDS. No definite heuristics are known for choosing all the appropriate constraints for an arbitrary problem, although there are fundamental reasons to expect that constraints expressible as moments of at most $O(x_i^4)$ should be sufficient^{18,†} [i.e., at most $O(q_i^2)$]. Also, the number of constraints must be kept small enough to implement numerically. One can at least partially test a set of constraints by decimating a full system which is small enough to solve exactly, and comparing the solutions of the full and decimated systems. If the decimated-system solution reproduces some desired statistical properties of the known full-system solution, it is plausible that a decimated-system solution with the same set of constraints will predict desired statistical properties of a full-system solution that is too large to find directly. One can also compare large- N results with any

[†] This is to cause the solution of the mean square of the Navier-Stokes equations.

existing theories which are exact in the limit $N \rightarrow \infty$.

The choice of certain constraints is suggested by the statistical and dynamical properties of the system to be decimated. Every known constant of the motion in the full system should suggest a constraint in the decimated system.

3. Enforcing the constraints

(a) Stochastic Newton-Raphson procedure

Each of the constraints can be written in the form of Eq. (8); that is,

$$\langle F_{(\alpha)} \rangle = 0 \quad \text{for } \alpha = 1, 2, \dots, C, \quad (9)$$

where C is the number of statistical constraints to be applied. In general F is a function of the explicit variables and stochastic forces with any combination of time arguments; for clarity, only the stochastic forces being determined by Eq. (9) ($\{q_i^{(v)}(t) \mid i=1, 2, \dots, S \mid v=1, 2, \dots, R\}$) will be indicated as arguments for F in subsequent algebra.

The constraints are enforced by the use of a stochastic Newton-Raphson iterative procedure.¹⁷ This procedure seeks an ensemble of stochastic forces $\{\tilde{q}_i^{(v)}(t) \mid i=1, 2, \dots, S \mid v=1, 2, \dots, R\}$ which solves the C equations in Eq. (9). That is,

$$\langle F_{(\alpha)}[\tilde{q}_1(t), \tilde{q}_2(t), \dots, \tilde{q}_S(t)] \rangle = 0 .$$

(See Appendix D for a general description of multidimensional Newton-Raphson procedures.) For q_i near \tilde{q}_i , a Taylor series expansion

of $F_{(\alpha)}$ about q_i yields

$$\begin{aligned} \langle F_{(\alpha)}[q_1(t), \dots] \rangle + \left\langle \sum_{i=1}^S \left[(\tilde{q}_i - q_i) \frac{\partial F_{(\alpha)}}{\partial q_i} \right] \right\rangle &\approx \langle F_{(\alpha)}[\tilde{q}_1(t), \dots] \rangle \\ &\approx 0 . \end{aligned}$$

From an initial guess ensemble of stochastic forcing values $\{\{q_{i(0)}^{(v)} | i=1,2,\dots,S\} | v=1,2,\dots,R\}$, the procedure iterates through a sequence of ensembles $\{\{\{q_{i(n)}^{(v)} | i=1,2,\dots,S\} | v=1,2,\dots,R\} | n=1,2,3,4,\dots\}$ toward a solution ensemble. In each iteration, the next member in the sequence is found by solving

$$\begin{aligned} \langle F_{(\alpha)}[q_{1(n)}, q_{2(n)}, \dots, q_{S(n)}] \rangle + \\ \left\langle \sum_{i=1}^S \left[[q_{i(n+1)} - q_{i(n)}] \frac{\partial F_{(\alpha)}}{\partial q_{i(n)}} \right] \right\rangle = 0 \quad \text{for } \alpha=1,2,\dots,C . \end{aligned} \quad (10)$$

If the iterates converge to the solution, every difference $[q_{i(n+1)}^{(v)} - q_{i(n)}^{(v)}]$ decreases in absolute value as $q_{i(n+1)}^{(v)}$ approaches $\tilde{q}_i^{(v)}$.

To solve Eq. (10), it is useful to express it as a matrix equation. The partial derivatives $\{\{\partial F_{(\alpha)} / \partial q_{i(n)}^{(v)} | i=1,2,\dots,S\} | v=1,2,\dots,R\}$ form the elements of an $SR \times C$ matrix ΔF :

$$[\Delta F]_{\alpha j} = \frac{\partial F_{(\alpha)} \left[q_{1(n)}^{(j \setminus S + 1)}, q_{2(n)}^{(j \setminus S + 1)}, \dots \right]}{\partial q_{(j \bmod S)(n)}^{(j \setminus S + 1)}} ,$$

where $j \setminus S$ denotes the integer part of the quotient j/S . The SR

q -differences $\{[q_{i(n+1)}^{(v)} - q_{i(n)}^{(v)}] | i=1,2,\dots,S | v=1,2,\dots,R\}$ form the components of an SR -dimensional vectors \mathbf{Q} :

$$Q_j = \left[q_{(j \bmod S)(n+1)}^{(\wedge S + 1)} - q_{(j \bmod S)(n)}^{(\wedge S + 1)} \right] .$$

The dot product of these vectors, divided by R , is the second term of Eq. (10). The C ensemble averages $\{\langle F_{(\alpha)} \rangle | \alpha=1,2,\dots,C\}$ form the components of a C -dimensional vector \mathbf{F} :

$$F_\alpha = \left\langle F_{(\alpha)} \left[q_{1(n)}, q_{2(n)}, \dots, q_{S(n)} \right] \right\rangle .$$

Equation (10) can now be reexpressed as

$$\Delta F \cdot \mathbf{Q} = -\mathbf{F} . \quad (11)$$

Since there are far fewer than SR constraints ($C \ll SR$), Eq. (11) is an underdetermined system.

(b) algebraic reduction to a determined matrix problem

One must choose some means of selecting a single SR -dimensional solution vector \mathbf{Q} for Eq. (11), such as requiring a least-squares minimization on the SR q -differences which are the components of \mathbf{Q} . A convenient way to do this is to express \mathbf{Q} as a linear combination of the rows of ΔF ,

$$Q_j = \sum_{\alpha=1}^C A_\alpha \left[\Delta F \right]_{\alpha j} .$$

Next construct a $C \times C$ matrix denoted by G whose elements are dot products of the rows of ΔF ,

$$[G]_{\alpha\beta} = \sum_{j=1}^S [\Delta F]_{\alpha j} [\Delta F]_{\beta j}$$

Finally, arrange the expansion coefficients $\{A_{\alpha} | \alpha=1,2,\dots,C\}$ into a C -dimensional column vector A . Now Eq. (11) can be expressed as the determined matrix problem

$$G \cdot A = -F . \quad (12)$$

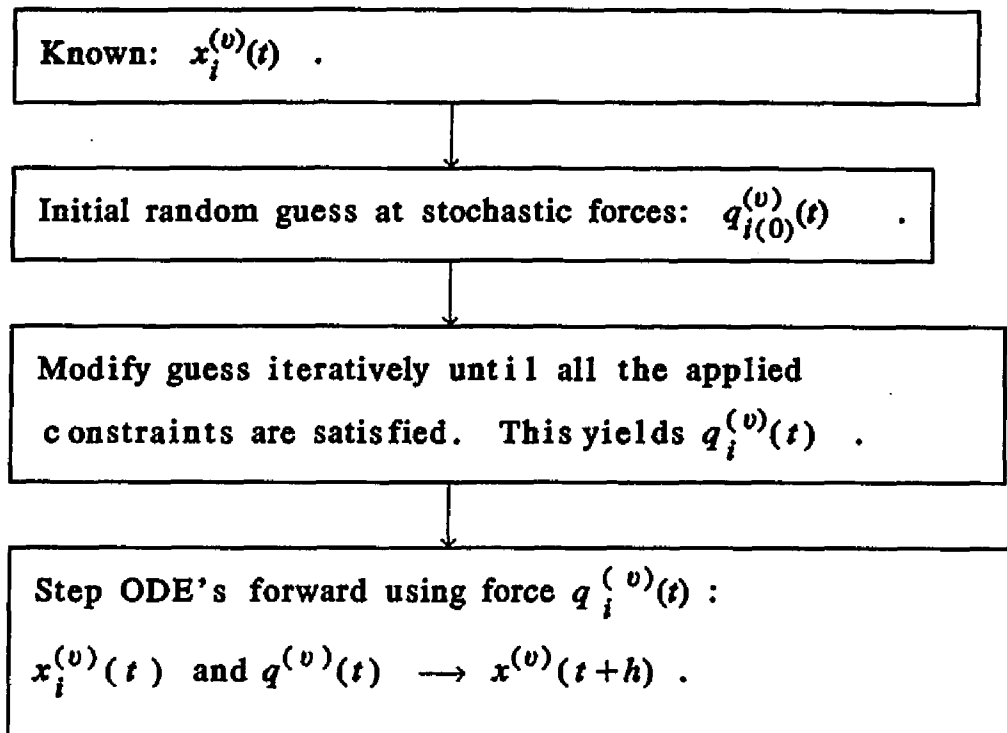
At every iteration in the Newton-Raphson procedure, this equation is solved for A ; A is used to construct Q , which yields $\{\{q_{i(n+1)}^{(v)} | i=1,2,\dots,S\} | v=1,2,\dots,R\}$. When the righthand side of Eq. (12) converges to the zero-vector, the iteration is halted and the last iterate of A is used to construct $\{\tilde{q}_i^{(v)} | i=1,2,\dots,C\} | v=1,2,\dots,R\}$.

E. Strong decimation limit

In the limit of strong decimation ($N/S \rightarrow \infty$), S/N can be used as a small parameter for perturbation analysis.¹⁸ An example of results from the strong decimation limit is the relationship between the DIA and the CDS derived in §VI.

F. Outline of numerical procedure

An ensemble of decimated systems is solved numerically from an ensemble of initial conditions $\{\{x_i^{(v)}(0) | i=1,2,\dots,S\} | v=1,2,\dots,R\}$. The same set of coupling coefficients is used for each realization in the ensemble. At every timestep, the ensemble of stochastic forces $\{\{q_i^{(v)}(t) | i=1,2,\dots,S\} | v=1,2,\dots,R\}$ is initialized at random then modified iteratively until all the statistical constraints are satisfied. The modified forces are then applied to the ensemble of systems of ODE's to step forward in time. This algorithm is summarized in the following block diagram for one timestep:



IV. THE BETCHOV SYSTEM

A. The system	23
1. ODE's	23
2. Statistical properties	25
3. Numerical solution	27
B. Reasons to choose this system for CDS analysis	28
C. Results from solving the full Betchov system	30
1. General parameters in the numerical studies	30
2. General results	31
3. Estimate of statistical fluctuations	35
4. Estimate of numerical operations	40

A. The system

1. ODE's

The Betchov system^{19,20} is a large set of coupled, quadratically nonlinear ordinary differential equations (ODE's):

$$\frac{dx_i}{dt} = \sum_{j,k=1}^N C_{ijk} x_j x_k \quad \text{for } i=1,2,\dots,N. \quad (13)$$

The C_{ijk} 's are constants. The variables $\{x_i(t) | i=1,2,\dots,N\}$ are like the mode amplitudes in the Fourier-analyzed form of the inviscid, incompressible Navier-Stokes equations; those mode amplitudes are coupled quadratically to each other in a way similar to the way in which the variables are coupled in Eq. (13).

The coupling coefficients $\{C_{ijk} | i,j,k=1,2,\dots,N\}$ in Eq. (13) are generated at random, with certain restrictions. This is one of the

significant differences between the Betchov system and the Navier-Stokes mode equations, whose couplings are nonrandom. The Betchov coefficients are chosen from a Gaussian distribution with zero mean and unit variance; this choice of all the coupling coefficients from the same distribution models the nonpreferential couplings within a given k -magnitude shell in isotropic turbulent flows.

The restrictions on the Betchov coupling coefficients are all designed to mimic some aspect of the Navier-Stokes mode coupling coefficients. The first restriction is that the coefficients satisfy a cyclic identity,

$$C_{ijk} + C_{jki} + C_{kij} = 0. \quad (14)$$

This insures that the energy E is a constant of the motion, where

$$E = \frac{1}{2} \sum_{i=1}^N x_i^2(t) = \text{constant.}$$

That is,

$$\begin{aligned} \frac{dE}{dt} &= \sum_{i=1}^N x_i(t) \frac{dx_i}{dt} \\ &= \sum_{i=1}^N \left\{ x_i(t) \left[\sum_{j,k=1}^N C_{ijk} x_j(t) x_k(t) \right] \right\} \\ &= \frac{1}{3} \sum_{i,j,k=1}^N x_i(t) x_j(t) x_k(t) [C_{ijk} + C_{jki} + C_{kij}] \\ &= 0, \end{aligned}$$

with the use of Eq. (14).

The second restriction is that only $O(N^2)$ of the possible N^3 couplings are nonzero. This models the requirement that the coupled Navier-Stokes modes satisfy the wavenumber triangle equality.⁷ In this paper, following the procedure of Betchov¹⁹ there are $4N^2/3$ nonzero couplings.

The third restriction prevents variables from coupling to themselves: $C_{ijk} = 0$ if any two or more of the indices $\{i,j,k\}$ are equal. This also models the structure of the Fourier-decomposed Navier-Stokes equations.⁷

2. Statistical properties

All of the statistical properties described in this paper are based on ensemble averages. A Betchov system with a single set of coupling coefficients is integrated from an ensemble of initial conditions $\{\{x_i^{(v)}(0) | i=1,2,\dots,N\} | v=1,2,\dots,R\}$ to determine an ensemble of time evolutions $\{\{x_i^{(v)}(t) | i=1,2,\dots,N\} | v=1,2,\dots,R\}$; R is the number of realizations in the ensemble. The initial conditions are chosen at random from a Gaussian ensemble with

$$\begin{aligned} \langle x_i(0) \rangle &= 0 \\ \text{and } \langle x_i^2(0) \rangle &= 1 \quad \text{for } i=1,2,\dots,N, \end{aligned}$$

and normalized to yield a microcanonical ensemble in which each member has the same energy. Specifically,

$$E^{(v)} = \frac{N}{2} \quad \text{for } v=1,2,\dots,R.$$

The Betchov system has three important statistical properties which result from the way that the coupling coefficients and initial conditions are generated. First, *all of the variables in the Betchov system are statistically similar.* At steady-state, no variable dominates any other, and there is no exchange of energy between the variables beyond the level of statistical fluctuations. Thus, the system is "isotropic."

Second, the Betchov system is "turbulent" in the sense that the variables have only a short memory of their previous values as time increases. The autocorrelation functions of the variables,

$$H_i(\tau;t) = \langle x_i(t) x_i(t+\tau) \rangle$$

for a fixed t , decay rapidly as functions of τ to small fluctuations about $H_i(t;\tau) = 0$. Because of the statistical similarity of all variables in the system, $H_i(t;\tau)$ is independent of i . A global indicator of the loss of memory of the variables is therefore the system-averaged autocorrelation function

$$H(t;\tau) = \frac{1}{N} \sum_{i=1}^N H_i(t;\tau) .$$

Third, because the initial conditions are an equilibrium ensemble, the Betchov system is time stationary; in particular, the autocorrelation functions $\{H_i(\tau;t) | i=1,2,\dots,N\}$ are independent of t . Hereafter $H_i(\tau;t)$ and $H(t;\tau)$ will often be written as $H_i(\tau)$ and $H(\tau)$.

3. Numerical solution

The full Betchov system is solved numerically using a simple ODE algorithm. First, the coupling coefficients are generated:¹⁹ Triplets of integers $\{i,j,k\}$ are generated at random from a uniform distribution between 1 and N until a set of $4N^2/9$ unique triplets allowing no self-couplings is determined. For each triplet $\{i,j,k\}$ three coupling coefficients are generated; they are

$$\begin{aligned} C_{ijk} &= \sqrt{\frac{1}{6}} (2a_1 - a_2 - a_3) , \\ C_{kij} &= \sqrt{\frac{1}{6}} (2a_2 - a_3 - a_1) , \\ \text{and } C_{jki} &= \sqrt{\frac{1}{6}} (2a_3 - a_1 - a_2) , \end{aligned}$$

where a_1 , a_2 , and a_3 are generated at random from a Gaussian distribution with zero mean and unit variance. The set of $4N^2/3$ coupling coefficients generated this way complies with the three restrictions previously described. Second, the initial conditions $\{x_i(0) | i=1,2,\dots,N\}$ are chosen at random from a Gaussian distribution and the system is integrated numerically to solve for $\{x_i(t) | i=1,2,\dots,N\}$. The ODE algorithm used is a second-order Runge-Kutta scheme:²¹

$$x_i(t+h) = x_i(t) + \frac{1}{2} [k_{1i} + k_{2i}] + O(h^3) , \quad (15)$$

$$\text{where } k_{1i} = h \frac{dx_i(t)}{dt}$$

$$\text{and } k_{2i} = h \frac{dx_j(t+h)}{dt} \Big|_{\{x_i = x_i(t) + k_{1i} | i=1,2,\dots,S\}}$$

In Eq. (15), h is the numerical timestep.

B. Reasons to choose this system for CDS analysis

The Navier-Stokes equations, even in simplified forms (incompressible, inviscid, two-dimensional, etc.) were not chosen to study this method in spite the method's arising from the field of fluid dynamics. Because of the wide range of important modes inherent to turbulence, one would have to choose a reasonable number of distinct statistical-symmetry groups; modes near in k -magnitude will be statistically similar, but their statistics will be different than those of modes far removed in k -magnitude.

The complications of the interactions of these statistical-symmetry groups, added to the complicated vector mode-coupling structure of the Navier-Stokes equations, would make it difficult to determine whether properties arose because of the physics of the system or artificial effects of the decimation procedure. Of particular importance is the exchange of energy between the statistical-symmetry groups. The Betchov system shares some important properties with the Navier-Stokes equations, and it lacks some properties which could lead to diagnostic difficulties; it was chosen for study for five basic reasons:

First, the Betchov system is "turbulent" in the sense that its variables exhibit nonperiodic fluctuating time evolution (dynamics). Because of the nature of the couplings ($C_{ijk} = 0$ for repeated indices),

the flow is divergence-free in its phase space (satisfies a Liouville property); this means that the system will move ergodically on the energy surface and never settle down onto an attractor in its phase space. Another dynamical indicator of the "turbulence" of the system is sensitive dependence on initial conditions. A *statistical* indicator of the "turbulence" is the loss of memory of the variables as evidenced by the decay of time correlations; a global measure of this is the system-averaged autocorrelation function $H(\tau)$. The time for this function to decay to zero is characteristic of the size of the Betchov system (i.e., it depends on N). Since there is only this one inherent time scale in the Betchov system, reproducing it is an important test for the CDS.

Second, the Betchov system has many degrees of freedom. The most commonly studied full Betchov system in this dissertation has 96 variables. Kraichnan originally tested the CDS on a system of 5 variables decimated to 3 variables.¹⁷ However, that system had several previously undiscovered conserved quantities which made it a less suitable model than the Betchov system. The work which led to this dissertation is the first application of the CDS to a many-variable system.

Third, the Betchov system has many similarities to the Fourier-mode form of the Navier-Stokes equations. The restriction to only $O(N^2)$ of the possible $O(N^3)$ couplings is similar to the results of the requirement that the coupled Navier-Stokes modes satisfy the wavenumber triangle equality.⁷ The lack of self-couplings is also seen in the Navier-Stokes equations.⁷ The constant E can be compared to the constant energy density in the inviscid form of the Navier-Stokes

Fourier mode equations.

Fourth, the Betchov system is highly statistically symmetric; all of the variables in the system are statistically similar. This feature eliminates dealing with separate statistical groups whose stochastic forces have different statistics. The interactions among these groups might obfuscate the results of the decimation. Eventually, the interaction of different statistical groups must be attacked using the CDS if the Navier-Stokes equations are to be solved; but for now, this system with one kind of statistics serves to test the fundamental workability of the CDS.

Fifth, a relatively simple DIA solution for the Betchov system exists. The Betchov system was originally designed to test the DIA; the integro-differential equation for $H_{\text{DIA}}(\tau)$ is simple to solve numerically for any N . (See Appendix B for derivation of the equation and an algorithm for solving it.) Furthermore, Kraichnan has shown that DIA solutions of systems with random couplings such as the Betchov system become exact as the size of the system (N) approaches infinity.²² These easily-obtained and accurate solutions for $H_{\text{DIA}}(\tau)$ can be compared with CDS results from decimation of systems too large to be solved computationally ($N = 10^3$ to 10^6).

C. Results from solving the full Betchov system

1. General parameters in the numerical studies

A system of $N = 96$ variables was chosen, with $4N^2/3 = 12288$ nonzero coupling coefficients. There were $R = 128$ realizations in the ensemble. The timestep was chosen sufficiently small so that there were at least

$O(30)$ timesteps in the decorrelation time interval.

2. General results

As an indicator of the "turbulent" nature of the dynamics of the variables in the system, Fig. 1a shows a typical variable's time evolution in a typical realization of the system. Figure 1b shows the time evolution of a single variable from a Betchov system integrated from several different initial conditions.

Figure 2 and Fig. 3 illustrate the statistical symmetry and time stationarity of the system. They show that the mean and variance of a typical variable do not change beyond the level of statistical fluctuations as t increases. The linearity of Fig. 3b is expected for a fixed-timestep numerical integration scheme which has constant local truncation error.

Figure 1

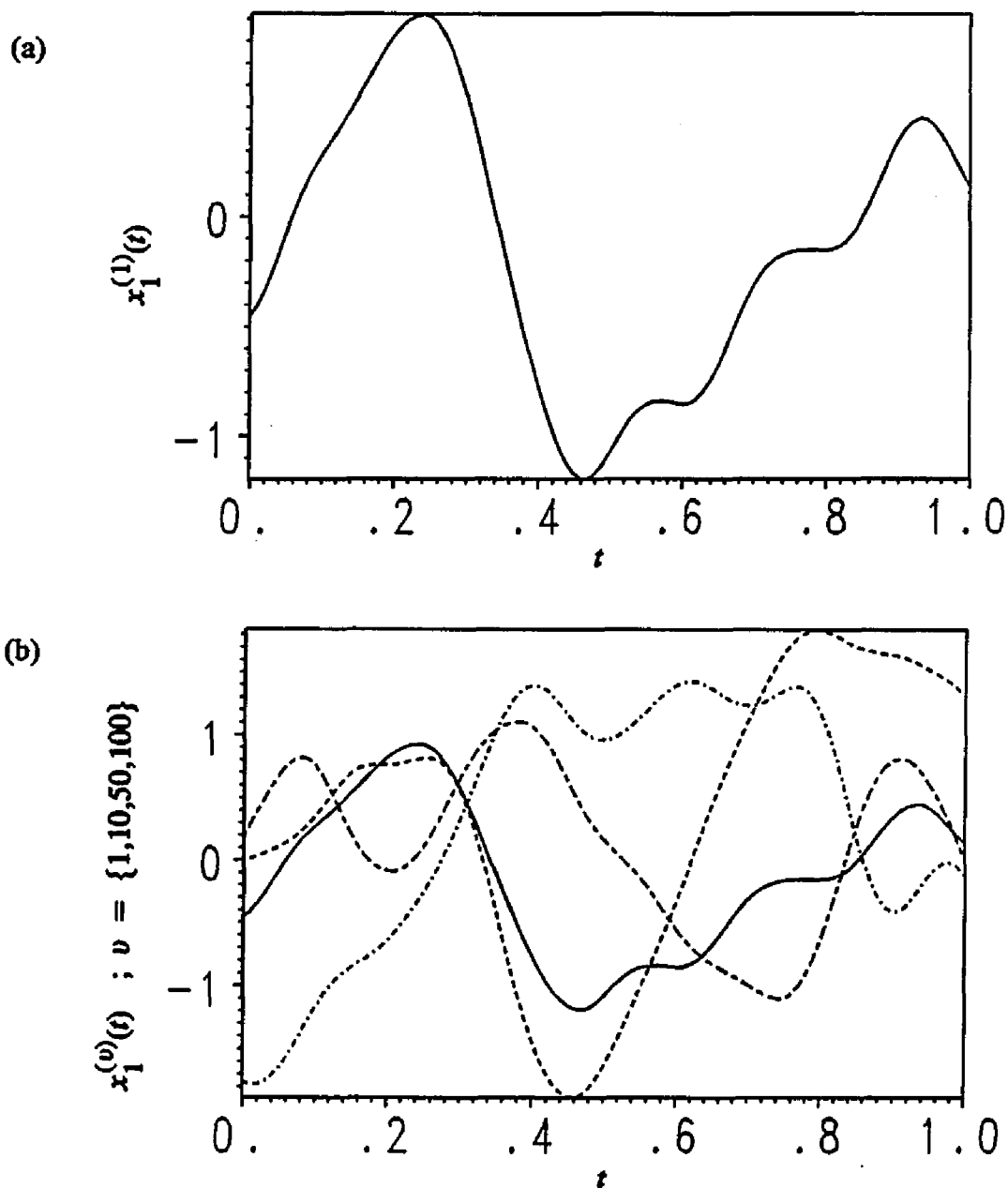


Figure 1. (a) A single variable x_1 , from a single realization of an $N = 96$ Betchov system. (b) A single variable, x_1 , from four different realizations of an $N = 96$ Betchov system; note the different initial conditions.

Figure 2

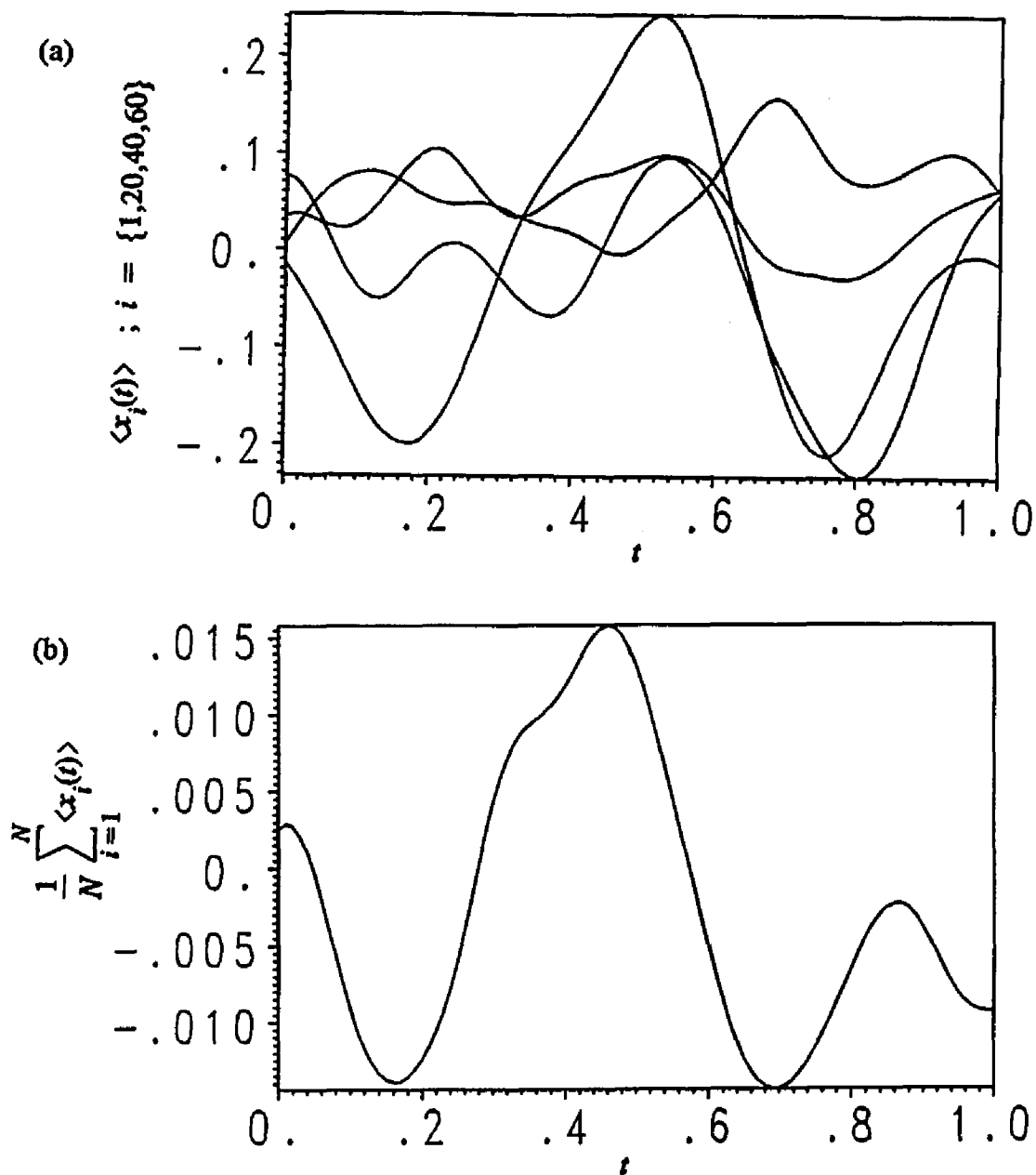


Figure 2. (a) The means of four different variables — $\langle x_1 \rangle$, $\langle x_{20} \rangle$, $\langle x_{40} \rangle$, $\langle x_{60} \rangle$ — from an ensemble of Betchov systems with $N = 96$. Note that no variable dominates any other. (b) The system-averaged mean of all the variables of an $N = 96$ Betchov system. For both (a) and (b), $R = 128$.

Figure 3

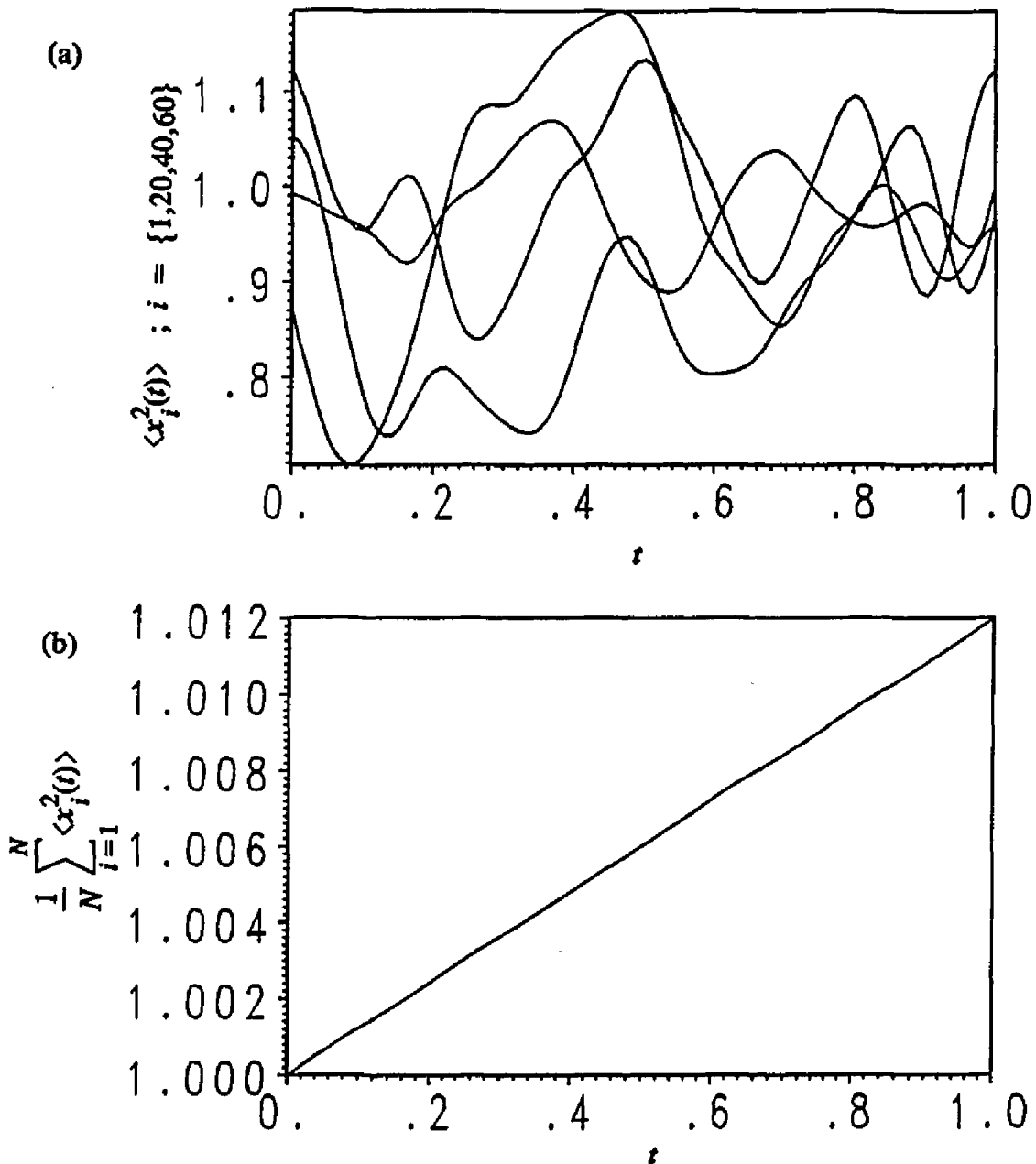


Figure 3. (a) The mean squares of four different variables — $\langle x_1^2 \rangle$, $\langle x_{20}^2 \rangle$, $\langle x_{40}^2 \rangle$, $\langle x_{60}^2 \rangle$ — from an ensemble of Betchov systems with $N = 96$. Note that no variable dominates any other. (b) The system-averaged mean square of all the variables of an $N = 96$ Betchov system. For both plots, $R = 128$.

An important statistical property of the system is the autocorrelation function, $H(t;\tau)$, where t is a fixed time. Figure 4 shows that the system is "turbulent" in the sense that the variables decorrelate with themselves after a finite time. Because the equations have no explicit time dependence and the initial conditions are an equilibrium ensemble, H should be independent of t . Figure 5 demonstrates this with computations of $H(\tau)$ for several values of t .

3. Estimate of statistical fluctuations

The biggest source of fluctuations is the finite size of the system, N , since the nonzero couplings are chosen at random among the N variables. Figure 6 shows calculations of $H(\tau)$ and its fluctuations for 5 different sets of 12288 random couplings, all for a 128-realization ensemble of a 96-variable system.

The fluctuations caused by the finite ensemble size are smaller. Figure 7 shows $H(\tau)$ and its fluctuations for 5 512-realization ensembles of 96-variable systems using the *same* 5 different sets of 12288 random couplings as for the $R = 128$ case. If the finite ensemble size were the primary cause of fluctuations in H , one would expect a the fluctuation levels for 512 realizations to be $O([128/512]^{1/2}) = 1/2$ times the fluctuations for $R = 128$; Figures 6 and 7 show the ratio of fluctuation levels to be $O(0.89)$.

Figure 4

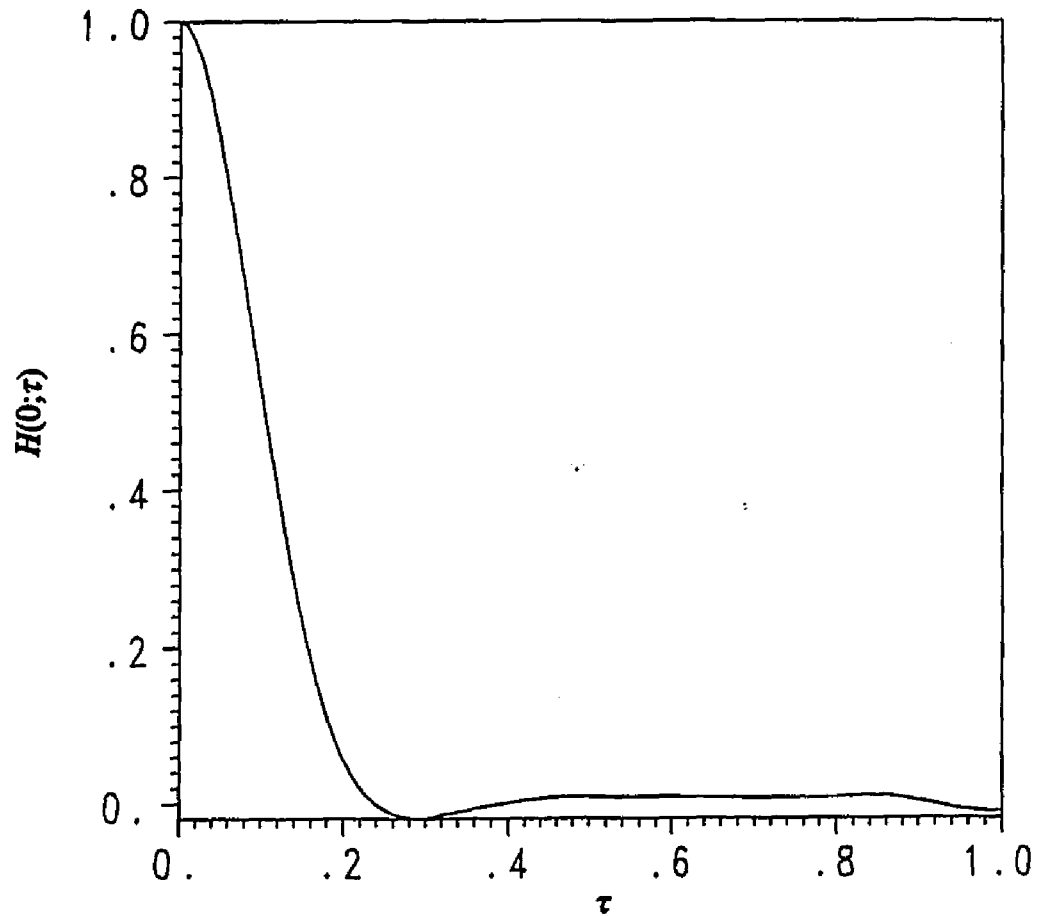


Figure 4. The autocorrelation function for an ensemble of 128 Betchov systems with $N = 96$.

Figure 5

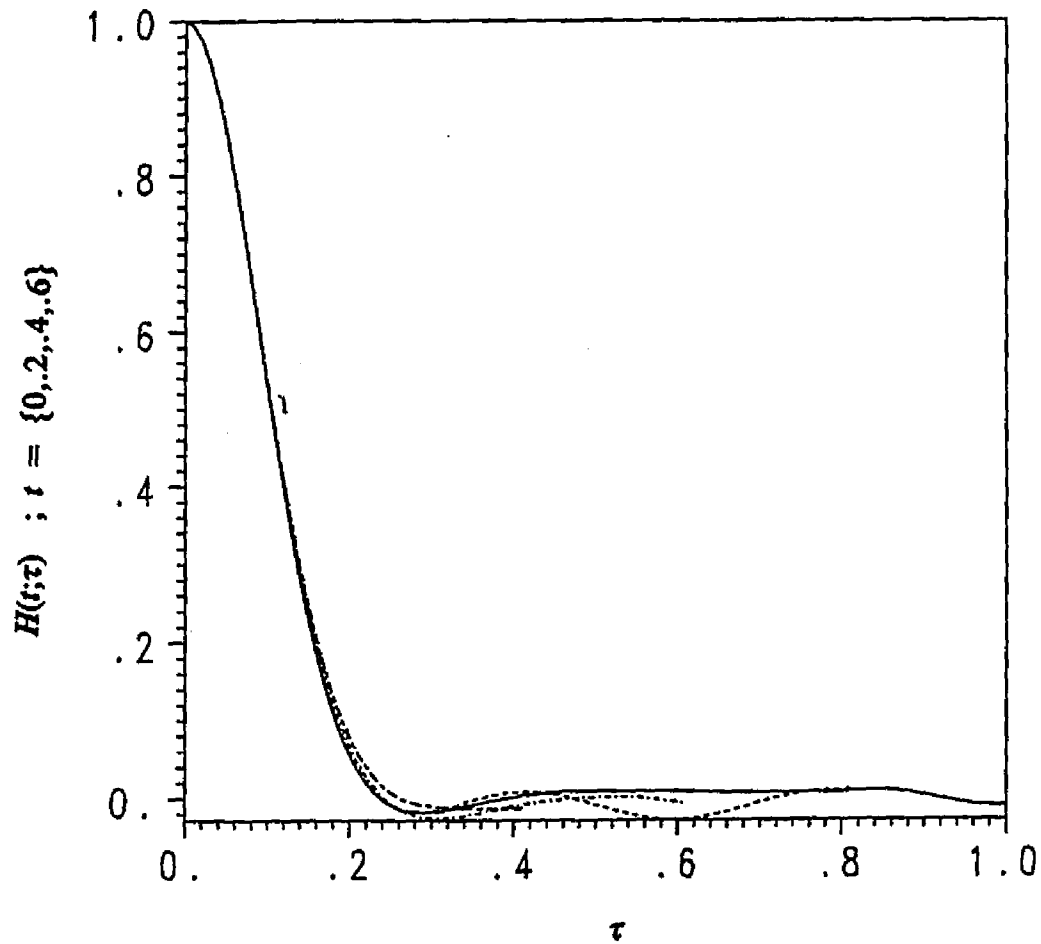


Figure 5. $H(t;\tau)$ with $t = \{0, .2, .4, .6\}$ for an $N = 96$ with an ensemble of $R = 128$ Betchov systems. This shows the time-stationarity of the system.

Figure 6

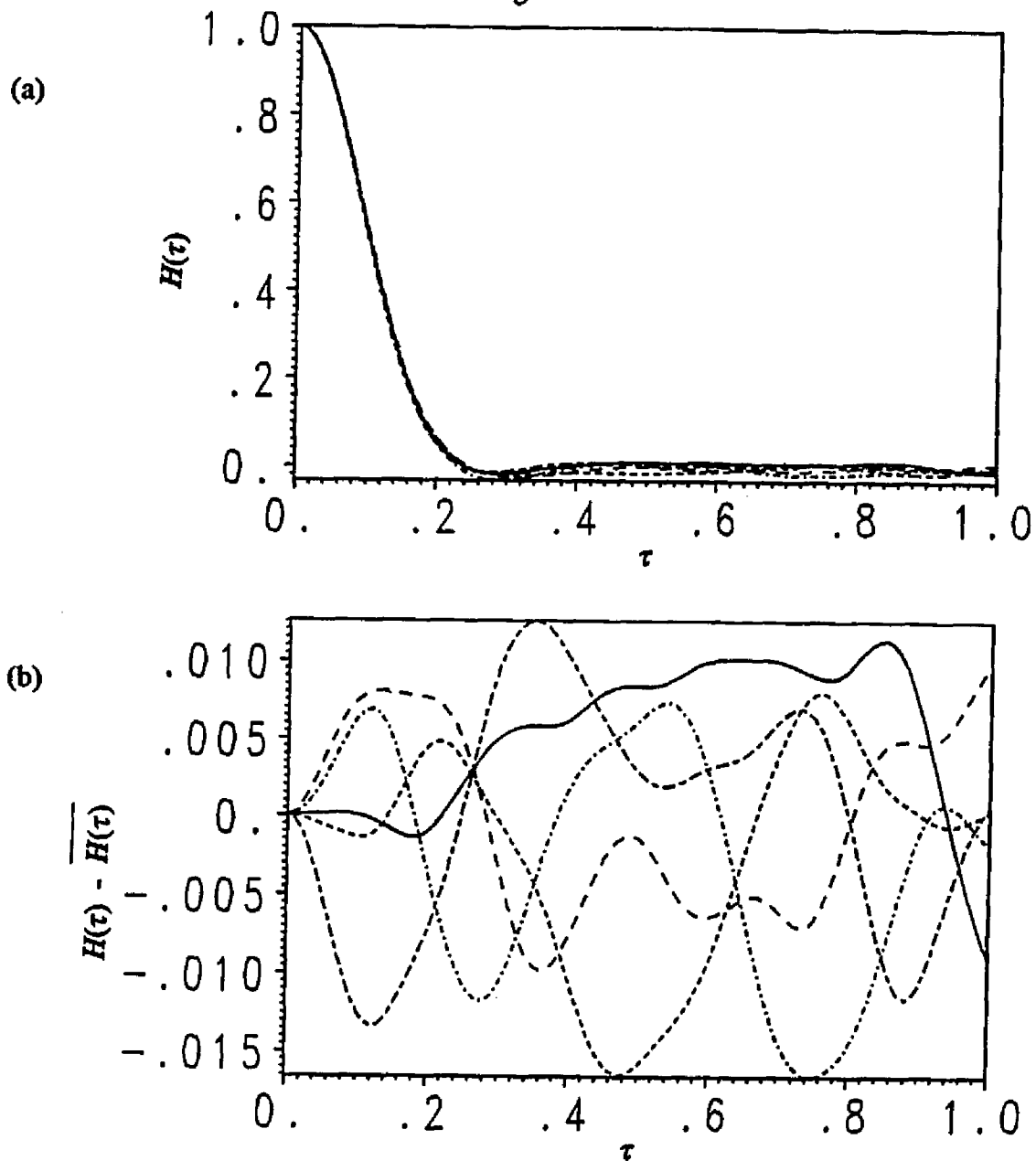


Figure 6. (a) $H(\tau)$ for five different ensembles ($R = 128$ for each) of an $N = 96$ Betheov system; each ensemble used a different set of random coupling coefficients. (But, as always, each realization within the ensembles used the same couplings.) (b) The fluctuations of the five curves in (a) about the average of those five curves, $\overline{H(\tau)}$.

Figure 7

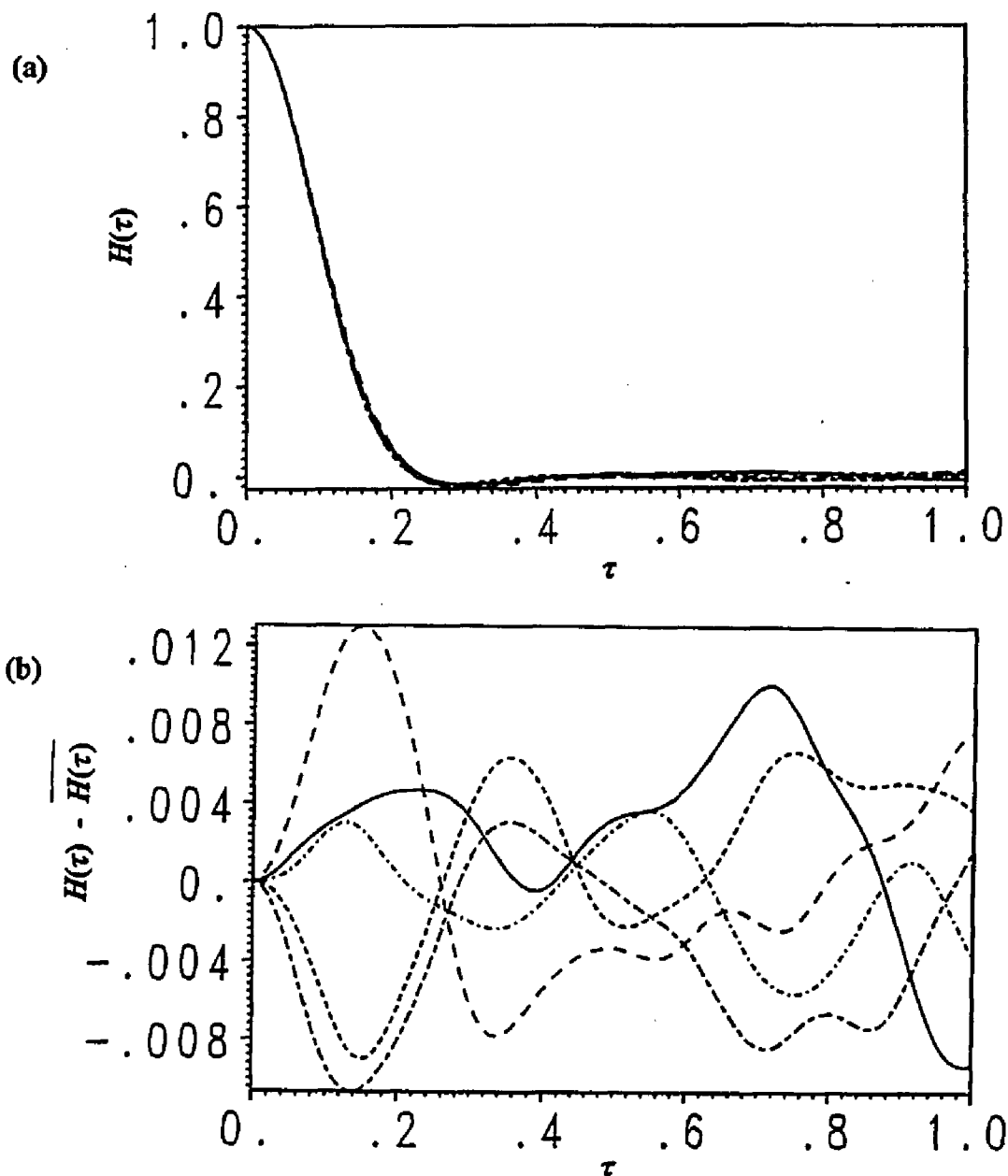


Figure 7. (a) $H(\tau)$ for five different ensembles ($R = 512$ for each) of an $N = 96$ Bethe system; each ensemble used a different set of random coupling coefficients. (But, as always, each realization within the ensembles used the same couplings.) (b) The fluctuations of the five curves in (a) about the average of those five curves, $\overline{H(\tau)}$. Compared with Fig. 6b, these fluctuation levels indicate that the primary source of fluctuations is finite- N rather than finite- R .

4. Estimate of numerical operations

The algorithm used for this dissertation stores only the nonzero coupling coefficients and calculates only the nonzero terms in the differential equations. Evaluation of the full-system time derivatives for an ensemble of R realizations requires $O(16RN^2/3 + 4RN)$ numerical operations each timestep (using a second-order Runge-Kutta method).

V. APPLICATION OF THE CDS TO THE BETCHOV SYSTEM

A. The decimated system	41
1. <i>Sample set</i>	41
2. <i>Stochastic forces</i>	42
(a) <i>Statistical interpolation: q^*</i>	43
3. <i>Statistical constraints</i>	44
(a) <i>Constraint set I</i>	45
(b) <i>Constraint set II</i>	48
(c) <i>General remarks about sets of constraints</i>	48
4. <i>General parameters in numerical studies</i>	49
5. <i>Estimate of statistical fluctuations</i>	50
6. <i>Estimate of numerical operations</i>	50
B. Results using constraint set I	55
1. <i>General results</i>	55
2. <i>Effects of the constraints</i>	64
(a) <i>Mean stochastic force constraint</i>	64
(b) <i>Mean energy constraint</i>	65
(c) <i>Force variance constraint</i>	65
(d) <i>Unequal-time constraints</i>	66
C. Results using constraint set II	73
1. <i>General results</i>	73
2. <i>Effects of the constraints</i>	83
(a) <i>Mean stochastic force constraint</i>	83
(b) <i>Equal-time force-variable constraint</i>	85
(c) <i>Unqual-time force-variable constraints</i>	85

A. The decimated system

1. *Sample set*

First, decimate the system: Replace the full set of variables $\{x_i \mid i=1,2,\dots,N\}$ with a much smaller sample set of variables

$\{x_i \mid i=1,2,\dots,S\}$ (where $S \ll N$). Because all the variables in the full Betchov system are statistically similar, the choice of sample set variables is completely arbitrary. Further, because of the random couplings in the Betchov system, it suffices to generate an independent set of $4S^2/9$ couplings. Numerical studies have showed no statistical difference between generating $4S^2/9$ independent couplings and extracting the sample-set couplings from a previously-generated full set of $4N^2/9$ couplings. Studies also indicated that S must be at least $O(20)$ to prevent spurious effects from fluctuations in random couplings.

Second, modify the system of ODE's to reflect its reduction from a set of N equations to a set of S equations. The original full-system ODE's [Eq. (024)] are replaced by the decimated-system equations

$$\frac{dx_i}{dt} = \sum_{j,k=1}^S C_{ijk} x_j x_k + q_i(t) \quad \text{for } i=1,2,\dots,S. \quad (16)$$

Each realization in the ensemble of decimated Betchov systems is one of these generalized-Langevin-like S -variable systems.

2. Stochastic forces

Each stochastic force q_i represents the statistical effects of couplings of variable x_i to variables outside the sample set, specifically

$$q_i(t) \leftrightarrow \sum_{j,k}^N{}' C_{ijk} x_j(t) x_k(t) ; \quad (17)$$

the symbol Σ' indicates a sum over all j and k such that at least one of

the two indices is greater than S . Since there are $4N^2/9$ coupling coefficients in the full system whose first indices are chosen at random, each variable couples to $O(N)$ others. The exact number of variables that any one couples to varies because N is finite.

(a) *Statistical interpolation: q^**

The sum in Eq. (17) is statistically similar to the following sum of sample set variables:

$$q_i^* = \left[\frac{N-S}{S} \right]^{1/2} \sum_{j,k=1}^S C_{ijk} x_j x_k \quad (18)$$

The factor $[(N-S)/S]^{1/2}$ is the weighting in the statistical interpolation; it gives each term in Eq. (18) the same weight as the corresponding $O(N/S)$ terms in Eq. (17). Specifically, it makes the mean squares of Eq. (18) and Eq. (17) equal, as will be shown:

Assume C_{ijk} , x_j , x_k are independent unit Gaussian random variables for all $\{i,j,k\}$. Then

$$\begin{aligned} \left\langle \left(\sum_{j,k=1}^S C_{ijk} x_j x_k \right)^2 \right\rangle &= \sigma_{N-S} \langle C_{ijk}^2 \rangle \langle x_j^2 \rangle \langle x_k^2 \rangle \\ &= \sigma_{N-S} \end{aligned}$$

where σ_{N-S} is the number of terms in the Σ' summation. Similarly,

$$\begin{aligned} \langle q_i^{*2} \rangle &= w_i^2 \sigma_S \langle C_{ijk}^2 \rangle \langle x_j^2 \rangle \langle x_k^2 \rangle \\ &= w_i^2 \sigma_S \end{aligned}$$

where σ_S is the number of terms in the summation and w_i is the statistical interpolation weighting.

For the (full) Betchov system, each variable has N terms in the summation in its time derivative (within fluctuations caused by finite N). Therefore $\sigma_{N-S} = (N-S)$ and $\sigma_S = S$. Thus

$$\begin{aligned} \langle q_i^{*2} \rangle &= \sum_{j,k}^N C_{ijk} x_j(t) x_k(t) \\ \Rightarrow w_i^2 \sigma_S &= \sigma_{N-S} \\ w_i &= [\sigma_{N-S}/\sigma_S]^{1/2} \\ &= \left[\frac{N-S}{S} \right]^{1/2} . \end{aligned}$$

3. Statistical constraints

As an example of a statistical constraint, consider the conservation of mean energy. Since E is conserved in the full Betchov system, so is $\langle E \rangle$. It is desirable, then, that a similarly-defined $\langle E_{\text{CDS}} \rangle$ should be conserved in the decimated system. This quantity $\langle E_{\text{CDS}} \rangle$ can be made constant by employing a statistical constraint:

$$\begin{aligned} \frac{d}{dt} \langle E_{\text{CDS}} \rangle &= 0 \\ \frac{d}{dt} \left\langle \frac{1}{2} \frac{N}{S} \sum_{i=1}^S x_i^2 \right\rangle &= \end{aligned}$$

$$\left\langle \frac{N}{2S} \sum_{i=1}^S \left[2x_i \frac{dx_i}{dt} \right] \right\rangle =$$

$$\left\langle \frac{N}{S} \sum_{i=1}^S \left[x_i \left[\sum_{j,k=1}^S C_{ijk} x_j x_k + q_i \right] \right] \right\rangle = 0 . \quad (19)$$

The factor N/S in the definition of E_{CDS} allows direct numerical comparison with E . By the construction of the Betchov coupling coefficients, the double sum in Eq. (19) is zero; this leaves

$$\left\langle \sum_{i=1}^S x_i(t) q_i(t) \right\rangle = 0 . \quad (20)$$

(a) *Constraint set I*

In constraint set I, four types of constraints are enforced. The first type constrains the system-averaged mean of the forces:

$$\left\langle \frac{1}{S} \sum_{i=1}^S q_i(t) \right\rangle = \left\langle \frac{1}{S} \sum_{i=1}^S q_i^*(t) \right\rangle , \quad (21)$$

where $q_i^*(t)$ is defined by Eq. (18). The second type constrains the system-averaged variance of the forces:

$$\left\langle \frac{1}{S} \sum_{i=1}^S \left[q_i(t) - \langle q_i(t) \rangle \right]^2 \right\rangle = \left\langle \frac{1}{S} \sum_{i=1}^S \left[q_i^*(t) - \langle q_i^*(t) \rangle \right]^2 \right\rangle \quad (22)$$

The third type constrains the two-time moments of the stochastic forces. Specifically, it constrains the system-averaged product of the current

forces with the forces at other times:

$$\left\langle \frac{1}{S} \sum_{i=1}^S q_i(t) q_i(t') \right\rangle = \left\langle \frac{1}{S} \sum_{i=1}^S q_i^*(t) q_i^*(t') \right\rangle \quad (23)$$

Because the numerical integration algorithm is primarily explicit (see §IVA3 for details), $q_i(t')$ and $q_i^*(t')$ for $t' > t$ are unknown. In general, somewhere between 2 and 10 t' points are used; these time-history points are spread out to span backwards at least one decorrelation time for most runs. Details are discussed in the results section (§VB).

These first three constraint-types constrain moments of the stochastic forces. The three system-averaged constraints were found to serve as well as similar constraints on the moments of the individual stochastic forces [e.g., $\langle q_i(t) \rangle = \langle q_i^*(t) \rangle$, etc.]; this reduced the number of constraints to apply by a factor of S . Off-diagonal constraints (moments of variables with unequal indices) were found to have little effect. [For example, $\langle q_i q_j \rangle = \langle q_i^* q_j^* \rangle$, etc.]

The fourth type of constraint is based on conservation of mean, decimated-system energy. Rather than the constraint derived in Eq. (19), a constraint based specifically on the finite time-differencing in the numerical ODE solution algorithm is used. The reason for this modification is that Eq. (19) allows a drift in the energy which is N/S times the error in the finite differencing; at strong decimation ($N/S \gg 1$), this error becomes significant. The modified constraint is formally expressed as

$$\frac{1}{h} \left\langle E_{\text{CDS}}(t+h) - E_{\text{CDS}}(t) \right\rangle = 0 ; \quad (24)$$

h is the numerical timestep. Eq. (24) and Eq. (15), together with the definition of E_{CDS} , yield the energy constraint:

$$\left\langle \frac{N}{2S} \sum_{i=1}^S \left\{ \left[x_i + \frac{1}{2} [k_{1i} + k_{2i}] \right]^2 - x_i^2 \right\} \right\rangle = 0 .$$

In this and other expressions in this paper, all time arguments are t unless otherwise noted. The time derivatives in k_{1i} and k_{2i} are evaluated using the decimated system equations, Eq. (16), to yield

$$\begin{aligned} \left\langle \frac{N}{2S} \sum_{i=1}^S \left\{ \left[x_i + \frac{h}{2} \left[\sum_{j,k=1}^S C_{ijk} x_j x_k + q_i(t) \right. \right. \right. \right. \\ + \sum_{j,k=1}^S C_{ijk} \left\{ \left[x_j + h \left[\sum_{l,m=1}^S C_{jlm} x_l x_m + q_j(t) \right] \right] \times \right. \\ \left. \left. \left[x_k + h \left[\sum_{l,m=1}^S C_{klm} x_l x_m + q_k(t) \right] \right] \right\} + \right. \\ \left. \left. \left. \left. q_i(t+h) \right] \right] \right]^2 - x_i^2 \right\} \right\rangle = 0 . \quad (25) \end{aligned}$$

In Eq. (25), $\{q_i(t) | i=1,2,\dots,S\}$ is assumed to be known, and $\{q_i(t+h) | i=1,2,\dots,S\}$ is to be adjusted to satisfy this constraint. This is also true for the other constraints.

(b) *Constraint set II*

In constraint set II, two types of constraints are enforced. The first type constrains the system-averaged mean of the forces:

$$\left\langle \frac{1}{S} \sum_{i=1}^S q_i(t) \right\rangle = \left\langle \frac{1}{S} \sum_{i=1}^S q_i^*(t) \right\rangle, \quad (26)$$

where $q_i^*(t)$ is defined by Eq. (18). This is the same as Eq. (21).

The second type constrains the stochastic forces against the system variables:

$$\left\langle \frac{1}{S} \sum_{i=1}^S q_i(t) x_i(t') \right\rangle = \left\langle \frac{1}{S} \sum_{i=1}^S q_i^*(t) x_i(t') \right\rangle. \quad (27)$$

For $t = t'$, the righthand side of Eq. (27) is zero because of the construction of the Betchov coupling coefficients (buried in the definition of q^* , which involves a sum over couplings). In this case, this constraint is just the time-derivative-based $\langle E \rangle$ conservation constraint described at the beginning of the section [Eq. (20)]. As in constraint set I, system-averaged constraints rather than constraints on individual forces are used. Again as in constraint set I, only time *history* constraints for which $t' < t$ are enforced. In general, somewhere between 4 and 20 t' points are used; these time-history points are spread out to span backwards at least one decorrelation time for most runs. Details are discussed in the results section (§VC).

(c) *General remarks about sets of constraints*

The effect of the constraints is not simply the sum of their

individual effects. Constraints have synergistic effects when used in combination. Furthermore, it is possible to design sets of constraints which are mutually incompatible. For example, if the partial derivatives of two constraint functions with respect to the stochastic forces are the same, the matrix procedure to enforce the constraints (see §III D 3) will produce a singular matrix. Table I lists constraint sets I and II for the reader's reference.

4. General parameters in numerical studies

In all of the results in this dissertation, the full Betchov system to be studied (specified by its size, N) is decimated to a system of $S = 32$ variables, with $O(4S^2/3) = 1365$ nonzero coupling coefficients. As in the full-system solution described in §IV C, there were $R = 128$ realizations of the system in the ensemble. If the full system was decimated to a system with significantly fewer than 32 variables, the fluctuations in the random couplings in the decimated system produced significant errors. (Note that the system-averaged constraints specified in §III C 1 rely on every variable coupling to approximately S others. If S is too small, this approximation is bad.) As in the full-system solution, the timestep in the Runge-Kutta algorithm was chosen so that there were at least $O(30)$ steps in the decorrelation time interval. Unless otherwise stated, the times constrained against each other in the two-time constraints were spaced out by a sufficient number of timesteps so that the maximum of the time interval $|t - t'|$ roughly spanned the decorrelation time.

5. Estimate of statistical fluctuations

Even more than in the full system, the biggest source of fluctuations is the finite size of the decimated system, S , for the same reason mentioned concerning the full system. Figure 8 shows calculations of $H_{\text{CDS}}(\tau)$ and its fluctuations for five different sets of 1365 random couplings, all for a 128-realization ensemble of a 32-variable decimated system. The autocorrelation function is defined as

$$H_{\text{CDS}}(\tau) = \frac{1}{S} \sum_{i=1}^S \langle x_i(t) x_i(t+\tau) \rangle,$$

where t is a fixed time.

Again, the fluctuations caused by the finite ensemble size are smaller. Figure 9 shows $H(\tau)$ and its fluctuations for five 512-realization ensembles of 32-variable decimated systems using the same five different sets of 1365 random couplings as in the 128-realization case. Again the ratio of these fluctuations to those for the 128-realization case indicates that finite S , not finite R , is the primary cause of fluctuations.

6. Estimate of numerical operations

Evaluation of the decimated-system time derivatives requires $O(16RS^2/3 + 9RS)$ operations (the additional $5RS$ operations over the number for a full system of size S are for adding the stochastic forces to the ODE's). Each timestep, the stochastic Newton-Raphson procedure requires $O(17RS^2 + 41RSC + 2RSC^2 + C^3)$ numerical operations for each iteration: $O(17RS^2)$ to calculate q^* , $O(41RSC)$ to compute \mathbf{F} and \mathbf{F} ,

$O(2SC^2)$ to set up G , and $O(C^3)$ to solve the G -matrix equation (see §III D3a and §III D3b). Generally the procedure converges in less than five iterations, and it almost always converges in less than ten iterations. For most of the cases discussed in this dissertation C was around ten, R was 128, and S was 32.

Assume $N^2 \gg N$, $S^2 \gg S$, $C < S$, $C \ll R$, and that 10 iterations of the Newton-Raphson procedure per timestep are needed; then the full and decimated systems require $O(16RN^2/3)$ and $O(175RS^2)$ numerical operations per timestep, respectively. As long as $N^2/S^2 > 175 \times 16/3$ (i.e., $N/S > 31$), the decimated system requires fewer operations than the full system. It is easy to see that for any reasonable relative values of N , S , and C , the decimated system requires fewer operations to solve than the full system. (Recall that the goal is to make N/S as high as possible.)

Table I

CONSTRAINT SETS AND SOME NOTED EFFECTS OF CONSTRAINTS

Set I[†]

Ia. $\frac{1}{S} \sum_{i=1}^S [q_i(t) - q_i^*(t)]$

Ib. $E(t+h) - E(t)$

Ic. $\frac{1}{S} \sum_{i=1}^S \left\{ [q_i(t) - \langle q_i(t) \rangle]^2 - [q_i^*(t) - \langle q_i^*(t) \rangle]^2 \right\}$

Id. $\frac{1}{S} \sum_{i=1}^S [q_i(t) q_i(t') - q_i^*(t) q_i^*(t')]$

Set II

IIa. $\frac{1}{S} \sum_{i=1}^S [q_i(t) - q_i^*(t)]$

IIb. $\frac{1}{S} \sum_{i=1}^S [q_i(t) x_i(t') - q_i^*(t) x_i(t')]$

Constraint	Noted effects
Ia	Prevents slow increase in $\langle q_i \rangle$ and $\langle q_i^* \rangle$ at $N/S = 100$.
Ib	Prevents $\langle E_{\text{CDS}} \rangle$ blowup.
Ic	Keeps variance of q_i from blowing up or collapsing.
Id	Gives correct $H(\tau)$ timescale. System sensitivity to exact number and spacing of t' points.
IIa	Slows $\langle E_{\text{CDS}} \rangle$ decay at strong decimation.
IIb	For $t = t'$, forces approximate $\langle E_{\text{CDS}} \rangle$ conservation. For $t \neq t'$, gives correct $H(\tau)$ timescale. System insensitivity to exact number and spacing of t' points.

[†] The quantity displayed here, when ensemble averaged and set equal to zero, defines the constraint

Figure 8

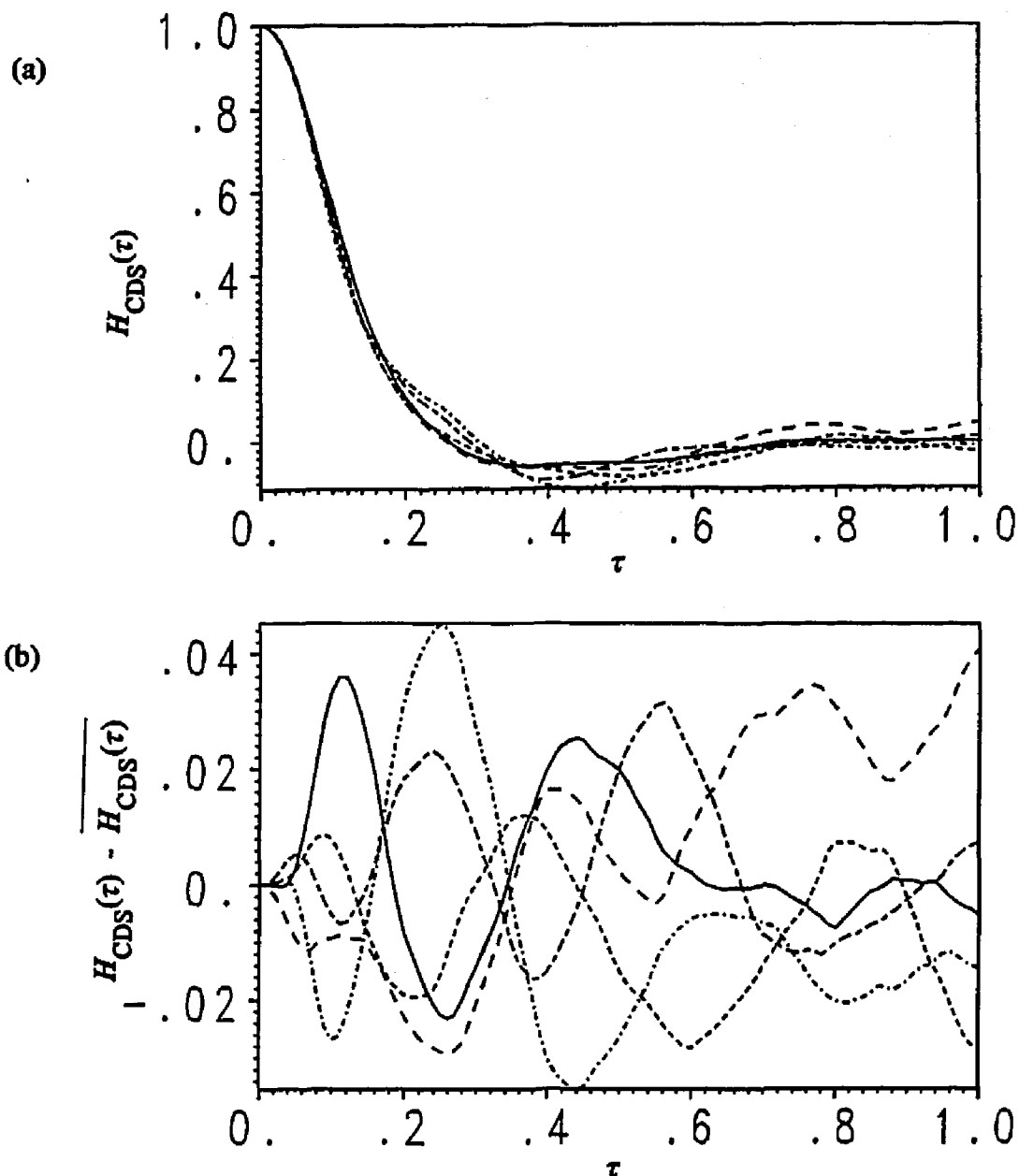


Figure 8. (a) $H_{\text{CDS}}(\tau)$ for five different ensembles ($R = 128$ for each) of an $S = 32$ system (decimated from $N = 96$) Betchov system; each ensemble used a different set of random coupling coefficients. (But, as always, each realization within the ensembles used the same couplings.) (b) The fluctuations of the five curves in (a) about the average of those five curves, $\overline{H_{\text{CDS}}(\tau)}$.

Figure 9

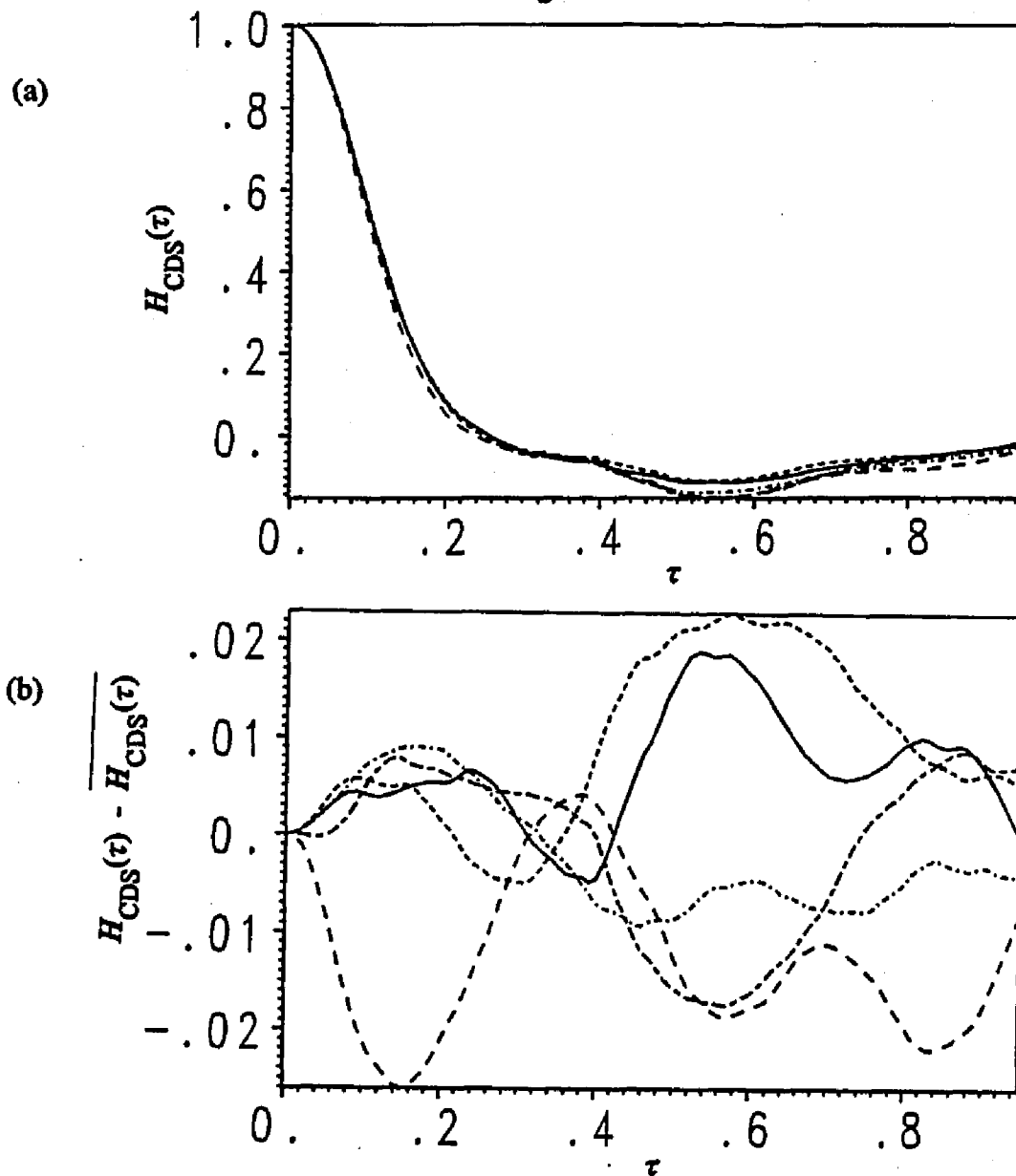


Figure 9. (a) $H_{\text{CDS}}(\tau)$ for five different ensembles ($R = 512$ for each) of an $S = 32$ system (decimated from $N = 96$) Betheov system under constraint set I; each ensemble used a different set of random coupling coefficients. (b) The fluctuations of the five curves in (a) about the average of those five curves, $\overline{H_{\text{CDS}}(\tau)}$. Comparison with Fig. 8b indicates that the primary source of fluctuations is finite- S rather than finite- R . Comparison with Figures 6 and 7 shows that the $S = 32$ size of the decimated yields higher fluctuations in random couplings than the $N = 96$ size of the full systems, both for $R = 128$ and $R = 512$.

B. Results using constraint set I

Constraint set I is listed in Table I. Some of the results from the following sections are also summarized in that table.

1. General results

As an indicator that the "turbulent" nature of the dynamics of the variables is not destroyed by the decimation, Fig. 10 shows a typical variable's time evolution in a typical realization of the decimated system. Of course, the exact dynamics of the full system are lost because many variables have been removed; this is no drawback since the primary interest is in the calculation of statistical properties of the system.

The isotropy of the Betchov system is not destroyed by the decimation; no variables in the decimated system become artificially dominant over any others. Figure 11 and Fig. 12 show $\langle x_i \rangle$ and $\langle x_i^2 \rangle$ for several i ; none are different from the others outside the level of statistical fluctuations. These plots also indicate the time stationarity of the decimated system; they show that the mean and variance of the variables do not change beyond the level of statistical fluctuations as t increases.

Figure 10

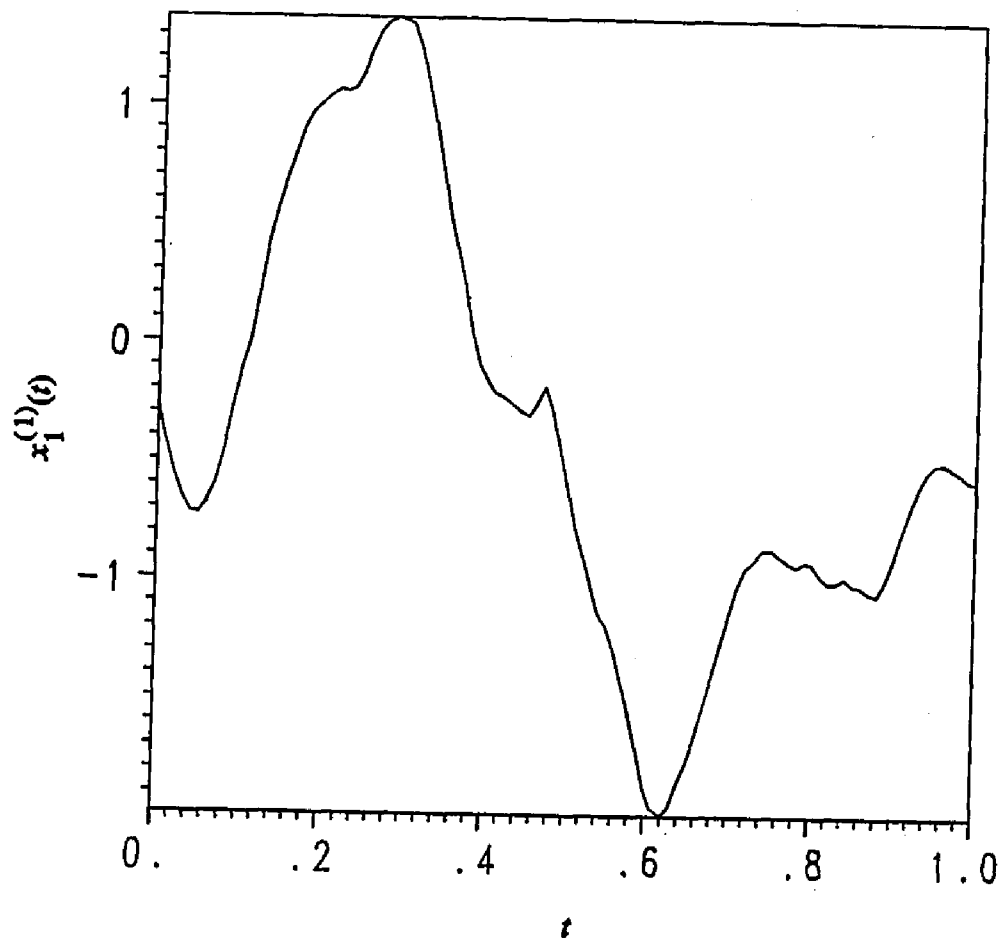


Figure 10. A single variable, x_1 , from a single realization of an $S = 32$ decimated Betchov system (decimated from $N = 96$) under constraint set I. There were 100 timesteps in the run, with 4 unequal-time constraints spaced out by 8 timesteps.

Figure 11

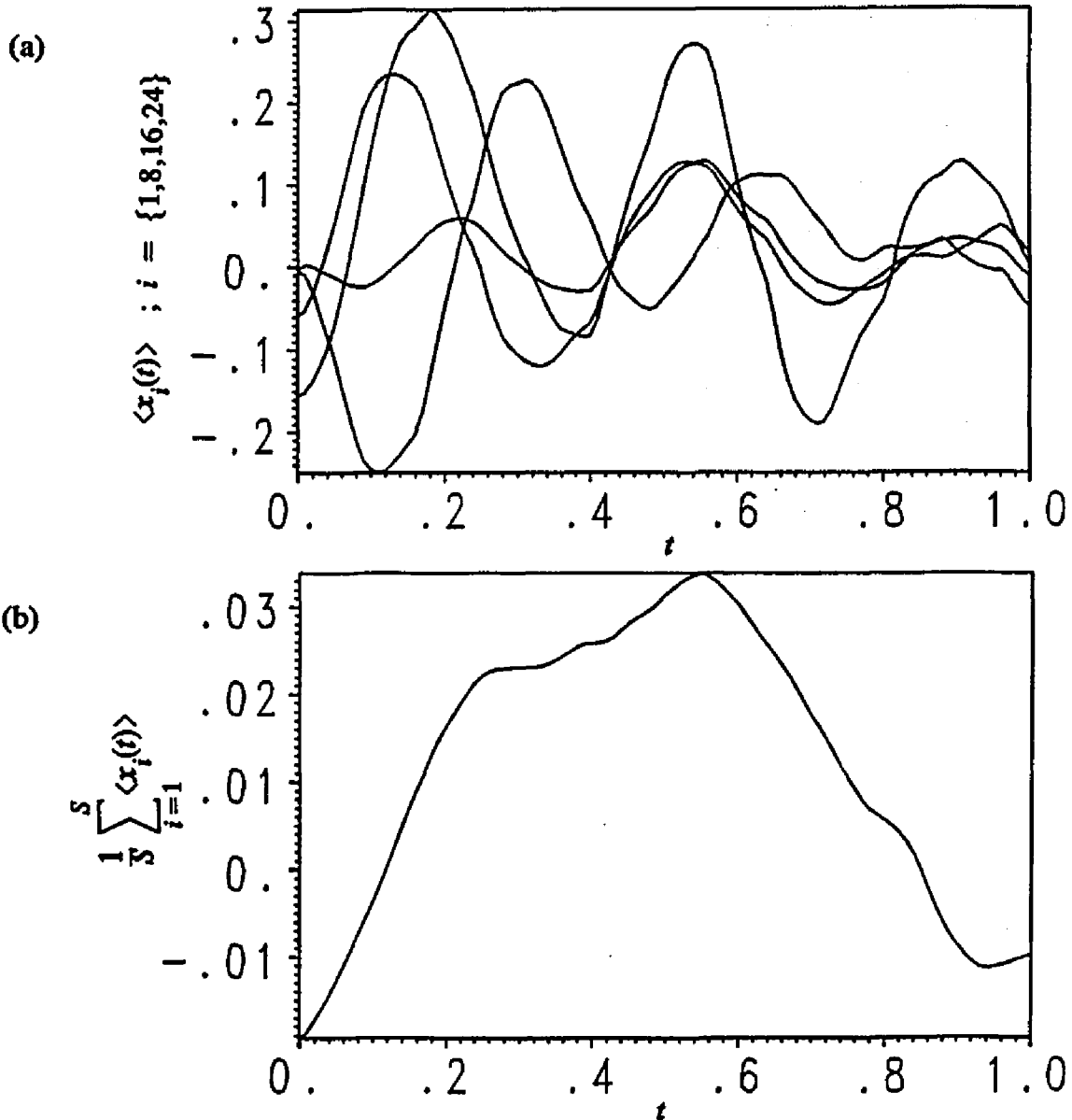


Figure 11. (a) The means of four different variables — $\langle x_1 \rangle$, $\langle x_8 \rangle$, $\langle x_{16} \rangle$, $\langle x_{24} \rangle$ — from an ensemble of $S = 32$, $N = 96$ decimated Betchov system under constraint set I. Note that no variable dominates any other. (b) The system-averaged mean of all the variables of that same realization of the decimated system. For both plots, $R = 128$; there were 100 timesteps in the run, with 4 unequal-time constraints spaced out by 8 timesteps.

Figure 12

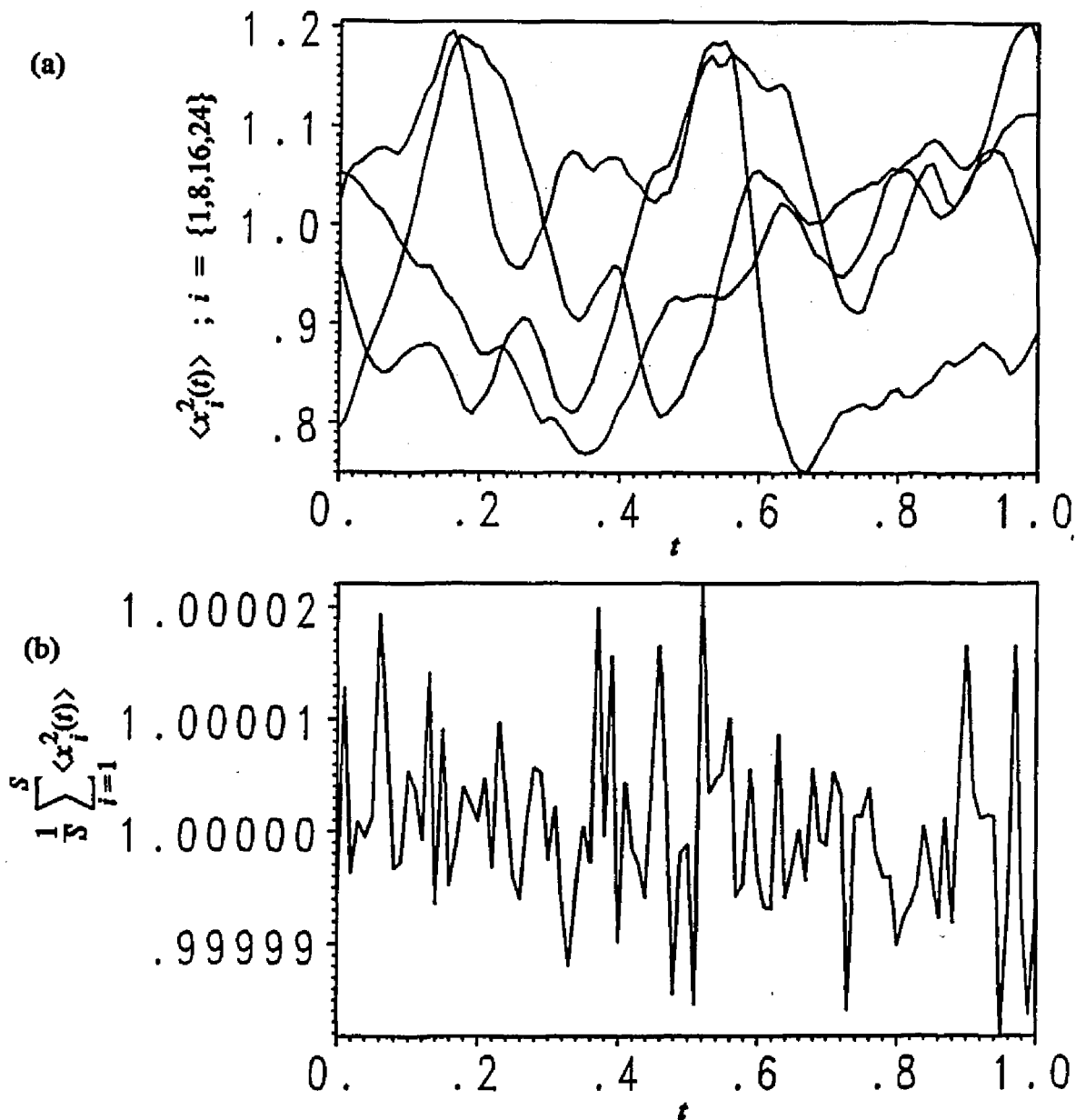


Figure 12. (a) The mean squares of four different variables — $\langle x_1^2 \rangle$, $\langle x_8^2 \rangle$, $\langle x_{16}^2 \rangle$, $\langle x_{24}^2 \rangle$ — from an ensemble of $S = 32$, $N = 96$ decimated Betchov system under constraint set I. Note that no variable dominates any other. (b) The system-averaged mean square of all the variables. For both plots, $R = 128$; there were 100 timesteps in the run, with 4 unequal-time constraints spaced out by 8 timesteps.

A test of the decimated system's ability to reproduce important statistical properties of the full system is the calculation of the autocorrelation function. Figures 13 through 16 show autocorrelation functions for decimated systems under constraint set I at various decimation strengths from $N/S = 33/32$ to $N/S = 100$. The DIA results are plotted for comparison of decorrelation time scales[†]; the full-system results are plotted for the values of N for which the full Betchov system was small enough to solve (affordably) numerically. The weaker decimation results are promising; the autocorrelation curves from the CDS, DIA, and full system are within statistical fluctuations of each other.

The striking problem with these results is the development of oscillations in $H_{\text{CDS}}(\tau)$ as N/S becomes large. These oscillations are visible in all decimated systems with these constraints with $N/S \geq O(10)$. Their maximum amplitude saturates at strong decimation, and they always damp out as τ increases. Furthermore, the half-period of the oscillations always matches the decorrelation time (as known from the DIA results). However, this phenomenon is definitely unacceptable and is certainly an artifice of the decimation scheme. It is the reason that constraint set II was developed; constraint set II eliminates the problem of the oscillations in H_{CDS} .

[†] Replacing τ in the equation for $H_{\text{DIA}}(\tau)$ [Eq. (B28)] with $\tau' = [3M\tau/N]^{1/2}$ shows that the timescale for $H_{\text{DIA}}(\tau)$ scales with $[1/N]^{1/2}$, while the shape of the curve remains the same for all N .

Figure 13

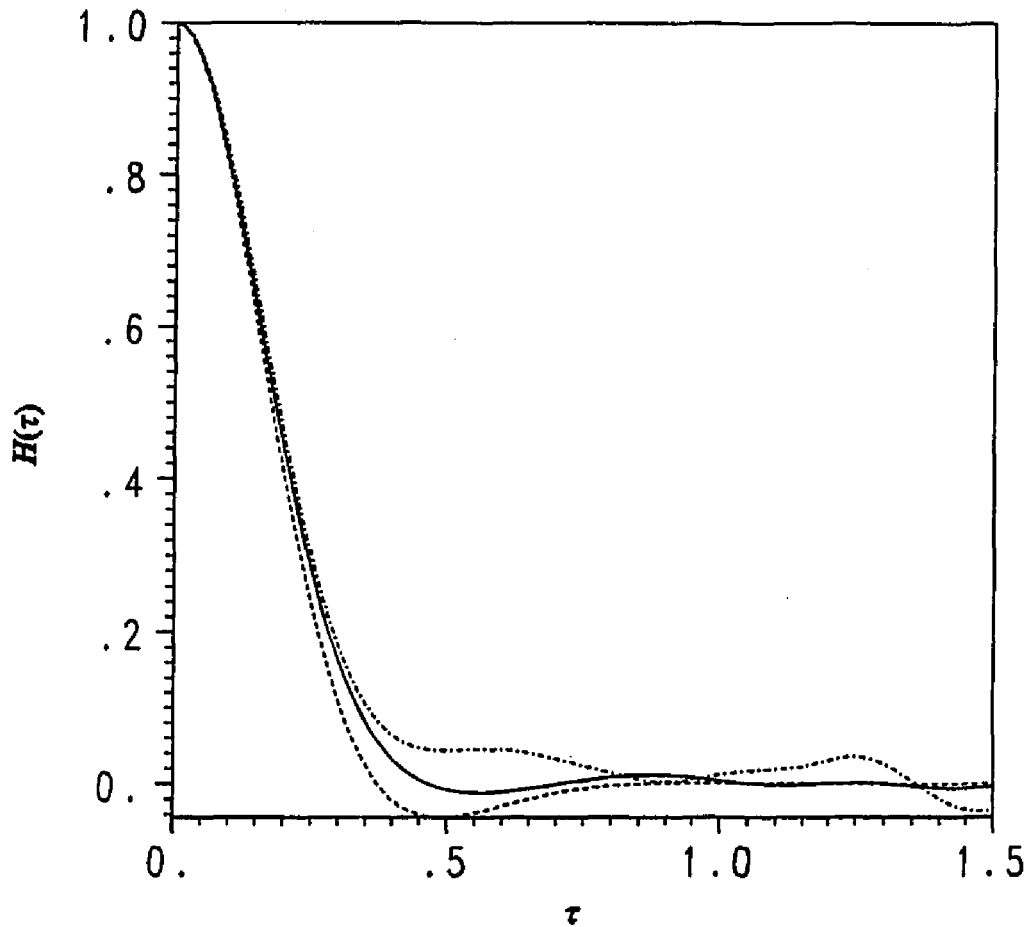


Figure 13. $H_{\text{CDS}}(\tau)$ for an $S = 32$, $N = 33$ decimated Betchov system under constraint set I (solid curve); $H_{\text{DIA}}(\tau)$ for $N = 33$ (dashed curve); $H(\tau)$ for a full $N = 33$ Betchov system (dot-dashed curve).

Figure 14

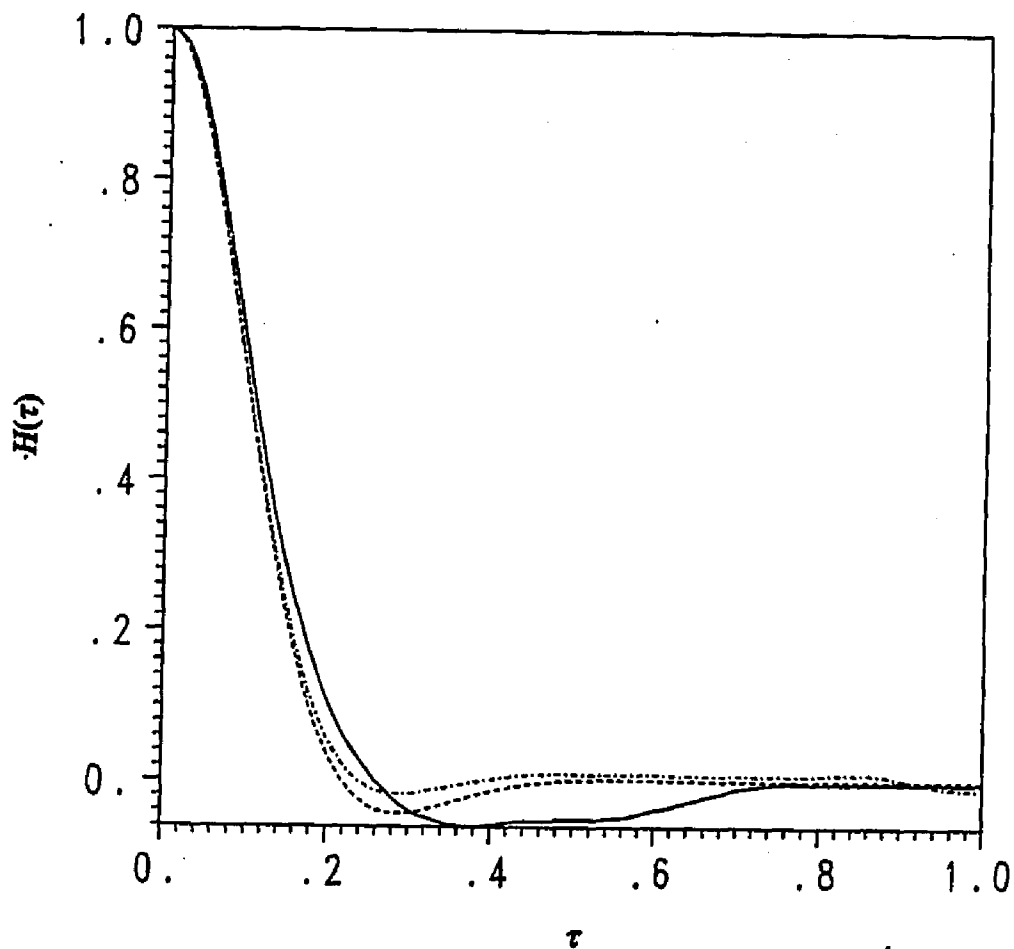


Figure 14. $H_{\text{CDS}}(\tau)$ for an $S = 32$, $N = 96$ decimated Betchov system under constraint set I (solid curve); $H_{\text{DIA}}(\tau)$ for $N = 96$ (dashed curve); $H(\tau)$ for a full $N = 96$ Betchov system (dot-dashed curve).

Figure 15

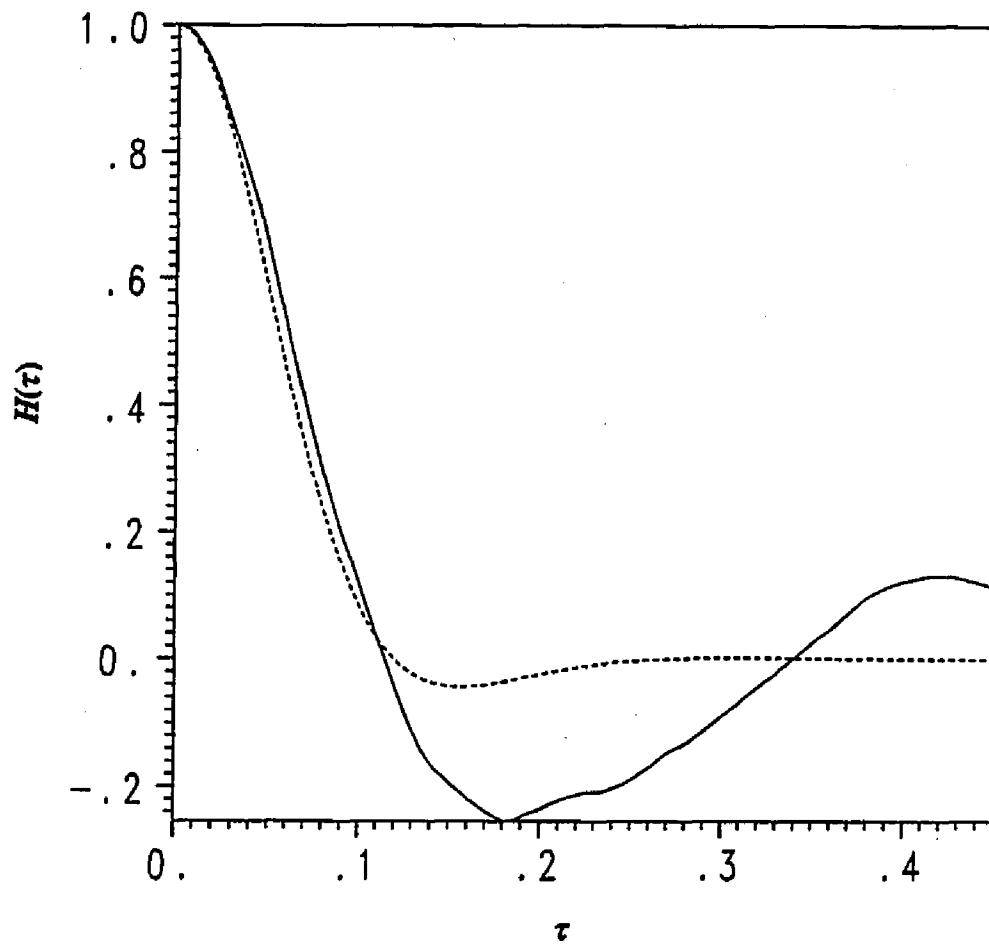


Figure 15. $H_{\text{CDS}}(\tau)$ for an $S = 32$, $N = 320$ decimated Betchov system under constraint set I (solid curve); $H_{\text{DIA}}(\tau)$ for $N = 320$ (dashed curve).

Figure 16

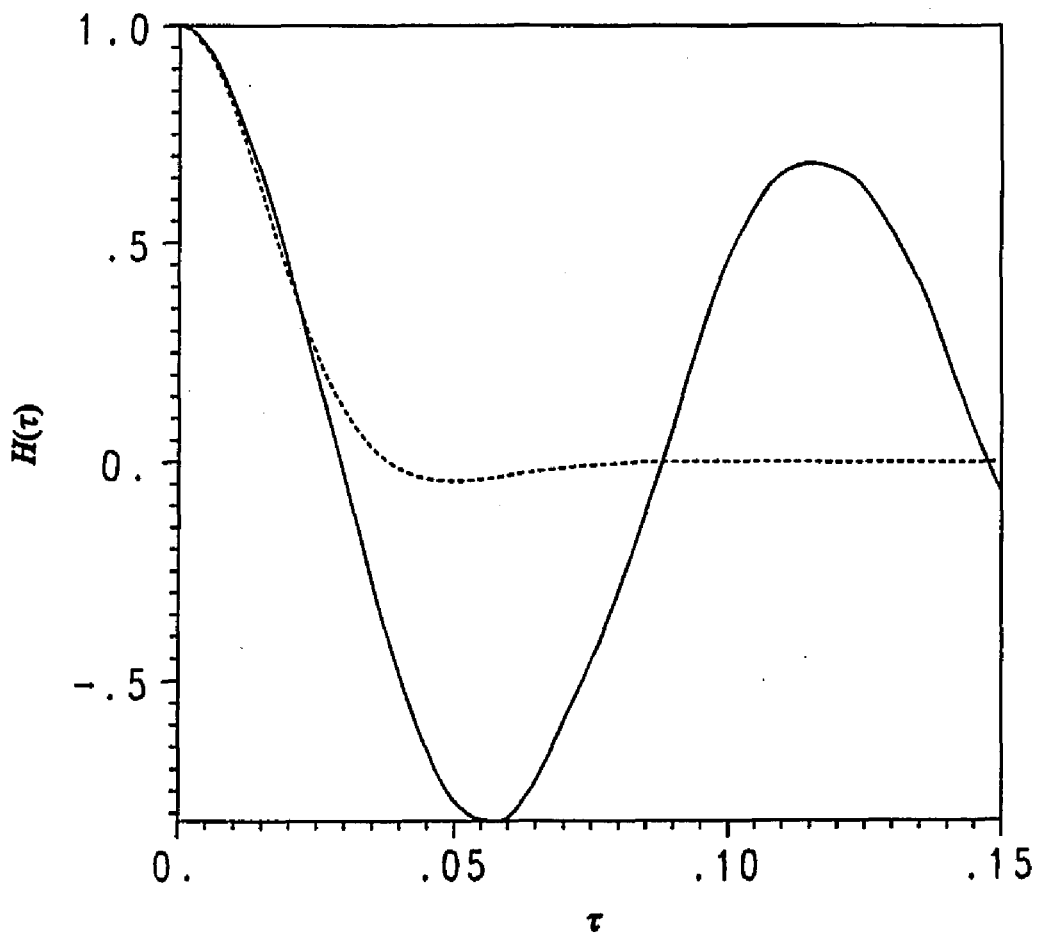


Figure 16. $H_{\text{CDS}}(\tau)$ for an $S = 32$, $N = 3200$ decimated Betchov system under constraint set I (solid curve); $H_{\text{DIA}}(\tau)$ for $N = 3200$ (dashed curve).

The cause of these oscillations is unknown, though seems likely that the unequal-time constraints are the culprits. It is virtually impossible to carefully study the role of these constraints in the oscillations, however, because of a second problem with the decimated system under constraint set I at strong decimation: The system fails to converge when too many unequal-time constraints are enforced. At $N/S = 100$, at most 3 unequal-time constraints can be successfully enforced; the Newton-Raphson procedure eventually fails to converge before enough time has elapsed to plot an adequately-long autocorrelation function curve.

2. Effects of the constraints

(a) Mean stochastic force constraint

The mean of q_i and q_i^* are zero within statistical fluctuations. This constraint [Eq. (21)] forces the two means to be equal, but not necessarily zero. At moderate decimation levels, such as $N/S = 3$, the effects of removing this constraint are unmeasurable. At stronger decimation, such as $N/S = 3200$, the effects are measurable (as a slow monotonic decrease in the system average of $\langle q_i \rangle$, for example); but the means of q_i and q_i^* do not wander significantly from zero. It was believed that this constraint would play an important role at much stronger decimation, so it was left in the program. Much stronger decimation never worked with constraint set I, though, so that could not be tested.

(b) Mean energy constraint

The mean energy constraint [Eq. (25)], as expected, causes exact conservation of $\langle E_{\text{CDS}} \rangle$. With $N = 96$, $S = 32$, $h = 0.01$ (numerical timestep), and 4 unequal-time constraints [Eq. (23)], removal of the mean energy constraint allows $\langle E_{\text{CDS}} \rangle$ to increase by a factor of 6.8 in the span of 6 timesteps. The constraints cannot be satisfied at the seventh timestep (the Newton-Raphson procedure fails to converge), at which point the numerical solution stops. In contrast, the full-system $N = 96$ run with the same timestep conserved $\langle E \rangle$ within 1.25 percent for the entire run of 100 steps.

With $N = 3200$, $S = 32$, and $h = 7.5 \times 10^{-4}$, removal of the mean energy constraint allows $\langle E_{\text{CDS}} \rangle$ to increase by a factor of 5 in one timestep. The constraints cannot be successfully enforced at the second timestep. Note that this h would allow 67 timesteps in the decorrelation interval, while the h from the previously-mentioned $N = 96$, $S = 32$ run allows only 30 timesteps in that system's decorrelation interval. It is clear that the mean energy constraint is more important for strong decimation with constraint set I. This is reasonable, since the stochastic forces play a bigger role in the ODE's as N/S increases.

(c) Force variance constraint

The system-average stochastic force variance constraint [Eq. (22)] not only forces the system average of the variances of q_i and q_i^* to be equal, but also keeps the variance of q_i from blowing up or collapsing. With $N = 96$, $S = 32$, $h = 0.01$, and 4 unequal-time constraints [Eq. (23)], removal of the variance constraint allows the system average q -variance

$$\left\langle \frac{1}{S} \sum_{i=1}^S [q_i(t) - \langle q_i(t) \rangle]^2 \right\rangle$$

to increase by a factor of 50 in the span of 9 timesteps. The system fails to converge at the tenth timestep.

With $N = 3200$, $S = 32$, and $h = 7.5 \times 10^{-4}$, removal of the variance constraint causes the system-average q -variance to plunge to zero in one timestep. The system fails to converge at the second timestep. Since this h is a smaller fraction of the decorrelation interval than was h in the $N = 96$ run and this run failed in *fewer* timesteps, it is clear that the variance constraint plays a bigger role for strong decimation with constraint set I.

(d) *Unequal-time constraints*

With no unequal-time constraints [Eq. (23)], the decay of the autocorrelation function $H_{\text{CDS}}(\tau)$ is radically altered. The function decays in a decorrelation interval closer to that of an *undecimated* Betchov system of size S than a Betchov system decimated from some $N > S$ to a system of size S . Figures 17 and 18 show this effect for $N/S = 3$ and $N/S = 100$.

Figure 17

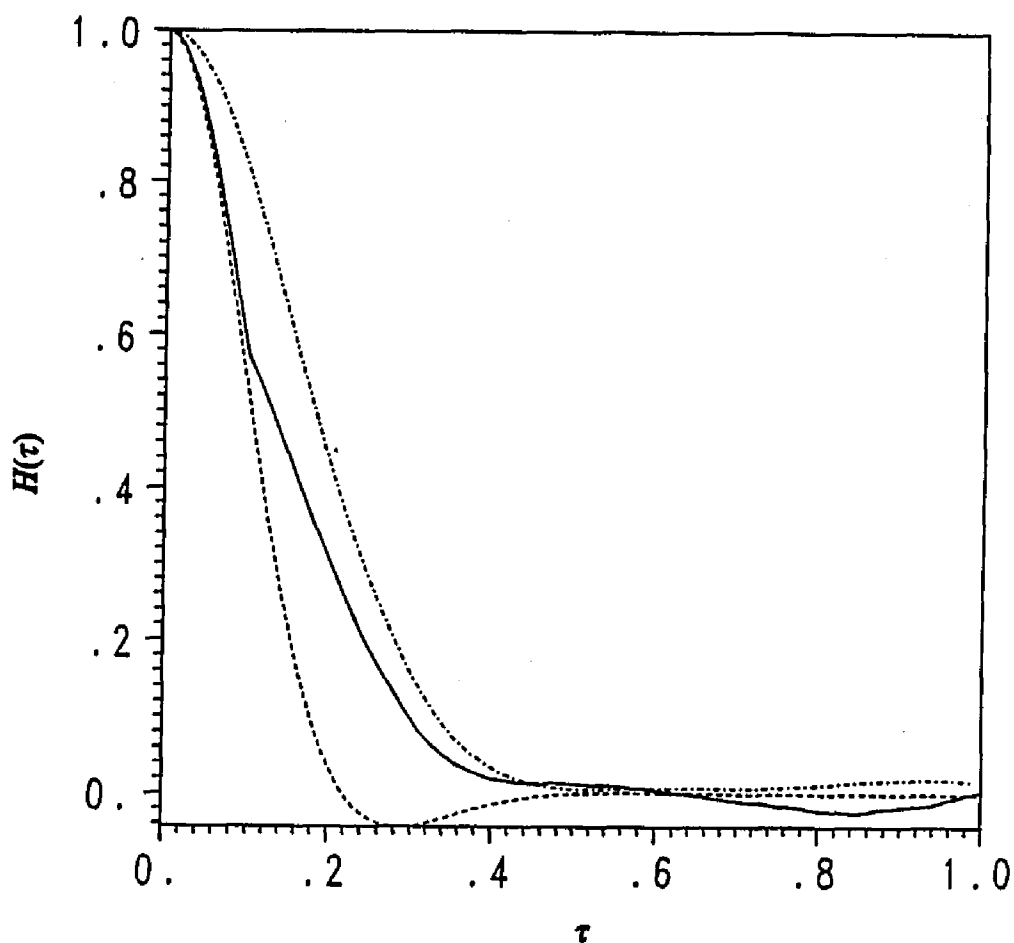


Figure 17. $H_{\text{CDS}}(\tau)$ for an $S = 32$, $N = 96$ decimated Betchov system under constraint set I with the unequal-time constraints switched off at $t = 0.1$ (solid curve); $H_{\text{DIA}}(\tau)$ for $N = 96$ (dashed curve); $H(\tau)$ for a full $N = 32$ Betchov system (dot-dashed curve).

Figure 18

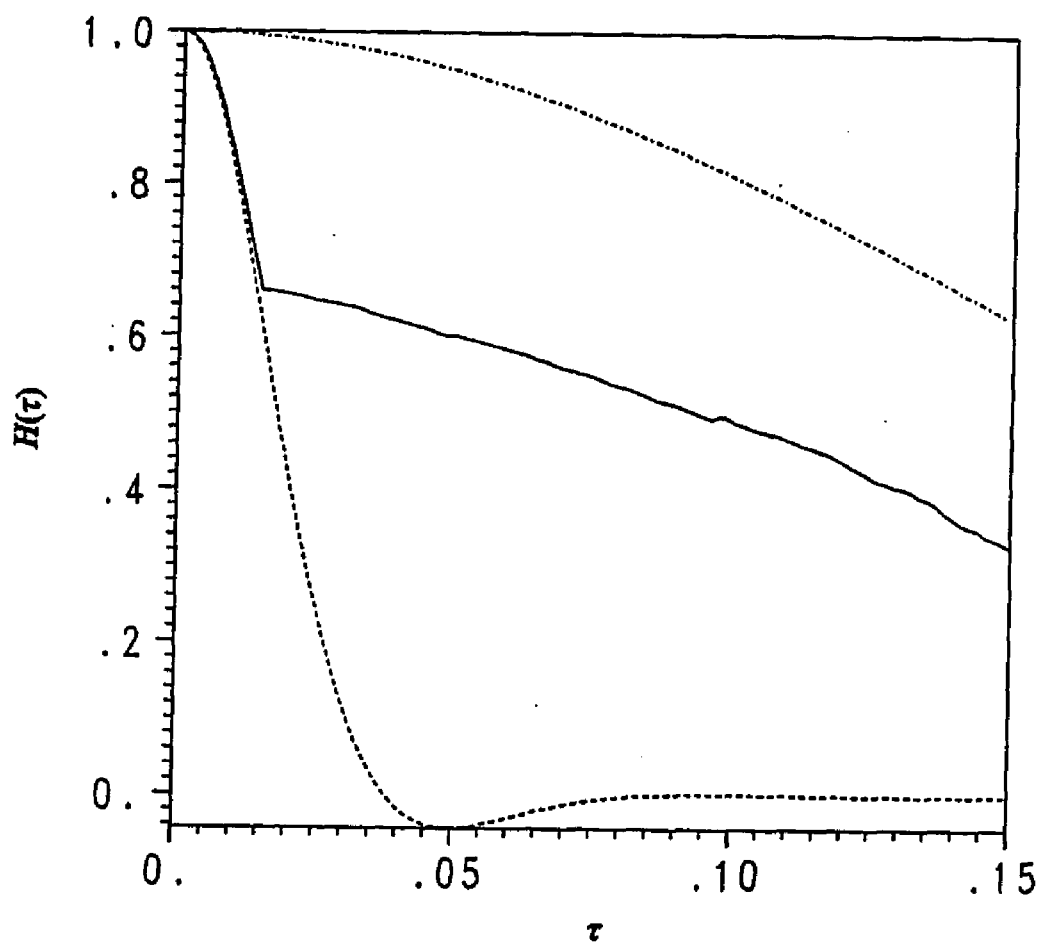


Figure 18. $H_{\text{CDS}}(\tau)$ for an $S = 32$, $N = 3200$ decimated Betchov system under constraint set I with the unequal-time constraints switched off at $t = 0.015$ (solid curve); $H_{\text{DIA}}(\tau)$ for $N = 3200$ (dashed curve); $H(\tau)$ for a full $N = 32$ Betchov system (dot-dashed curve).

The effects of changing the (nonzero) number and spacing between the unequal-time constraints are not entirely understood. Nonetheless, there are some comments worth making concerning the effect of the spacing between the unequal-time points $\{t', t'', \dots\}$ constrained against and the length of the maximal window $|t - t'|$.

First, consider the effects of adding additional unequal-time constraints to a system to extend the window while keeping the spacing between the unequal-time points the same. For $N/S = 3$ and for $N/S = 100$, this produces no noticeable effects, except for the earlier convergence failure at $N/S = 100$ mentioned in §VB1.

Second, consider the effects of adding additional unequal-time constraints to a system but decreasing the spacing between the unequal-time points to keep the size of the window unchanged. For $N/S = 3$, this causes a noticeable loss of time stationarity of the system. This can be seen in Fig. 19, which superimposes autocorrelation functions calculated from different base times in the run; for an exactly time stationary system, the curves would all overlap within statistical fluctuations. For $N/S = 100$, the only observable effect of this change of constraints was the aforementioned convergence failure problems. (But early convergence failure prevents making a plot like Fig. 19, so it is unknown whether this constraint change effects the time stationarity of the $N/S = 100$ system.)

Third, consider the behavior of a system whose window spans only a small fraction of the decorrelation interval. For $N/S = 3$, with the window spanning 25 percent of the decorrelation interval, there is a noticeable lack of time stationarity, as Fig. 20 shows; there is an indication of the development of oscillations in the autocorrelation

functions in Fig. 20, but this has not been studied enough to definitely conclude that.

Figure 19

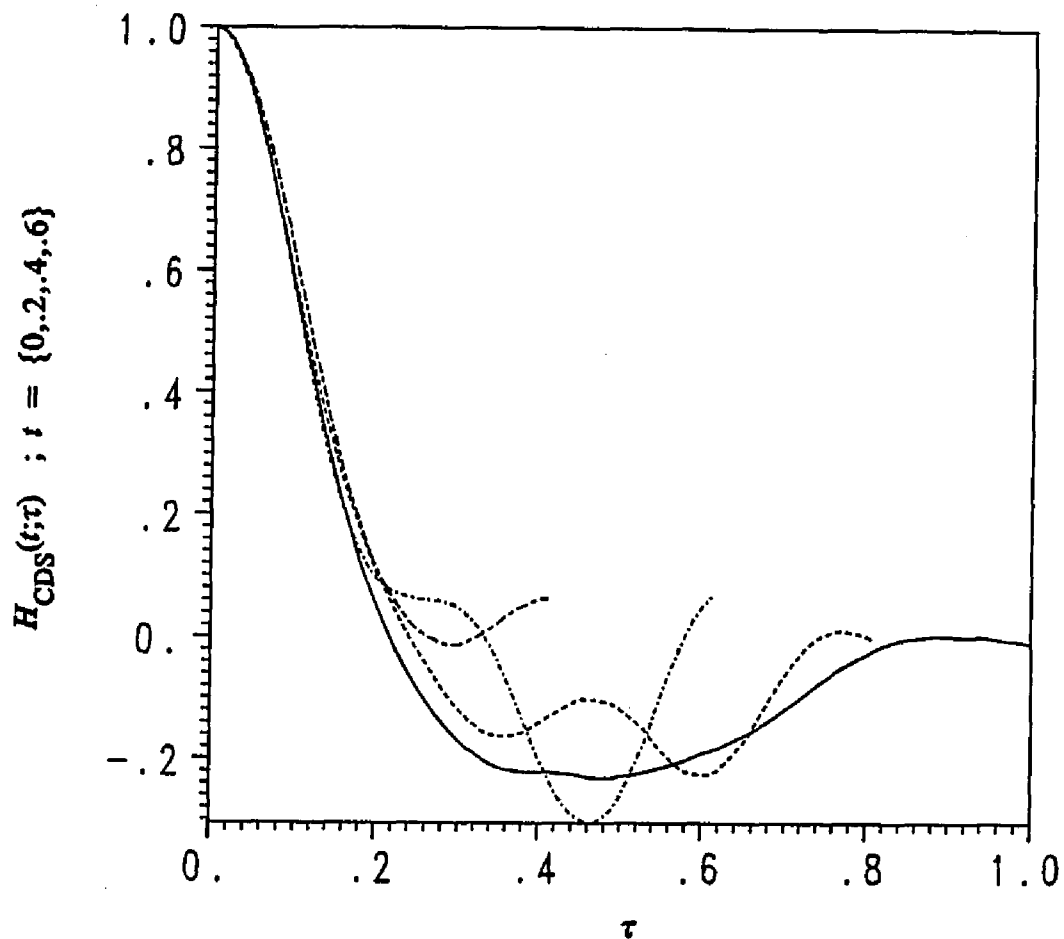


Figure 19. $H_{\text{CDS}}(t;\tau)$ for $t = \{0, .2, .4, .6\}$ with $S = 32$, $N = 96$, $R = 128$, 100 timesteps, and with 8 unequal-time constraints (constraint set I) spaced out by 4 timesteps. This is a modification of the parameters used to generate Fig. 13, which had 4 unequal-time constraints spaced out by 8 timesteps.

Figure 20

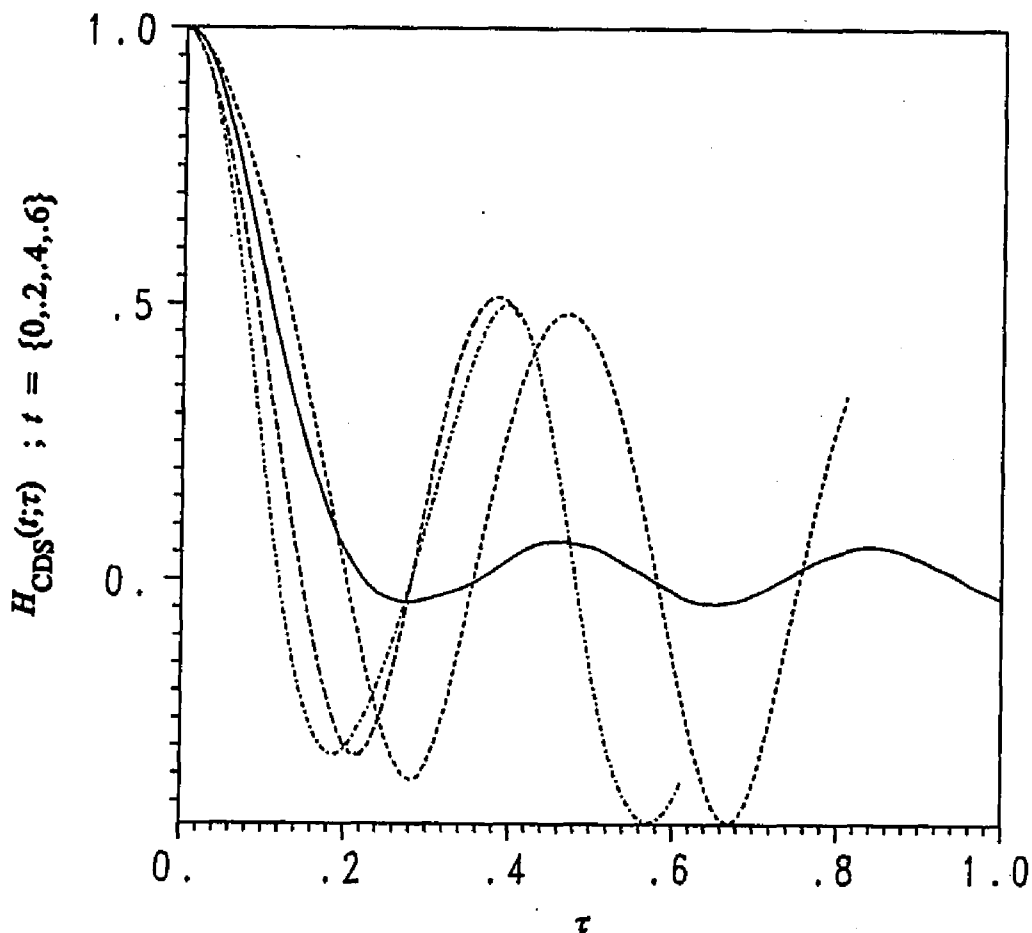


Figure 20. $H_{\text{CDS}}(t;\tau)$ for $t = \{0, .2, .4, .6\}$ with $S = 32$, $N = 96$, $R = 128$, 100 timesteps, and with 8 unequal-time constraints (constraint set I) spaced out by 8 timesteps. This is a modification of the parameters used to generate Fig. 13, which had 4 unequal-time constraints spaced out by 8 timesteps.

C. Results using constraint set II

Again, the reader is referred to Table I for a list the constraint set II. Some of the results from the following sections are summarized in that table.

1. General results

As with constraint set I, the "turbulence," isotropy, and time-stationarity of the Betchov system are not destroyed by decimation under constraint set II. These conclusions are supported by Fig. 21 Fig. 22, and Fig. 23.

Because constraint set II has no exact mean energy constraint like Eq. (25), the mean energy $\langle E_{\text{CDS}} \rangle$ does wander a bit as time evolves because of discretization errors. (Example: $\langle E_{\text{CDS}} \rangle$ varies by 1 percent for $N = 96$, $S = 32$, $h = .002$, 10 unequal-time constraints.) As mentioned before, the equal-time case of Eq. (27) is equivalent to the time-derivative-based energy constraint Eq. (20). With constraint set II, this wandering is always downward; the mean energy of the system decays as time evolves. This decay becomes more pronounced as N/S increases, and it is necessary to use increasingly small timesteps (relative to the decorrelation interval) to maintain desired $\langle E_{\text{CDS}} \rangle$ conservation. The Newton-Raphson procedure fails to converge if the equal-time case of Eq. (27) is replaced or supplemented by the exact energy conservation constraint from constraint set I [Eq. (25)].

Figure 21

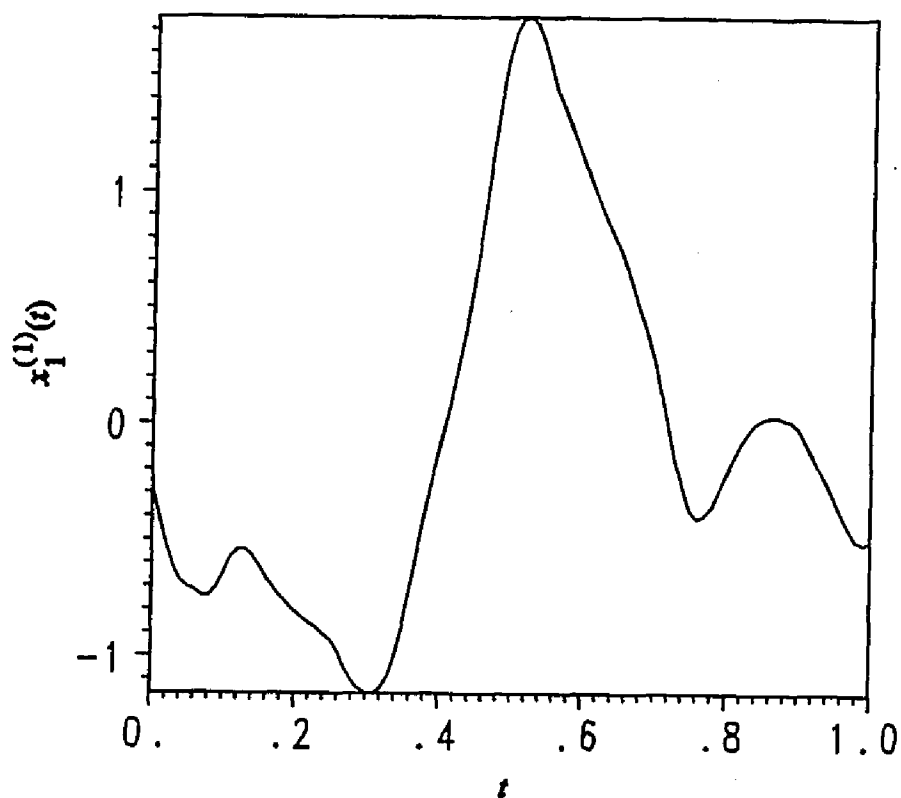


Figure 21. A single variable, x_1 , from a single realization of an $S = 32$ decimated Betchov system (decimated from $N = 96$) under constraint set II. There were 500 timesteps in the run, with 10 unequal-time constraints spaced out by 14 timesteps.

Figure 22

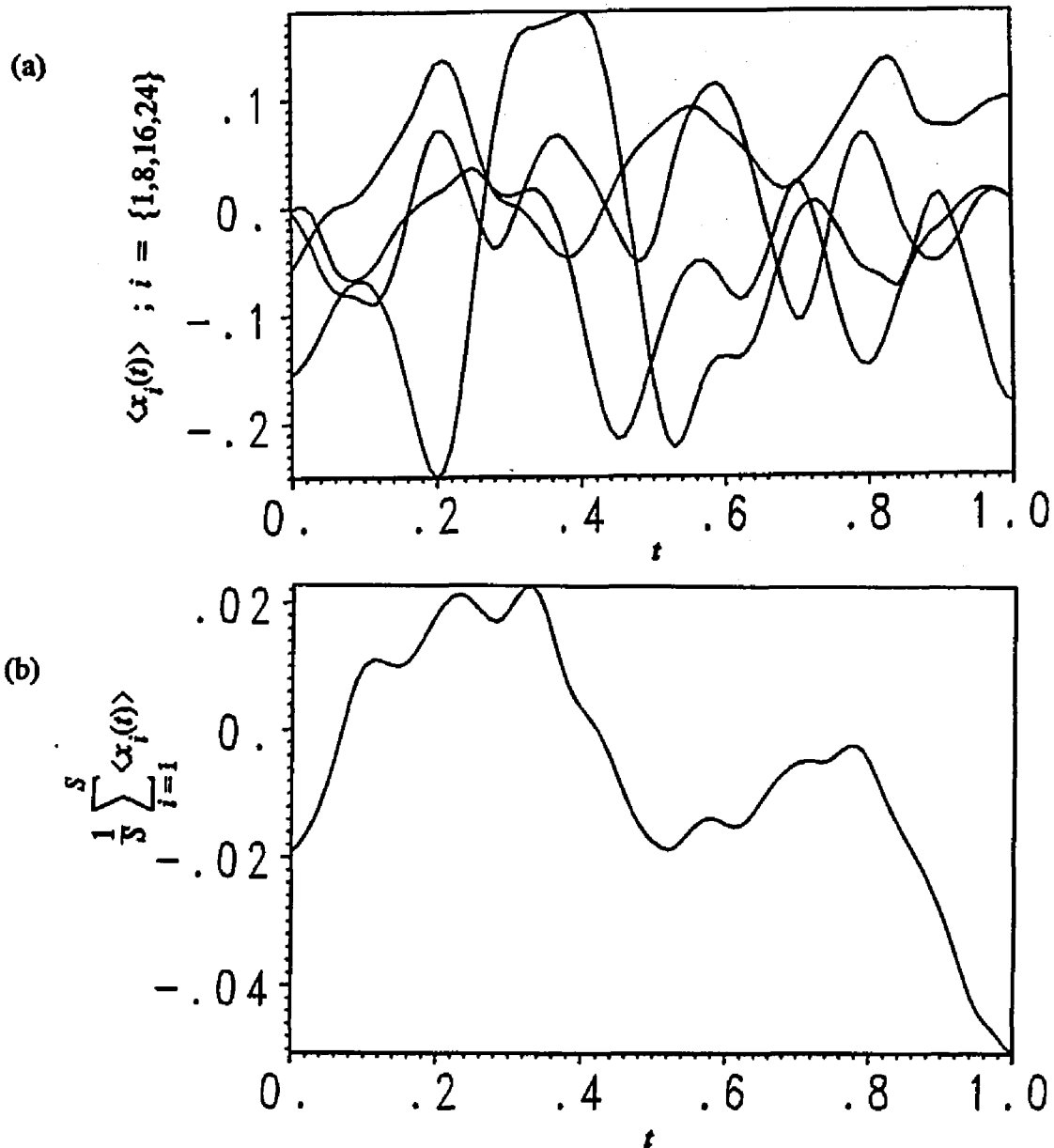


Figure 22. (a) The means of four different variables — $\langle x_1 \rangle$, $\langle x_8 \rangle$, $\langle x_{16} \rangle$, $\langle x_{24} \rangle$ — from an ensemble of $S = 32$, $N = 96$ decimated Betchov system under constraint set II. Note that no variable dominates any other. (b) The system-averaged mean of all the variables of that same realization of the decimated system. For both plots, $R = 128$; there were 500 timesteps in the run, with 10 unequal-time constraints spaced out by 14 timesteps.

Figure 23

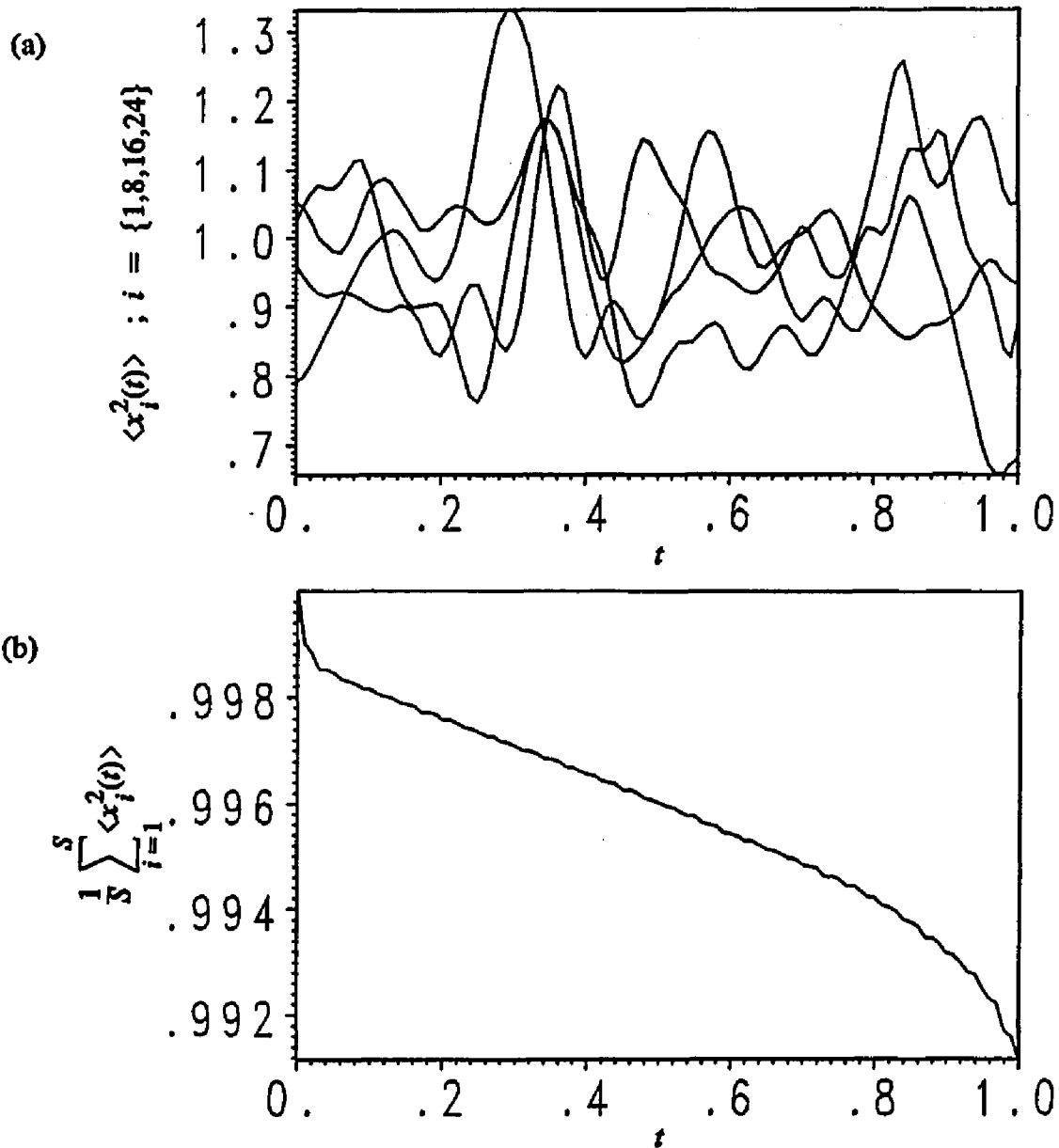


Figure 23. (a) The mean squares of four different variables — $\langle x_1^2 \rangle$, $\langle x_8^2 \rangle$, $\langle x_{16}^2 \rangle$, $\langle x_{24}^2 \rangle$ — from an ensemble of $S = 32$, $N = 96$ decimated Betchov system under constraint set I. Note that no variable dominates any other. (b) The system-averaged mean square of all the variables. For both plots, $R = 128$; there were 500 timesteps in the run, with 10 unequal-time constraints spaced out by 14 timesteps.

Figures 24 through 28 show autocorrelation functions for decimated systems under constraint set II at various decimation strengths from $N/S = 33/32$ to $N/S = 10^6$. The DIA results (and full-system results, where possible) are plotted for comparison of decorrelation time scales. The clear success of constraint set II is at strong decimation. The oscillations in H_{CDS} produced by constraint set I are noticeably absent in these results. The only problem with the results from constraint set II is the deviation of H_{CDS} from H_{DIA} and H for intermediate decimation strength, such as $N/S = 3$ (Fig. 23). This deviation is slight, but just outside the level of statistical fluctuations.

The H_{CDS} curve for $N/S = 3$ can be brought within fluctuations of the full-system and DIA curves with the addition of a variance constraint of the form of Eq. (22). However, this causes convergence failure of the Newton-Raphson procedure at stronger decimation levels. Perhaps it is not surprising that the properties of a single constraint set as simple as set II vary a bit through the wide decimation-level range investigated. In any case, one of the more interesting conclusions to be drawn from constraint set II concerns the strong decimation limit and its relationship with the DIA; this will be discussed later in the dissertation (§ VI).

Figure 24

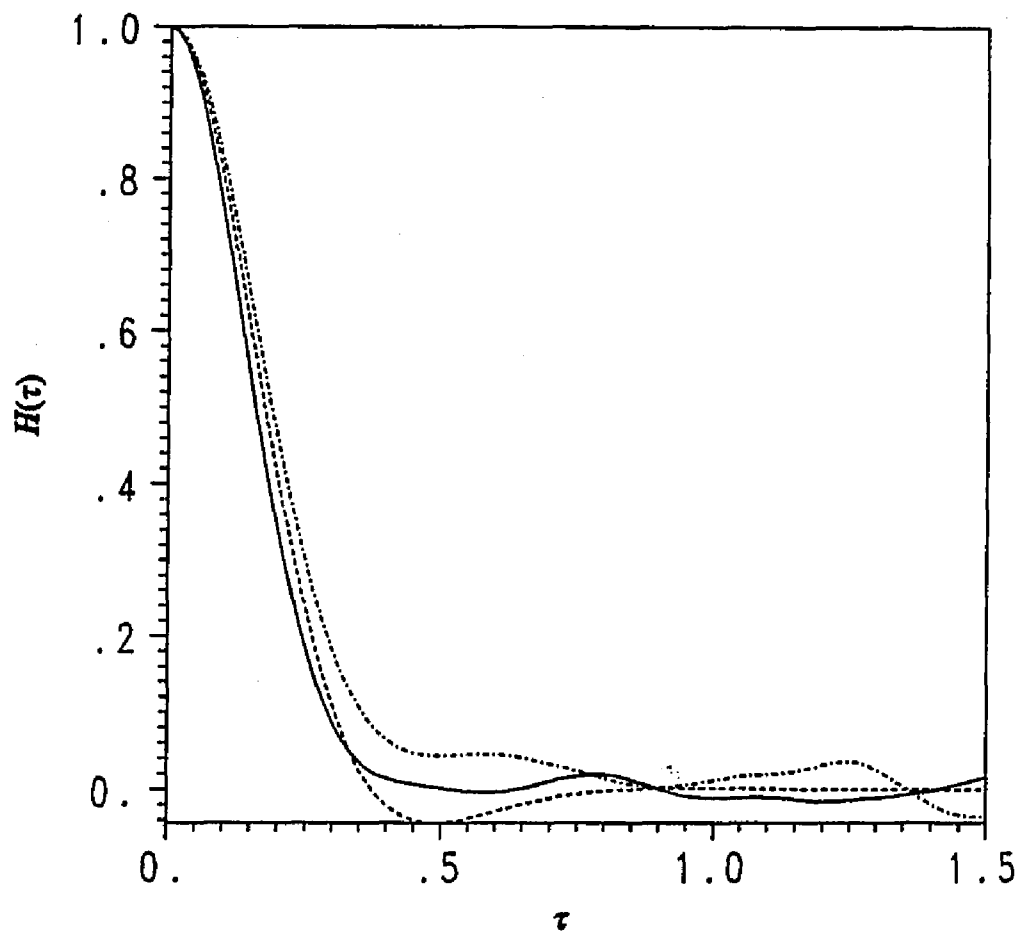


Figure 24. $H_{\text{CDS}}(\tau)$ for an $S = 32$, $N = 33$ decimated Betchov system under constraint set II (solid curve); $H_{\text{DIA}}(\tau)$ for $N = 33$ (dashed curve); $H(\tau)$ for a full $N = 33$ Betchov system (dot-dashed curve).

Figure 25

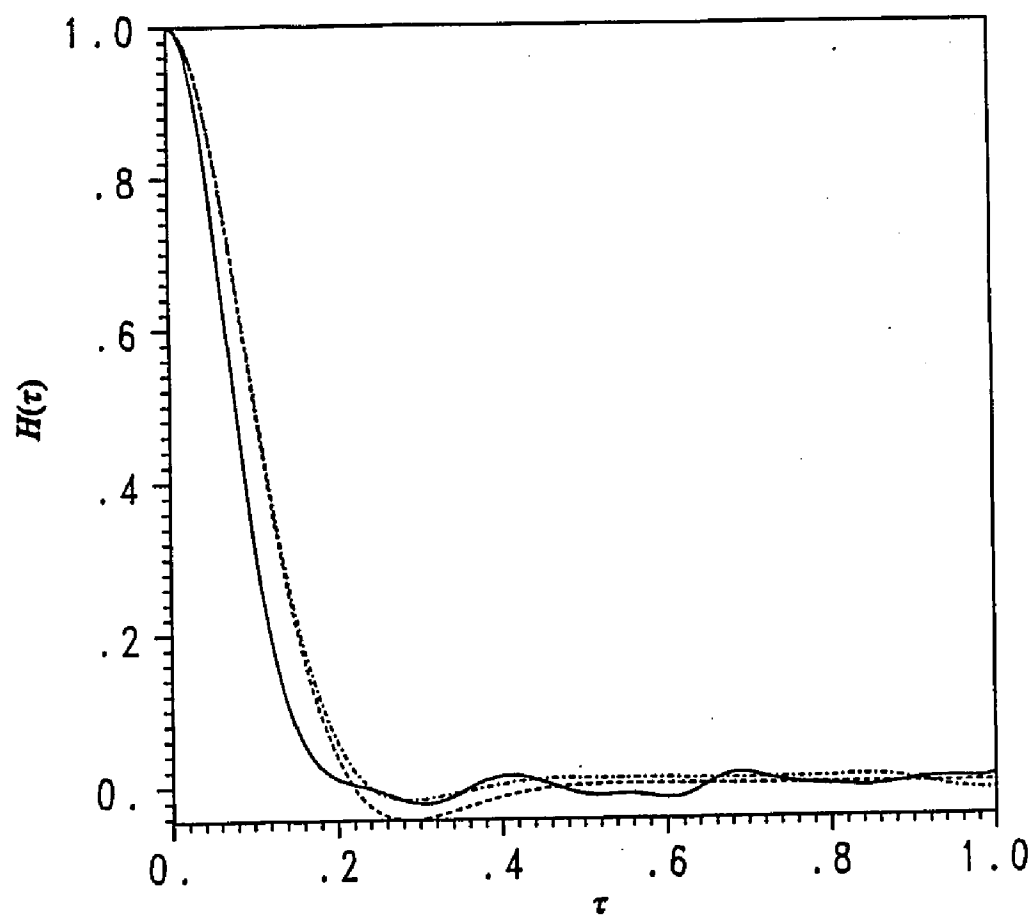


Figure 25. $H_{\text{CDS}}(\tau)$ for an $S = 32, N = 96$ decimated Betchov system under constraint set Π (solid curve); $H_{\text{DIA}}(\tau)$ for $N = 96$ (dashed curve); $H(\tau)$ for a full $N = 96$ Betchov system (dot-dashed curve).

Figure 26

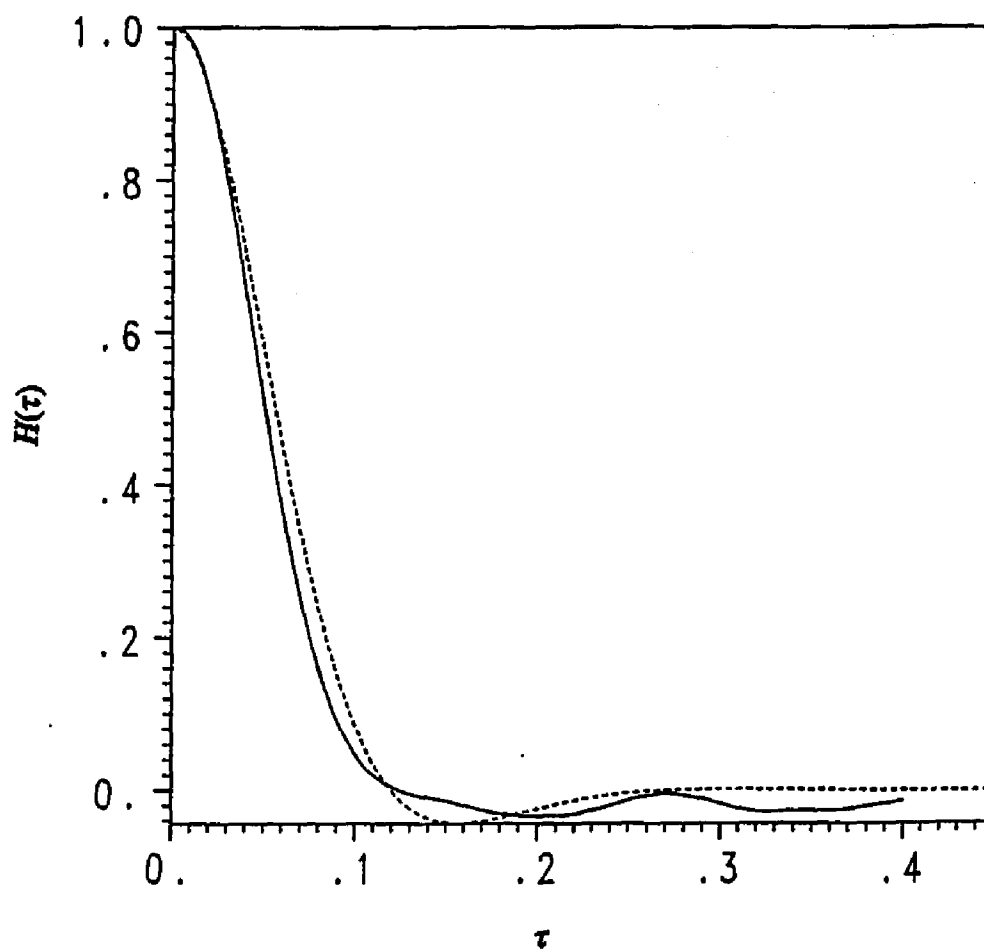


Figure 26. $H_{\text{CDS}}(\tau)$ for an $S = 32$, $N = 320$ decimated Betchov system under constraint set Π (solid curve); $H_{\text{DIA}}(\tau)$ for $N = 320$ (dashed curve).

Figure 27

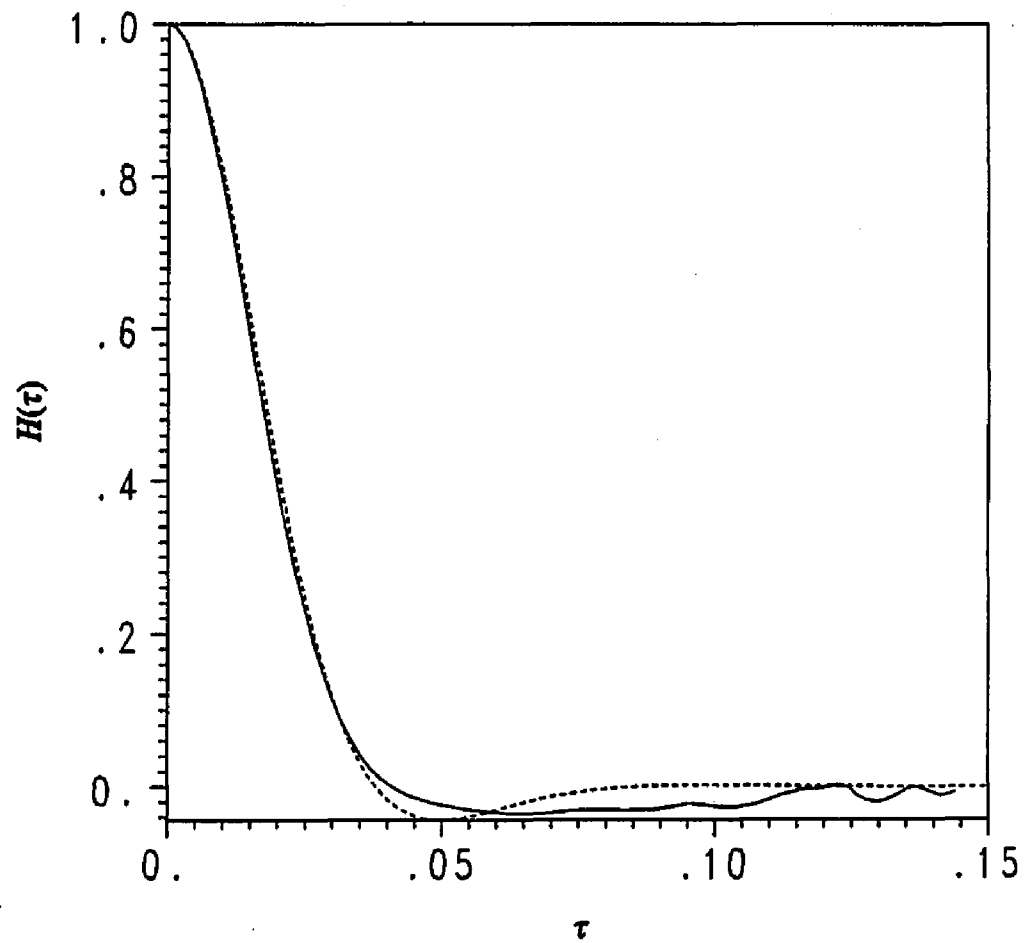


Figure 27. $H_{\text{CDS}}(\tau)$ for an $S = 32$, $N = 3200$ decimated Betchov system under constraint set II (solid curve); $H_{\text{DIA}}(\tau)$ for $N = 3200$ (dashed curve).

Figure 28

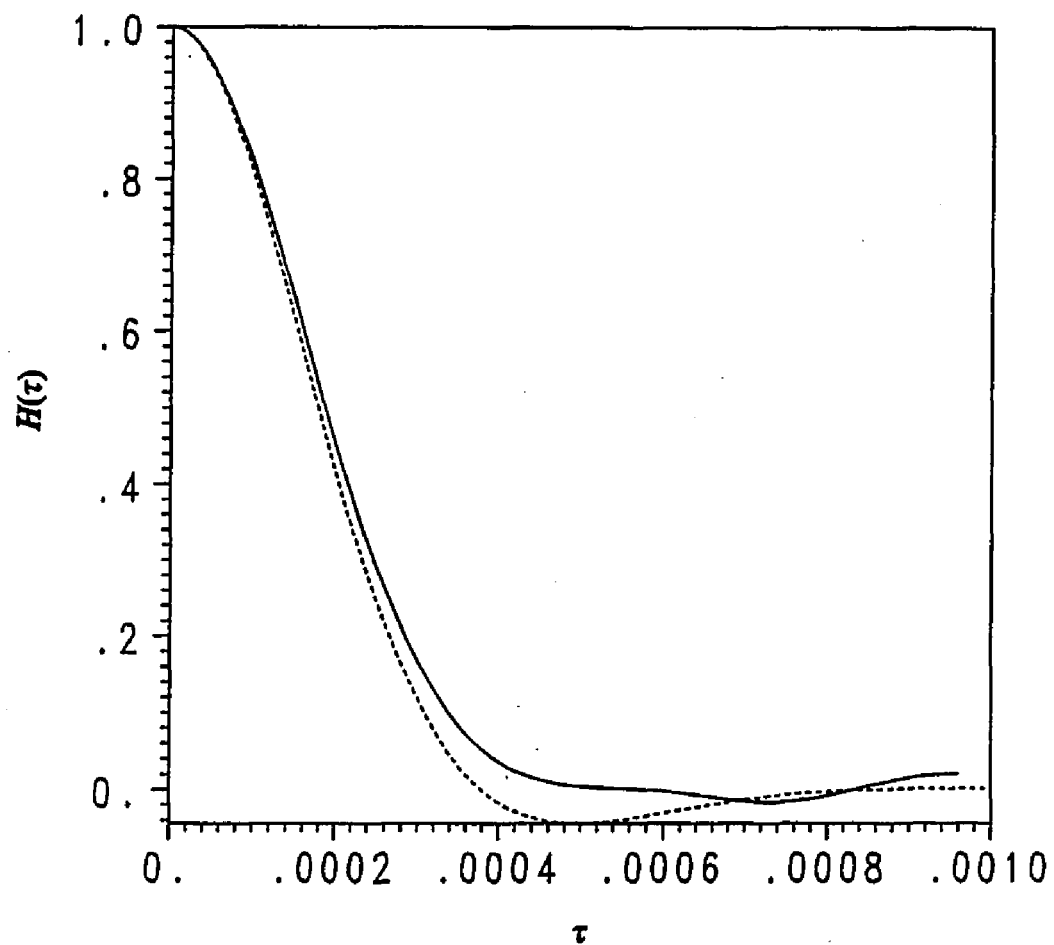


Figure 28. $H_{\text{CDS}}(\tau)$ for an $S = 32, N = 32 \times 10^6$ decimated Betchov system under constraint set II (solid curve); $H_{\text{DIA}}(\tau)$ for $N = 32 \times 10^6$ (dashed curve).

Sometimes, particularly at strong decimation, the mean energy is observed to suddenly depart from its slow decay and plunge to smaller and smaller values. This usually coincides with an obvious disruption in the autocorrelation function, following which the curve fluctuates strongly. Figure 29 shows these two effects on an $N/S = 100$ run. At very strong decimation, such as $N/S = 10^6$, the breakup of H_{CDS} is sometimes observed when $\langle E_{\text{CDS}} \rangle$ has not yet noticeably plunged. Nonetheless, it is concluded that the two phenomena are linked; the instability is stronger as N/S increases. The instability can always be avoided by choosing smaller timesteps and appropriate unequal-time constraints (including constraint over a longer time-history). Study of this instability is the goal of possible future analysis.

2. Effects of the constraints

(a) Mean stochastic force constraint

At moderate decimation levels, such as $N/S = 3$, the effects of removing this constraint [Eq. (26)] are unmeasurable. At stronger decimation, such as $N/S = 3200$, the effects are measurable as a slight slowing in the decay rate of $\langle E_{\text{CDS}} \rangle$ (by 3 percent in the most extreme case observed) or even a temporary increase in $\langle E_{\text{CDS}} \rangle$ (one percent in the most extreme case observed).

Figure 29

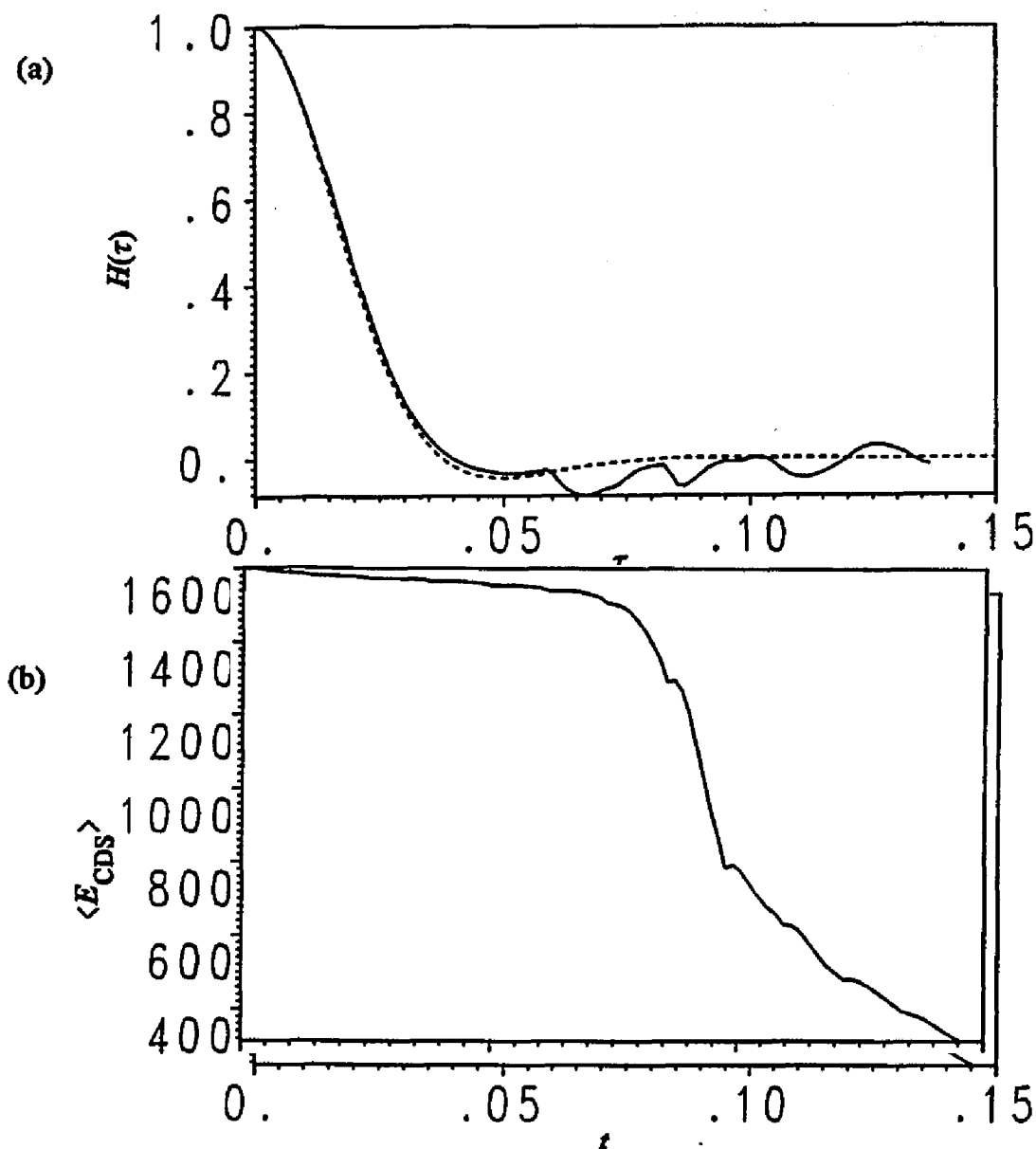


Figure 29. (a) $H_{\text{CDS}}(t=0.015; \tau)$ for an $S = 32$, $N = 3200$ decimated Betchov system under constraint set II (solid curve) with 100 timesteps and 4 unequal-time constraints spaced out by 8 timesteps. Note the disruption in the curve around $\tau = .06$; this corresponds to $t = .075$ in the system's time evolution. The dashed curve is $H_{\text{DIA}}(\tau)$ for $N = 3200$. (b) $\langle E_{\text{CDS}} \rangle$ for the same decimated system. Note the drastic drop in $\langle E_{\text{CDS}} \rangle$ around $t = .075$ corresponding to the disruption in the H_{CDS} curve.

(b) *Equal-time force-variable constraint*

This constraint [Eq. (27) with $t' = t$], as explained before, causes approximate $\langle E_{\text{CDS}} \rangle$ conservation. Systems run without it fail after a few timesteps; they run longer if h is decreased, since the unequal-time force-variable constraints approach this one if the spacing between unequal-time points is also small. For $N/S = 3$, a typical system without this constraint failed to converge at the third timestep, before which $\langle E_{\text{CDS}} \rangle$ had increased by 3 percent. For $N/S = 100$, a typical system failed with numerical overflow errors at the third timestep, before which $\langle E_{\text{CDS}} \rangle$ had only increased 0.0009 percent; however, the overflow error suggests that $\langle E_{\text{CDS}} \rangle$ is skyrocketing during the attempt to apply the constraints at the third timestep.

(c) *Unequal-time force-variable constraints*

With no unequal-time constraints [Eq. (046) with $t' < t$], as with constraint set I, the decay of the autocorrelation function $H_{\text{CDS}}(\tau)$ is radically altered toward that of an *undecimated* Betchov system of size S . Figures 30 and 31 show this effect for $N/S = 3$ and $N/S = 100$.

The effects of changing the number and spacing between the unequal-time constraints are subtler, but more consistent than the effects observed under constraint set I. Again, consider the effect of the spacing between the unequal-time points $\{t', t'', \dots\}$ constrained against and the length of the maximal window $|t - t'|$.

First, add more constraints to a system to extend the window while keeping the spacing between the unequal-time points the same. For $N/S = 3$ and for $N/S = 100$, this produces no noticeable effects, except for a slight improvement in $\langle E_{\text{CDS}} \rangle$ conservation: For $N/S = 3$, the total

percentage decrease in $\langle E_{\text{CDS}} \rangle$ goes from 11 percent to 4.5 percent — a change in percentage drop of 6.5 percent [with $N = 96$, $S = 32$, $h = 0.003$, (a) 7 unequal-time constraints spaced by 10 timesteps, and (b) 16 unequal-time constraints spaced by 10 timesteps]. For $N/S = 100$ with these same two sets of parameters (except now $h = 0.0005$) the energy-related instability sets in after about two decorrelation times, before which $\langle E_{\text{CDS}} \rangle$ decays only one percent in each case. The subsequent plunging of $\langle E_{\text{CDS}} \rangle$ is lessened by 1 percent in the second case (at three decorrelation times).

Second, add more constraints to the system but decrease the spacing between the unequal-time points to keep the size of the window unchanged. For $N/S = 3$ and $N/S = 100$, the major noticeable effect is improved $\langle E_{\text{CDS}} \rangle$ conservation: For $N/S = 3$, the change in percentage drop in $\langle E_{\text{CDS}} \rangle$ is 10.8 percent [with $N = 96$, $S = 32$, $h = 0.003$, (a) 7 unequal-time constraints spaced by 10 timesteps, and (b) 16 unequal-time constraints spaced by 5 timesteps]. For $N/S = 100$ with the same parameters (except now $h = 0.0005$) the onset of the instability is not observed during the entire three decorrelation times of the run, and $\langle E_{\text{CDS}} \rangle$ decays less than 1 percent.

Third, use a window spanning only a small fraction of the decorrelation time. For $N/S = 3$ and $N/S = 100$, with the window spanning 20 percent of the decorrelation interval, $\langle E_{\text{CDS}} \rangle$ decays by less than 0.1 percent and no instability occurs (with 9 unequal-time constraints and h giving 100 timesteps in the decorrelation time; the runs go out to 3 decorrelation times). For the same parameters, but with the unequal-time constraints spanning the entire decorrelation time, the instability sets in after two decorrelation times; $\langle E_{\text{CDS}} \rangle$ decays by 11

percent for $N/S = 3$ and 21 percent for $N/S = 100$. However, for the same timesteps but with only one unequal-time constraint, the instability sets in before one decorrelation time; $\langle E_{\text{CDS}} \rangle$ decays by 83 percent for $N/S = 3$ and 60 percent for $N/S = 100$. This behavior is complicated, but it need not be understood in detail since the main interest is a stable solution that conserves $\langle E_{\text{CDS}} \rangle$; any parameters which yield such a solution are acceptable. For consistency, the unequal-time constraints always span one decorrelation time in the results presented here (where possible).

Figure 30

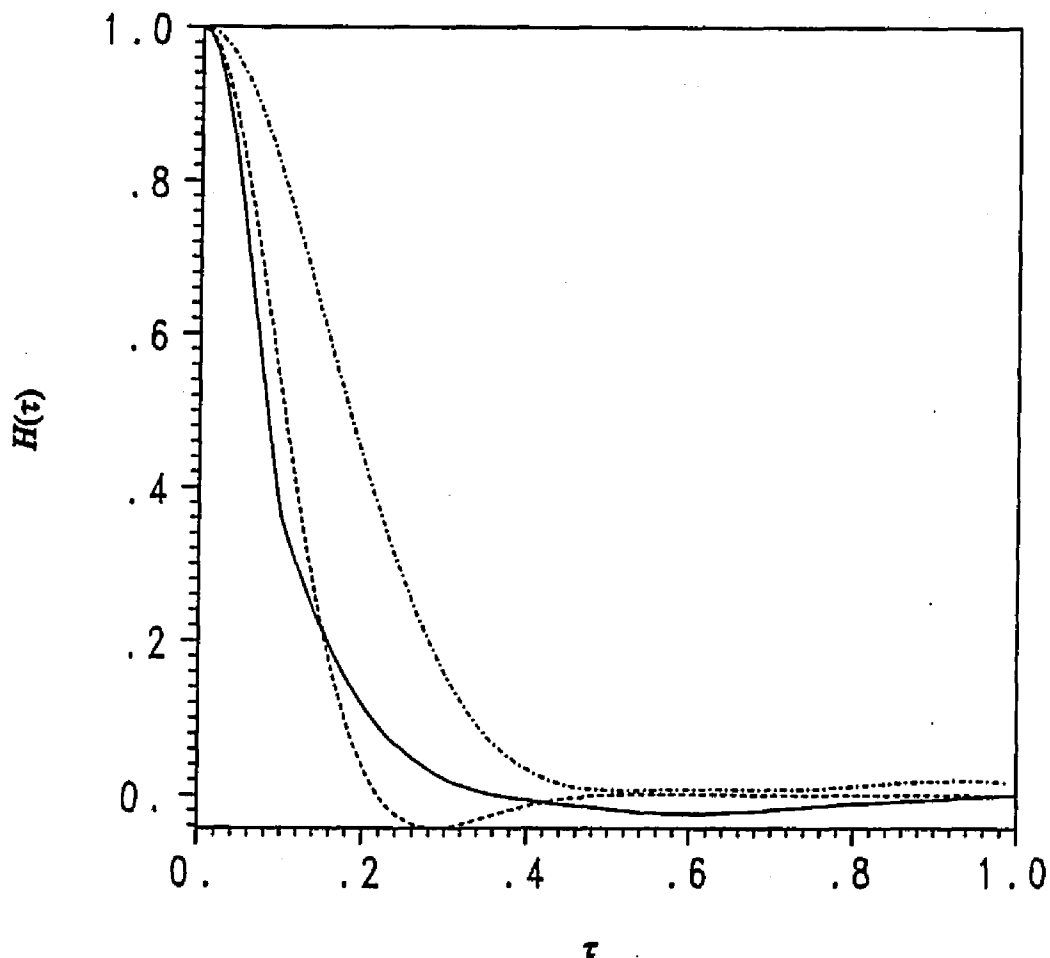


Figure 30. $H_{\text{CDS}}(\tau)$ for an $S = 32$, $N = 96$ decimated Betchov system under constraint set Π with the unequal-time constraints switched off at $t = 0.1$ (solid curve); $H_{\text{DIA}}(\tau)$ for $N = 96$ (dashed curve); $H(\tau)$ for a full $N = 32$ Betchov system (dot-dashed curve).

Figure 31

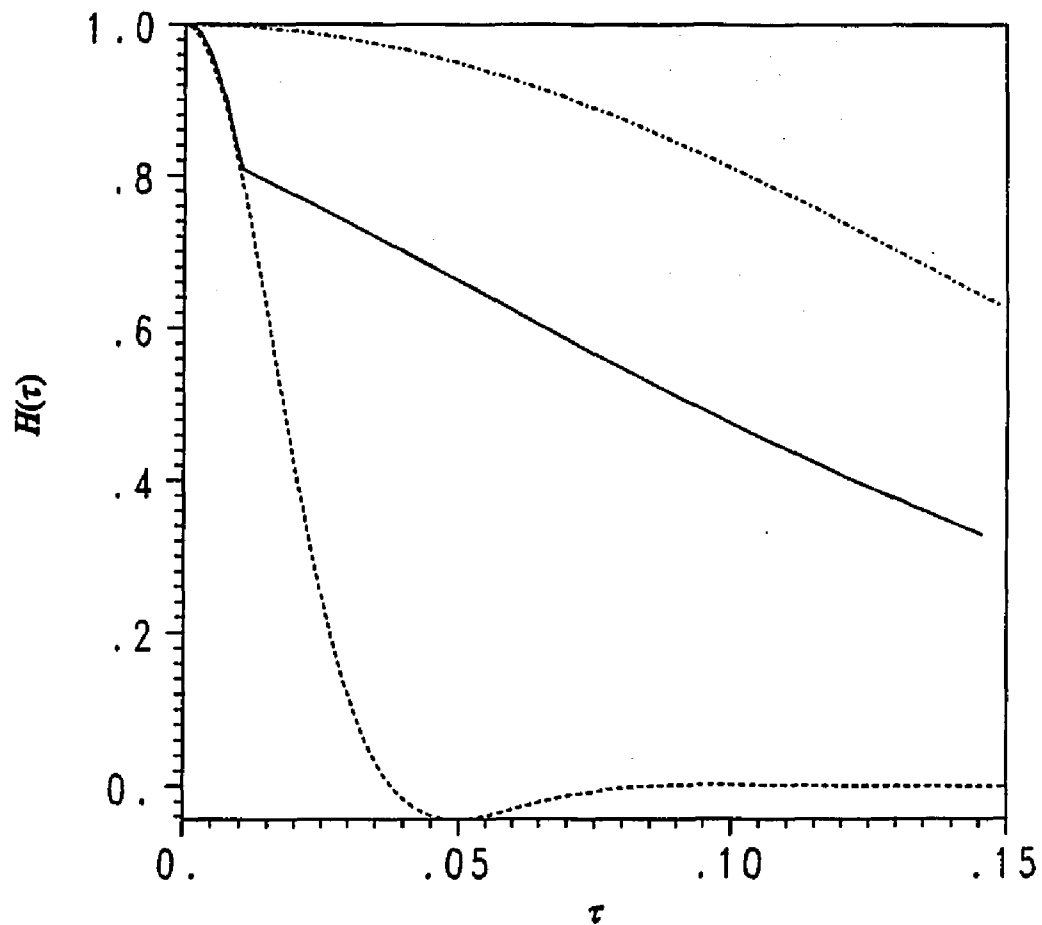


Figure 31. $H_{\text{CDS}}(\tau)$ for an $S = 32$, $N = 3200$ decimated Betchov system under constraint set I with the unequal-time constraints switched off at $t = 0.01$ (solid curve); $H_{\text{DIA}}(\tau)$ for $N = 3200$ (dashed curve); $H(\tau)$ for a full $N = 32$ Betchov system (dot-dashed curve).

VI. RELATION BETWEEN THE CDS AND THE DIA

A. DIA via CDS	90
B. Constraint set II as "DIA constraints"	100

A. DIA via CDS

Recent work of Robert Kraichnan^{17,18,23} has suggested that the CDS under constraint set II is related to the DIA in the limit as $N \rightarrow \infty$. There is no rigorous proof for this claim, but plausible support for it is lent by the following:

First, note that the DIA can be recovered beginning with the following intuitive leap: instead of the full-system Bethe equations [Eq. (13)], consider

$$\frac{dx_i}{dt} = b_i(t) + \int_0^t R_i(t,s) x_i(s) ds \quad \text{for } i=1,2,\dots,N, \quad (28)$$

where $b_i(t)$ is a random function satisfying

$$\langle b_i(t) x_i(t') \rangle = 0 \quad (29)$$

for all t and t' . The function $R_i(t,s)$ is defined by

$$R_i(t,s) = \int_0^t \left\langle \sum_{j,k=1}^N C_{ijk} x_j(t) x_k(t) x_i(s') \right\rangle \mathcal{K}_i(s,s' | 0,t) ds', \quad (30)$$

where the kernel $\mathcal{K}_i(s,s' | 0,t)$ is the inverse of the autocorrelation

function; that is,

$$\int_0^t \mathcal{K}_i(s, s' | 0, t) \langle x_i(t') x_i(s) \rangle ds = \delta(t' - s') .$$

Note that \mathcal{K}_i is statistically sharp ($\langle \mathcal{K}_i \rangle = \mathcal{K}_i$). With the use of the expressions for R_i and \mathcal{K}_i , Eq. (28) becomes

$$\frac{dx_i}{dt} = b_i(t) +$$

$$\int_0^t \left[\int_0^t \left\langle \sum_{j, k=1}^N C_{ijk} x_j(t) x_k(t) x_i(s') \right\rangle \mathcal{K}_i(s, s' | 0, t) ds' \right] x_i(s) ds$$

$$\text{for } i=1, 2, \dots, S . \quad (30)$$

The reasons for setting up this equation will become clear in the end. One justification for it is that Eq. (28) follows the pattern of Orszag's derivation of the DIA,⁷ which begins by replacing differential equations of the form

$$\frac{dy_i}{dt} = \sum_{j, k}^S A_{ijk} y_j y_k - v_i y_i$$

with integro-differential equations of the form

$$\frac{dy'_i}{dt} = \int_0^t \eta_i(t, s) y'_i(s) ds - v_i y'_i ,$$

where η_i is a nonrandom eddy-damping factor. In Eq. (28), R_i plays the same conceptual role as η_i .

At this point, if both sides of Eq. (30) were multiplied by $x_i(t+\tau)$ and averaged and the DIA moment expressions from Appendix B employed, the *same* expression for $H_{\text{DIA}}(\tau)$ as derived in Appendix B would result. This is another justification for replacing the Betchov system with this new integro-differential system — they have the same DIA solution.

In preparation for decimation of system of N equations to a system of S equations, split the summation in Eq. (30) into two parts:

$$\left\langle \sum_{j,k=1}^N C_{ijk} x_j(t) x_k(t) x_i(s') \right\rangle = \left\langle \sum_{j,k=1}^S C_{ijk} x_j(t) x_k(t) x_i(s') \right\rangle + \left\langle \sum_{j,k}^{\prime N} C_{ijk} x_j(t) x_k(t) x_i(s') \right\rangle ,$$

where Σ' is the sum over all j and k such that at least one of the two indices is greater than S . Next, replace

$$\left\langle \sum_{j,k}^{\prime N} C_{ijk} x_j(t) x_k(t) x_i(s') \right\rangle$$

with

$$\langle q_i^*(t) x_i(s') \rangle .$$

As always in this dissertation, $q_i^*(t)$ is defined as

$$q_i^*(t) = \sum_{j,k}^N C_{ijk} x_j(t) x_k(t) .$$

The decimated-system equations are then

$$\begin{aligned} \frac{dx_i}{dt} = & b_i(t) + \int_0^t \left[\int_0^t \langle q_i^*(t) x_i(s') \rangle \mathcal{K}_i(s, s' | 0, t) ds' \right] x_i(s) ds + \\ & \int_0^t \left[\int_0^t \left\langle \sum_{j,k=1}^S C_{ijk} x_j(t) x_k(t) x_i(s') \right\rangle \mathcal{K}_i(s, s' | 0, t) ds' \right] x_i(s) ds \\ & \text{for } i=1,2,\dots,S . \end{aligned} \quad (31)$$

Now introduce a new quantity Q_i and rewrite Eq. (31) as

$$\frac{dx_i}{dt} = \sum_{j,k=1}^S C_{ijk} x_j(t) x_k(t) + Q_i(t) \quad \text{for } i=1,2,\dots,S, \quad (32)$$

where

$$\begin{aligned} Q_i(t) = & b_i(t) + \int_0^t \left[\int_0^t \langle q_i^*(t) x_i(s') \rangle \mathcal{K}_i(s, s' | 0, t) ds' \right] x_i(s) ds + \\ & \int_0^t \left[\int_0^t \left\langle \sum_{j,k=1}^S C_{ijk} x_j(t) x_k(t) x_i(s') \right\rangle \mathcal{K}_i(s, s' | 0, t) ds' \right] x_i(s) ds \\ & - \sum_{j,k=1}^S C_{ijk} x_j(t) x_k(t) . \end{aligned} \quad (33)$$

The transformation from Eq. (31) to Eq. (32) is a formal one, whose

purpose will become clear at the next step in the argument.

Next, take the moment of $Q_i(t)$ with $x_i(t')$; after interchanging the order of the integrations over s and s' and taking averaged quantities outside the new moment brackets,

$$\begin{aligned}
\langle Q_i(t) x_i(t') \rangle &= \langle b_i(t) x_i(t') \rangle + \\
&+ \int_0^t \left[\int_0^{t'} \langle x_i(s) x_i(t') \rangle \mathcal{K}_i(s, s' | 0, t) ds \right] \langle q_i^*(t) x_i(s') \rangle ds' \\
&+ \int_0^t \left[\int_0^t \langle x_i(s) x_i(t') \rangle \mathcal{K}_i(s, s' | 0, t) ds \right] \left\langle \sum_{j, k=1}^S C_{ijk} x_j(t) x_k(t) x_i(s') \right\rangle ds' \\
&\quad - \left\langle \sum_{j, k=1}^S C_{ijk} x_j(t) x_k(t) x_i(t') \right\rangle \\
&= 0 + \int_0^t \delta(t' - s') \langle q_i^*(t) x_i(s') \rangle ds' \\
&\quad + \int_0^t \delta(t' - s') \left\langle \sum_{j, k=1}^S C_{ijk} x_j(t) x_k(t) x_i(s') \right\rangle ds' \\
&\quad - \left\langle \sum_{j, k=1}^S C_{ijk} x_j(t) x_k(t) x_i(t') \right\rangle \\
\langle Q_i(t) x_i(t') \rangle &= \langle q_i^*(t) x_i(t') \rangle . \tag{34}
\end{aligned}$$

Finally, identify $Q_i(t)$ with the stochastic force $q_i(t)$ in the decimated Betchov system equations Eq. (16). Now Eq. (32) is identical with Eq. (16), and the force-variable constraints in constraint set II [Eq. (26)] are system-averaged versions of Eq. (34). The

least-squares-minimization $q_i(t)$ determined by the Newton-Raphson procedure in the implementation of the CDS discussed in §IID3 and Appendix D is intimately related to the $Q_i(t)$ defined in Eq. (33). The remainder of this section is dedicated to clarifying that relationship.

In the numerical determination of $q_i(t)$ under constraint set II only a finite set of discrete time values $t \leq t'$ are used in the force-variable constraints:

$$\sum_{i=1}^S \langle q_i(t) x_i(t') \rangle = \sum_{i=1}^S \langle q_i^*(t) x_i(t') \rangle . \quad (35)$$

For simplicity, assume that every timestep is constrained against, so that t' takes the values $\{0, h, 2h, 3h, 4h, \dots, Lh\}$; L is defined so that $t = Lh$. Now the time integrals in the preceding equations in this section become discrete sums over the t' values. That is, Eq. (33) becomes

$$\begin{aligned} Q_i(Lh) = & b_i(Lh) + \sum_{m=0}^L \sum_{n=0}^L x_i(mh) \langle q_i^*(Lh) x_i(nh) \rangle \mathcal{K}_i(m, n | L) \\ & + \sum_{m=0}^L \sum_{n=0}^L x_i(mh) \left\langle \sum_{j, k=1}^S C_{ijk} x_j(Lh) x_k(Lh) x_i(nh) \right\rangle \mathcal{K}_i(m, n | L) \\ & - \sum_{j, k=1}^S C_{ijk} x_j(Lh) x_k(Lh) , \quad (36) \end{aligned}$$

where

$$\sum_{j=0}^L \langle x_i(mh) x_i(jh) \rangle \mathcal{K}_i(j,n | L) = \delta_{mn} . \quad (37)$$

Next, define the $(L+1)$ -dimensional matrices κ_i and \mathcal{K}_i :

$$\begin{aligned} [\kappa_i]_{mj} &= [\kappa_i]_{jm} = \langle x_i(mh) x_i(jh) \rangle . \\ [\mathcal{K}_i]_{mj} &= \mathcal{K}_i(m,j | L) . \end{aligned} \quad (38)$$

It is straightforward to show that $\kappa_i = \kappa_i^{-1}$. Now define the $(L+1)$ -dimensional vectors \mathbf{x}_i and \mathbf{Q}_i^* :

$$\begin{aligned} [\mathbf{x}_i]_m &= x_i(mh) \\ [\mathbf{Q}_i^*]_m &= \langle q_i^*(Lh) x_i(mh) \rangle . \end{aligned} \quad (39)$$

Using these definitions, the second term in the righthand side of Eq. (36) can be expressed compactly:

$$\sum_{m=0}^L \sum_{n=0}^L x_i(mh) \langle q_i^*(Lh) x_i(nh) \rangle \mathcal{K}_i(m,n | L) = \mathbf{x}_i \cdot \kappa_i^{-1} \cdot \mathbf{Q}_i^* .$$

Using Eq. (36), calculate the moment $\langle Q_i(Lh) x_i(ph) \rangle$:

$$\begin{aligned}
\langle Q_i(Lh) x_i(ph) \rangle &= \langle b_i(Lh) x_i(ph) \rangle \\
&+ \left\langle \sum_{m=0}^L \sum_{n=0}^L x_i(mh) \langle q_i^*(Lh) x_i(nh) \rangle \mathcal{K}_i(m,n | L) x_i(ph) \right\rangle \\
&+ \left\langle \sum_{m=0}^L \sum_{n=0}^L x_i(mh) \left\langle \sum_{j,k=1}^S C_{ijk} x_j(Lh) x_k(Lh) x_i(nh) \right\rangle \mathcal{K}_i(m,n | L) x_i(ph) \right\rangle \\
&- \left\langle \sum_{j,k=1}^S C_{ijk} x_j(Lh) x_k(Lh) x_i(ph) \right\rangle .
\end{aligned}$$

This expression can be simplified by switching orders of summation and using Eq. (29), Eq. (37), Eq. (38), and Eq. (39); the result is

$$\langle Q_i(Lh) x_i(ph) \rangle = \sum_{n=0}^L [x_i \cdot x_i^{-1}]_{pn} [Q_i^*]_n .$$

Thus, using Eq. (066),

$$\begin{aligned}
\langle Q_i(Lh) x_i \rangle &= x_i \cdot x_i^{-1} \cdot Q_i^* \\
&= Q_i^* \\
\langle Q_i(Lh) x_i \rangle &= \langle q_i^*(Lh) x_i \rangle .
\end{aligned}$$

Next consider the $q_i(Lh)$ calculated using the Newton-Raphson technique in the CDS as described in §IID3 and Appendix D. The Newton-Raphson process iteratively modifies an initial guess $q_i^{(0)}(Lh)$ until it satisfies constraints of the form Eq. (35). This is equivalent to modifying $q_i^{(0)}(Lh)$ only once with a $\delta q_i(Lh)$ which is equal to the sum

of all the small changes from the sequence of iterations. That is, an initial $q_i^{(0)}(Lh)$ is guessed for which in general

$$\langle q_i^{(0)}(Lh) \mathbf{x}_i \rangle \neq \langle q_i^*(Lh) \mathbf{x}_i \rangle .$$

This is modified by $\delta q_i(Lh)$, so that

$$\langle [q_i^{(0)}(Lh) + \delta q_i(Lh)] \mathbf{x}_i \rangle = \langle q_i^*(Lh) \mathbf{x}_i \rangle . \quad (40)$$

Express $\delta q_i(Lh)$ as a linear combination of the components of \mathbf{x}_i [note that this is exactly the procedure described in §III D 3(b)]:

$$\delta q_i(Lh) = \sum_{m=0}^L A_m x_i(mh) .$$

The n th component of $\langle \delta q_i(Lh) \mathbf{x}_i \rangle$ is then

$$\begin{aligned} \langle \delta q_i(Lh) x_i(nh) \rangle &= \sum_{m=0}^L A_m [x_i]_{mn} \\ &= [x_i \cdot \mathbf{A}]_n . \end{aligned}$$

Here $[\mathbf{A}]_m = A_m$. Now Eq. (40) is

$$\begin{aligned} [x_i \cdot \mathbf{A}]_n &= [Q_i^*]_n - \langle q_i^{(0)}(Lh) x_i(nh) \rangle \\ &= [Q_i^*]_n - [Q_i^{(0)}]_n . \end{aligned}$$

Generalizing,

$$\begin{aligned} \mathbf{x}_i \cdot \mathbf{A}_i &= \mathbf{Q}_i^* - \mathbf{Q}_i^{(0)} \\ \mathbf{A}_i &= \mathbf{x}_i^{-1} \cdot [\mathbf{Q}_i^* - \mathbf{Q}_i^{(0)}] . \end{aligned}$$

Thus

$$\begin{aligned} q_i(Lh) &= q_i^{(0)}(Lh) + \delta q_i(Lh) \\ &= q_i^{(0)}(Lh) + \mathbf{x}_i \cdot \mathbf{A}_i \\ &= q_i^{(0)}(Lh) + \mathbf{x}_i \cdot \mathbf{x}_i^{-1} \cdot [\mathbf{Q}_i^* - \mathbf{Q}_i^{(0)}] . \quad (41) \end{aligned}$$

Now this can be compared with $Q_i(Lh)$ derived earlier. Comparison of Eq. (41) with Eq. (36) shows that

$$\begin{aligned} q_i(Lh) - Q_i(Lh) &= \left[q_i^{(0)}(Lh) - \mathbf{x}_i \cdot \mathbf{x}_i^{-1} \cdot \mathbf{Q}_i^{(0)} \right] - \left[b_i(Lh) \right. \\ &+ \sum_{m=0}^L \sum_{n=0}^L x_i(mh) \left\langle \sum_{j,k=1}^S C_{ijk} x_j(Lh) x_k(Lh) x_i(nh) \right\rangle \mathcal{K}_i(m,n | L) \\ &\quad \left. - \sum_{j,k=1}^S C_{ijk} x_j(Lh) x_k(Lh) \right] . \end{aligned}$$

Both terms in parentheses satisfy $\langle (\dots) \mathbf{x}_i \rangle = 0$, so

$$\left\langle \left[q_i(Lh) - Q_i(Lh) \right] \mathbf{x}_i \right\rangle = 0 .$$

Thus the difference $q_i(Lh) - Q_i(Lh)$ contributes nothing to the moments in the constraints being discussed and is irrelevant to the formalism of the CDS.

B. Constraint set II as "DIA constraints"

Based on the argument from the previous section, it was suspected that constraint set II might give results comparable with the DIA results for the Betchov system. The observed convergence of $H_{\text{CDS}}(\tau)$ under constraint set II toward $H_{\text{DIA}}(\tau)$ as $N/S \rightarrow \infty$ (and consequently $N \rightarrow \infty$, since S is finite) supports that suspicion. It may be that similar "DIA constraints" can be configured for other systems to be studied with the CDS. This would be a valuable tool for two reasons: (1) CDS results could be compared with existing DIA results for systems whose DIA solutions have been calculated, and (2) it would provide a relatively simple way to generate DIA results for systems not previously solved with the DIA (solution of arbitrary systems with the DIA is a notoriously Herculean algebraic and computational task).

VII. CONCLUSIONS AND NEXT STEPS

A. Works with one symmetry group	101
B. Ideas behind derivation of DIA via CDS supported	104
C. Works where cumulant-discard approximation fails	105

A. Works with one symmetry group

The machinery of the CDS has been shown to function when applied to a many-variable system with one statistical symmetry group. The basic statistical character of the system is not altered by the decimation and constrained forcing. The isotropy and time-stationarity of the Betchov system are preserved in the decimated system. With constraint set II the autocorrelation function, a key statistical property of the Betchov system, is found to agree qualitatively and approximately over a range of decimation levels from $N/S = 33/32$ to $N/S = 10^6$. The agreement is quantitatively within statistical fluctuation levels both for very weak decimation [$N/S = O(1)$] and strong decimation [$N/S = O(100)$ and higher], with the results becoming better as N/S becomes larger. While it is possible that as yet untried additional constraints could improve quantitative agreement over the entire decimation range, it is also possible that it is simply unreasonable to expect a single formulation to work over the entire range.

Since the goal of the CDS is the reduction of very large systems, it is good enough that the scheme works best at strong decimation. More important than further refining results on decimation of the simple Betchov system is the application of the CDS to more complicated systems. Specifically, the CDS should next be applied to a system with

more than one statistical symmetry group. The interactions between groups of variables with different statistical properties must be studied. The CDS must be shown to preserve the average interactions between the groups. Work has begun on two more complicated systems.

The first system is a modified Betchov system which has two variable types. The two sets of variables in the modified Betchov system form two statistical symmetry groups; the variables within the sets are statistically similar, but the two groups have different statistics. The modified Betchov system is based on one used by Kraichnan in a recent paper.²⁴ The system equations are the same as the regular Betchov system:

$$\frac{dx_i}{dt} = \sum_{j,k=1}^N A_{ijk} x_j x_k \quad \text{for } i=1,2,\dots,N .$$

The variables fall into the groups $\{x_i \mid i=1,2,\dots,N_1\}$ and $\{x_i \mid i=N_1+1,2,\dots,N_2\}$, where $N_1 + N_2 = N$. The magnitude of the coupling coefficient A_{ijk} depends on which group variable x_i belongs to. Specifically,

$$A_{ikj} = \frac{1}{2} (B_{jki} - B_{kij})$$

where

$$B_{ijk} = \theta_{ijk} \frac{v_j v_k}{(v_i v_j v_k)^{1/2}} .$$

The θ_{ijk} are chosen at random from a uniform distribution on the interval $(-1,1)$, and the v_i are constant weights which determine the

relative character of the statistical groups. In the work so far,

$$v_i = \begin{cases} 1 & \text{for } i \leq N_1 \\ 9 & \text{for } N_1 < i \leq N \quad (\text{n.b.: } N - N_1 = N_2) \end{cases} .$$

As in this dissertation, tractable full modified Betchov systems will be solved then decimated for direct comparison. Particular attention will be paid to the exchange of energy between the two variable groups. Perhaps the depression of nonlinearity observed by Kraichnan in numerical studies of the full modified Betchov system²⁴ can be reproduced by decimated systems.

The second system under investigation is the 2D, inviscid, incompressible Navier-Stokes equations. Preliminary work on this system has begun, starting from the scalar vorticity formulation of the equations.²⁵ The Fourier mode formulation of these equations is

$$\frac{\partial}{\partial t} \rho(\mathbf{k}, t) = \sum_{\mathbf{p} + \mathbf{r} = \mathbf{k}} M(\mathbf{r}, \mathbf{p}) \rho(\mathbf{r}, t) \rho(\mathbf{p}, t) ,$$

where $\rho(\mathbf{k}, t)$ is a Fourier mode amplitude for the mode-series representation of the scalar vorticity (the magnitude of the curl of the two-dimensional flow velocity field; the direction of the curl is everywhere perpendicular to the 2D flow field) and

$$M(\mathbf{r}, \mathbf{p}) = -\frac{3}{2} (\mathbf{r} \times \mathbf{p}) \left[\frac{1}{r^2} - \frac{1}{p^2} \right]$$

are the mode coupling coefficients. This set of ODE's is of the generic form specified in Eq. (1), and the same decimation approach applies (now

with many groups of statistically similar modes). A preliminary computer code for a simple formulation with constraints based on conservation of energy density and enstrophy density (two conserved quantities in the full equations) has been constructed. Plans are to study the modified Betchov system to verify that the CDS can reproduce statistical-symmetry-group interactions faithfully, then advance this 2D Navier-Stokes calculation.

The eventual goal for neutral fluid turbulence study, of course, is the decimation of the full 3D Navier-Stokes equations with viscosity and compressibility. The addition of viscosity presents no difficulties for CDS solution; in fact, the inviscid equations (and the energy-conserving Betchov equations) may well be a more demanding numerical test of the CDS because there is no damping which could moderate spurious effects. There is also no reason that the CDS cannot be applied to the MHD equations to study plasma turbulence, which is the ostensible reason that the research leading to this dissertation took place.

B. Ideas behind derivation of DIA via CDS supported

Kraichnan's discussions^{17,18,23} about the link between the DIA and CDS have been supported. Kraichnan's discussions claim that the DIA can be recovered as a special case of the CDS. In particular, constraint set II in this dissertation is a system-averaged finite subset of the DIA constraints proposed by Kraichnan.^{17,18,23}

If the CDS works only as a means of finding DIA solutions, it is still a valuable tool. The application of the DIA to the Navier-Stokes and other physical equations is extremely difficult, both algebraically and numerically. A glance at DIA

literature^{26,27,28,29,e.g.} shows the magnitude of that difficulty, which can be both algebraic and numerical.

C. Works where cumulant-discard approximation fails

Finally, it should be noted that this application of the CDS to the Betchov system — particularly under constraint set II — has succeeded in calculating $H(\tau)$ where the cumulant-discard approximation fails. Certainly the DIA solution for $H(\tau)$ is a success for the Betchov system; but this is not a surprise, since the system was designed as a model for illustrating the DIA. Indeed, the DIA solution is much simpler to attain for the Betchov system than the CDS solution. However, as mentioned before, the DIA solution of more complicated systems is arduous, and the CDS holds promise for them. The research leading to this dissertation has been a first step (or perhaps a half-step), but a sensible one for studying a new method before applying it to a difficult problem about which little is known — strong fluid turbulence.

APPENDIX A: CUMULANT-DISCARD APPROXIMATION SOLUTIONS OF THE BETCHOV SYSTEM

The cumulant-discard approximation is a closure approximation for the moment hierarchy. It approximates quadruple moments with products of double moments. For Gaussian (normal) variables, quadruple moments are exactly equal to products of double moments; for this reason, this approximation is also called the *quasinormal approximation*. This appendix presents two different applications of the approximation to the problem of solving for the autocorrelation function of the Betchov system.

The first application begins with the Betchov system ODE's:

$$\frac{dx_i}{dt} = \sum_{j,k=1}^N C_{ijk} x_j x_k \quad \text{for } i=1,2,\dots,N. \quad (\text{A1})$$

Multiply each ODE by $x_i(t+\tau)$, sum over i , divide by N , and take the ensemble average of both sides of the resulting single equation:

$$\frac{1}{N} \left\langle \sum_{i=1}^N x_i(t+\tau) \frac{dx_i(t)}{dt} \right\rangle = \frac{1}{N} \left\langle \sum_{i,j,k=1}^N C_{ijk} x_i(t+\tau) x_j(t) x_k(t) \right\rangle \quad (\text{A2})$$

The lefthand side of Eq. (A2) is equal to $-dH(\tau)/d\tau$, as can be seen by explicitly calculating $dH(\tau)/d\tau$:

$$H(\tau) = \frac{1}{N} \sum_{i=1}^N \langle x_i(t) x_i(t+\tau) \rangle$$

$$\begin{aligned}
\frac{dH}{d\tau} &= \frac{1}{N} \sum_{i=1}^N \left\langle x_i(t) \frac{dx_i(t+\tau)}{d\tau} \right\rangle \\
&= \frac{1}{N} \sum_{i=1}^N \left[\frac{d}{dt} \langle x_i(t) x_i(t+\tau) \rangle - \left\langle x_i(t+\tau) \frac{dx_i(t)}{dt} \right\rangle \right] \quad (A3)
\end{aligned}$$

The second term on the righthand side of Eq. (A3) comes from the chain rule, followed by a trivial change of variable:

$$\begin{aligned}
\frac{d}{dt} \langle x_i(t) x_i(t+\tau) \rangle &= \left\langle \frac{dx_i(t)}{dt} x_i(t+\tau) \right\rangle + \left\langle x_i(t) \frac{dx_i(t+\tau)}{dt} \right\rangle \\
&= \left\langle \frac{dx_i(t)}{dt} x_i(t+\tau) \right\rangle + \left\langle x_i(t) \frac{dx_i(t+\tau)}{dt} \right\rangle .
\end{aligned}$$

The first term on the righthand side of Eq. (A3) is zero because the statistics of the Betchov system are time-stationary; with that term removed, Eq. (A3) yields .

$$-\frac{dH}{d\tau} = \frac{1}{N} \sum_{i=1}^N \left\langle x_i(t+\tau) \frac{dx_i(t)}{dt} \right\rangle .$$

From Eq. (A2), then,

$$-\frac{dH}{d\tau} = \frac{1}{N} \left\langle \sum_{i,j,k=1}^N C_{ijk} x_i(t+\tau) x_j(t) x_k(t) \right\rangle . \quad (A4)$$

It is useful now to introduce the shorthand notation

$$x_j = x_j(t)$$

and

$$x'_j = x_j(t+\tau) .$$

Now take the τ -derivative of both sides of Eq. (A4), make a trivial variable change, and use the ODE's again:

$$\begin{aligned} \frac{d^2 H}{d\tau^2} &= -\frac{1}{N} \left\langle \sum_{i,j,k=1}^N C_{ijk} x_j x_k \frac{dx'_i}{d\tau} \right\rangle \\ &= -\frac{1}{N} \left\langle \sum_{i,j,k=1}^N C_{ijk} x_j x_k \frac{dx'_i}{d\tau} \right\rangle \\ &= -\frac{1}{N} \left\langle \sum_{i,j,k=1}^N \left[C_{ijk} x_j x_k \sum_{p,q=1}^N C_{ipq} x'_p x'_q \right] \right\rangle \\ &= -\frac{1}{N} \sum_{i,j,k,p,q=1}^N C_{ijk} C_{ipq} \langle x_j x_k x'_p x'_q \rangle . \end{aligned}$$

Now make the cumulant-discard approximation on the quadruple moment $\langle x_j x_k x'_p x'_q \rangle$:

$$\begin{aligned} \frac{d^2 H_{CD}}{d\tau^2} &= -\frac{1}{N} \sum_{i,j,k,p,q=1}^N C_{ijk} C_{ipq} \left\{ \langle x_j x_k \rangle \langle x'_p x'_q \rangle + \langle x_j x'_p \rangle \langle x_k x'_q \rangle + \right. \\ &\quad \left. \langle x_j x'_q \rangle \langle x_k x'_p \rangle \right\} . \end{aligned} \quad (A5)$$

Now make use of the statistical independence of the variables in the Betchov system, which implies $\langle x_i x'_j \rangle = 0$ if $i \neq j$:

$$\frac{d^2 H_{\text{CD}}}{d\tau^2} = -\frac{1}{N} \sum_{i,j,k,p,q=1}^N C_{ijk} C_{ipq} \left\{ \delta_{jk} \delta_{pq} \langle x_j^2 \rangle \langle x_p'^2 \rangle + \delta_{jp} \delta_{kq} \langle x_j x_j' \rangle \langle x_k x_k' \rangle + \delta_{jq} \delta_{kp} \langle x_j x_j' \rangle \langle x_k x_k' \rangle \right\}. \quad (\text{A6})$$

A further consequence of the isotropy of the Betchov system is that $H_i = H_j = H \quad \forall i,j$. Using this, and $\langle x_j^2 \rangle = 1$, yields

$$\frac{d^2 H_{\text{CD}}}{d\tau^2} = -\frac{1}{N} \sum_{i,j,k,p,q=1}^N C_{ijk} C_{ipq} \left\{ \delta_{jk} \delta_{pq} + \delta_{jp} \delta_{kq} H_{\text{CD}}^2(\tau) + \delta_{jq} \delta_{kp} H_{\text{CD}}^2(\tau) \right\} \quad (\text{A7})$$

Next, note that since $C_{ijj} = 0$ the first term in the righthand side of Eq. (A7) is zero, and either the second or third term in braces is zero for all terms in the summation. This simplifies Eq. (A7) to

$$\frac{d^2 H_{\text{CD}}}{d\tau^2} = -\frac{1}{N} \left\{ \sum_{i,j,k=1}^N C_{ijk} C_{ijk} \right\} H_{\text{CD}}^2. \quad (\text{A8})$$

In the large- N limit, the quantity in braces in Eq. (A8) becomes $3M$ (where M is the number of coupling triplets) because of the random Gaussian coupling coefficients. Eq. (A8) becomes

$$\frac{d^2 H_{\text{CD}}}{d\tau^2} = -\frac{3M}{N} H_{\text{CD}}^2.$$

This equation can now be solved for $H_{\text{CD}}(\tau)$ with the initial condition $H_{\text{CD}}(0) = 1$. A numerical solution is plotted in Fig. A1 (solid curve);

it has the proper behavior near $\tau = 0$, then plummets to $-\infty$ as τ increases. This is clearly not a valid approximation for the true autocorrelation function, which goes to zero as τ becomes large.

Figure A1

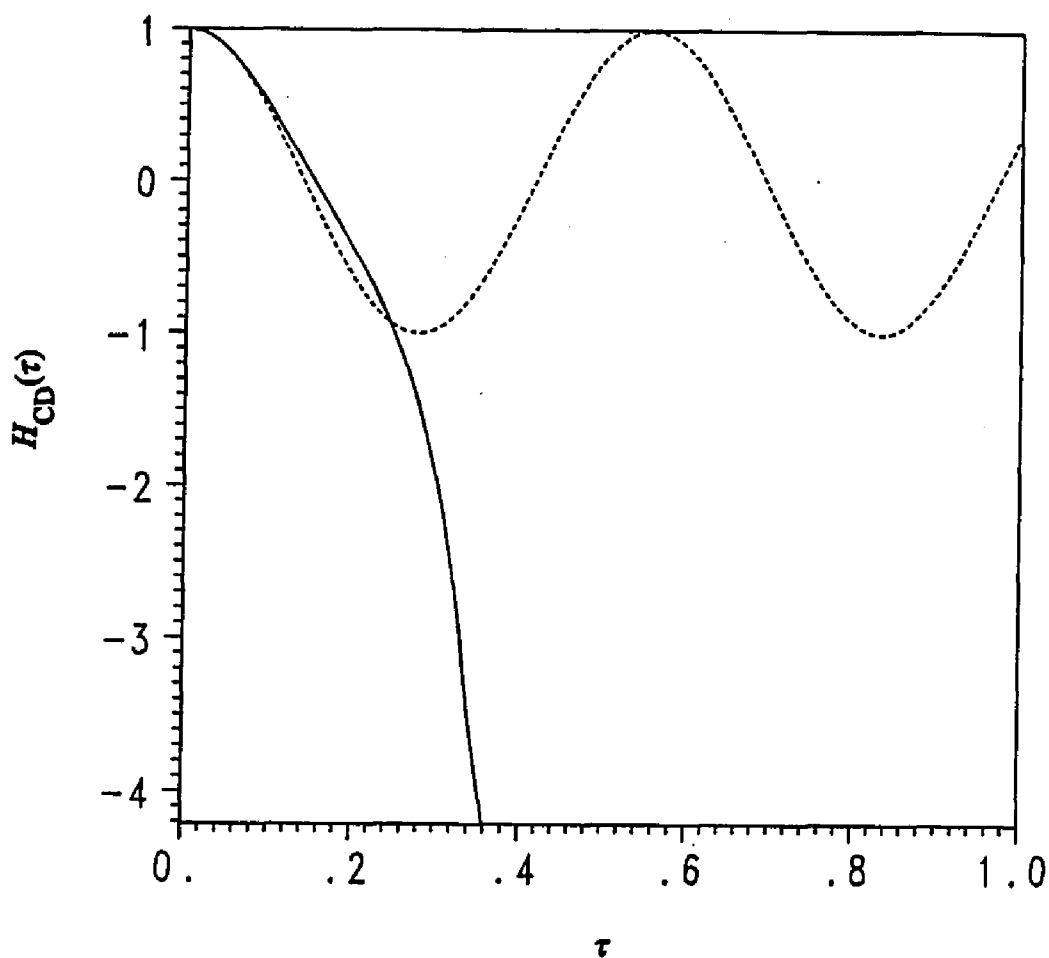


Figure A1. Two cumulant-discard approximations to the autocorrelation function for the Betchov system. The solid curve is the solution to the equation immediately following Eq. (A8); this function goes to $-\infty$. The dashed curve is the solution to the equation immediately following Eq. (A12), which is a cosine function. For both curves, $N = 96$ and $M = 4N^2/9$.

A second approach using the cumulant-discard approximation begins by time-differentiating both sides of Eq. (A1), then multiplying by $x_i(t+\tau)$, summing over i , and ensemble averaging as before:

$$\frac{1}{N} \sum_{i=1}^N \left\langle x'_i \frac{d^2 x_i}{dt^2} \right\rangle = \frac{1}{N} \left\langle \sum_{i=1}^N x'_i \sum_{j,k=1}^N C_{ijk} \left[x_j \frac{dx_k}{dt} + x_k \frac{dx_j}{dt} \right] \right\rangle \quad (\text{A9})$$

The lefthand side of Eq. (A9) is equal to $d^2 H(\tau)/d\tau^2$, as can be seen by explicit calculation; using the chain rule twice, trivial variable changes, and twice using the time-stationarity of the Betchov system,

$$\begin{aligned} \frac{1}{N} \sum_{i=1}^N \left\langle x'_i \frac{d^2 x_i}{dt^2} \right\rangle &= \frac{1}{N} \sum_{i=1}^N \left\langle \frac{d}{dt} \left[x'_i \frac{dx_i}{dt} \right] - \frac{dx_i}{dt} \frac{dx'_i}{dt} \right\rangle \\ &= \frac{1}{N} \sum_{i=1}^N \left\{ \frac{d}{dt} \left\langle x_i \frac{dx_i}{dt} \right\rangle - \left[\left\langle \frac{dx_i}{dt} \frac{dx'_i}{dt} \right\rangle \right] \right\} \\ &= \frac{1}{N} \sum_{i=1}^N \left\{ 0 - \left[\frac{d}{dt} \left\langle x_i \frac{dx'_i}{dt} \right\rangle - \left\langle x_i \frac{d^2 x'_i}{dt^2} \right\rangle \right] \right\} \\ &= \frac{1}{N} \sum_{i=1}^N \left\{ 0 - \left[0 - \left\langle x_i \frac{d^2 x'_i}{d\tau^2} \right\rangle \right] \right\} \\ &= \frac{1}{N} \sum_{i=1}^N \left\langle x_i \frac{d^2 x'_i}{d\tau^2} \right\rangle \\ &= \frac{d^2 H}{d\tau^2} . \end{aligned}$$

From Eq. (A9), then,

$$\frac{d^2 H}{d\tau^2} = \sum_{i,j,k=1}^N C_{ijk} \left\langle x'_i \left[x_j \frac{dx_k}{dt} + x_k \frac{dx_j}{dt} \right] \right\rangle .$$

Using the ODE's, this becomes

$$\begin{aligned} \frac{d^2 H}{d\tau^2} &= \frac{1}{N} \sum_{i,j,k=1}^N C_{ijk} \sum_{p,q=1}^N \left\langle x'_i \left\{ C_{kpq} x_j x_p x_q + C_{j pq} x_k x_p x_q \right\} \right\rangle \\ &= \frac{1}{N} \sum_{i,j,k=1}^N C_{ijk} \sum_{p,q=1}^N \left\{ C_{kpq} \langle x'_i x_j x_p x_q \rangle + C_{j pq} \langle x'_i x_k x_p x_q \rangle \right\} . \end{aligned}$$

Now make the cumulant-discard approximation on the quadruple moments $\langle x'_i x_j x_p x_q \rangle$ and $\langle x'_i x_k x_p x_q \rangle$:

$$\begin{aligned} \frac{d^2 H_{CD}}{d\tau^2} &= \\ &\frac{1}{N} \sum_{i,j,k=1}^N C_{ijk} \sum_{p,q=1}^N \left\{ C_{kpq} \left[\langle x'_i x_j \rangle \langle x_p x_q \rangle + \langle x'_i x_p \rangle \langle x_j x_q \rangle + \langle x'_i x_q \rangle \langle x_j x_p \rangle \right] \right. \\ &\quad \left. + C_{j pq} \left[\langle x'_i x_k \rangle \langle x_p x_q \rangle + \langle x'_i x_p \rangle \langle x_k x_q \rangle + \langle x'_i x_q \rangle \langle x_k x_p \rangle \right] \right\} . \end{aligned}$$

Now use the isotropy of the Betchov system and $\langle x_i^2 \rangle = 1$ (as was done before with Eq. (A5) and Eq. (A6)) to yield

$$\frac{d^2 H_{CD}}{d\tau^2} = \frac{1}{N} \sum_{i,j,k=1}^N C_{ijk} \sum_{p,q=1}^N \left\{ C_{kpq} \left[\delta_{ij} \delta_{pq} H_{CD} + \delta_{ip} \delta_{jq} H_{CD} + \delta_{iq} \delta_{jp} H_{CD} \right] \right\}$$

$$+ C_{j pq} \left[\delta_{ik} \delta_{pq} H_{CD} + \delta_{ip} \delta_{kq} H_{CD} + \delta_{iq} \delta_{kp} H_{CD} \right] \} . \quad (\text{A10})$$

Next, note that since $C_{ijj} = 0$ the first term in each pair of square brackets contributes zero to the total sum, and either the second or third term in each pair of brackets contributes zero for all terms in the total sum. This simplifies Eq. (A10) to

$$\begin{aligned} \frac{d^2 H_{CD}}{d\tau^2} &= \frac{1}{N} \sum_{i,j,k=1}^N C_{ijk} \left\{ C_{kij} H_{CD} + C_{kji} H_{CD} + C_{jik} H_{CD} + C_{jki} H_{CD} \right\} \\ &= \frac{1}{N} H_{CD}(\tau) \left\{ \sum_{i,j,k=1}^N C_{ijk} \left[C_{kij} + C_{kji} + C_{jik} + C_{jki} \right] \right\} . \quad (\text{A11}) \end{aligned}$$

In the large- N limit, the quantity in braces in Eq. (A11) can be simplified by using several relations which arise because of the independent random Gaussian coupling coefficients:

$$\sum_{i,j,k=1}^N C_{ijk} C_{jki} = 0 = \sum_{i,j,k=1}^N C_{ijk} C_{jik}$$

and

$$\sum_{i,j,k=1}^N C_{ijk} C_{kij} = -\frac{3}{2} M = \sum_{i,j,k=1}^N C_{ijk} C_{jki} . \quad (\text{A12})$$

Using these in Eq. (A11) yields

$$\begin{aligned} \frac{d^2 H_{\text{CD}}}{d\tau^2} &= \frac{1}{N} H_{\text{CD}}(\tau) \left\{ \sum_{i,j,k=1}^N C_{ijk} [C_{kij} + C_{jki}] \right\} \\ &= \frac{1}{N} H_{\text{CD}} \{-3M\} \end{aligned}$$

$$\frac{d^2 H_{\text{CD}}}{d\tau^2} = -\frac{3M}{N} H_{\text{CD}} .$$

This equation can now be solved for $H_{\text{CD}}(\tau)$. The solution (with $H_{\text{CD}}(0) = 1$) is

$$H_{\text{CD}}(\tau) = \cos\left[\sqrt{3M/N} \tau\right] ,$$

which is plotted in Fig. A1 (dashed curve). This is also clearly not a valid approximation for the true autocorrelation function.

APPENDIX B: DIA SOLUTION OF THE BETCHOV SYSTEM

A. Derivation of $H_{\text{DIA}}(\tau)$	116
B. Numerical solution: code	137

A. Derivation of $H_{\text{DIA}}(\tau)$

The DIA calculation of the autocorrelation function begins with the definition:

$$H(\tau) = \frac{1}{N} \sum_{i=1}^N \langle x_i(t) x_i(t+\tau) \rangle .$$

Now take the τ derivative of both sides, as done at the beginning of Appendix A. The result is

$$\frac{dH(\tau)}{d\tau} = - \frac{1}{N} \sum_{j,k=1}^N C_{ijk} \langle x_i(t+\tau) x_j(t) x_k(t) \rangle . \quad (\text{B1})$$

The DIA is a way to approximate the triple correlations on the righthand side of Eq. (B1) using a response function. Basically, it expresses the triple moments in terms of quadruple moments (the next stage in the moment hierarchy), then replaces the quadruple moments by response-function weighted products of double moments.

The cumulant discard approximation (Appendix A) made the same kind of moment-hierarchy truncation and yielded results for $H(\tau)$ that were good for small τ , then diverged from the correct form. The DIA is a

means to remove the high- τ errors resulting from the hierarchy truncation. It does so by the introduction of a decaying response function called the *regression function*.

To define the regression function, consider the effect of perturbing one variable in a Betchov system with a small impulse at a fixed time t_p . For a specific example, imagine that variable x_5 perturbed by an amount ε at time t_p . This perturbation changes the time evolution of x_5 from its unperturbed path; because of the turbulence of the system, the perturbed $x_5^p(t)$ eventually deviates strongly from the unperturbed $x_5^u(t)$. Define the difference between these two evolutions as Δx_5 :

$$\Delta x_5(t) = x_5^p(t) - x_5^u(t) . \quad (B2)$$

The general shape of this function Δx_5 is shown in Fig. B1. If different realizations of the Betchov system were perturbed at variable x_5 in the same way, their Δx_5 functions would deviate strongly from each other at long times; this is depicted by the curves in Fig. B2. The curves would average to zero, however. Define the regression function for variable 5 as

$$G_5(\tau) = \left\langle \frac{\Delta x_5(\tau)}{\varepsilon} \right\rangle ; \quad \tau = t - t_p .$$

This function is depicted in Fig. B3.

The ensemble of x_5 's is perturbed at time t_p from a Gaussian probability distribution. The regression function describes the "regression" of their distribution back to Gaussian. The energy ε of the impulse is redistributed among all variables in each realization.

Figure B1

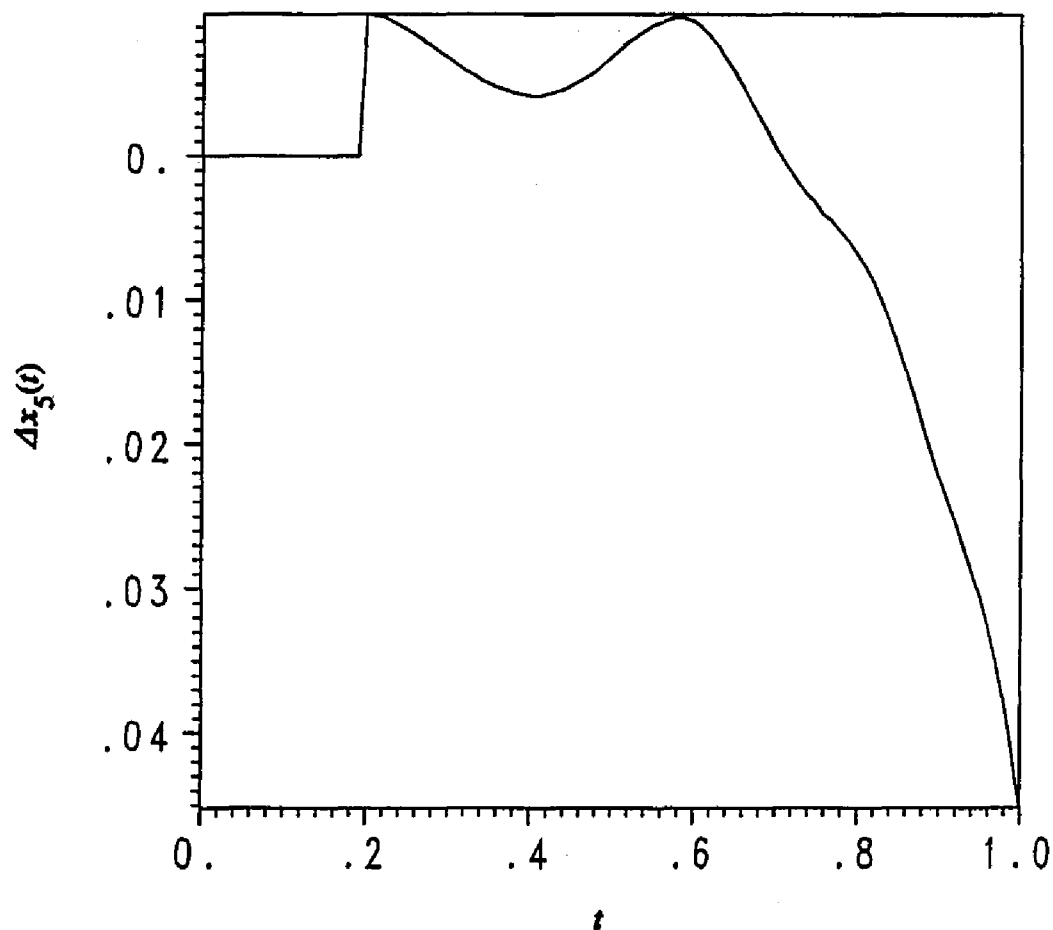


Figure B1. The function $\Delta x_5(t)$ calculated numerically for a single realization of a Betchov system with $N = 96$; in the perturbed system, variable x_5 was perturbed by $\varepsilon = 0.01$ at time $t_p = 0.2$. The long-time growth of this function indicates how the perturbed system deviates strongly from the unperturbed system.

Figure B2

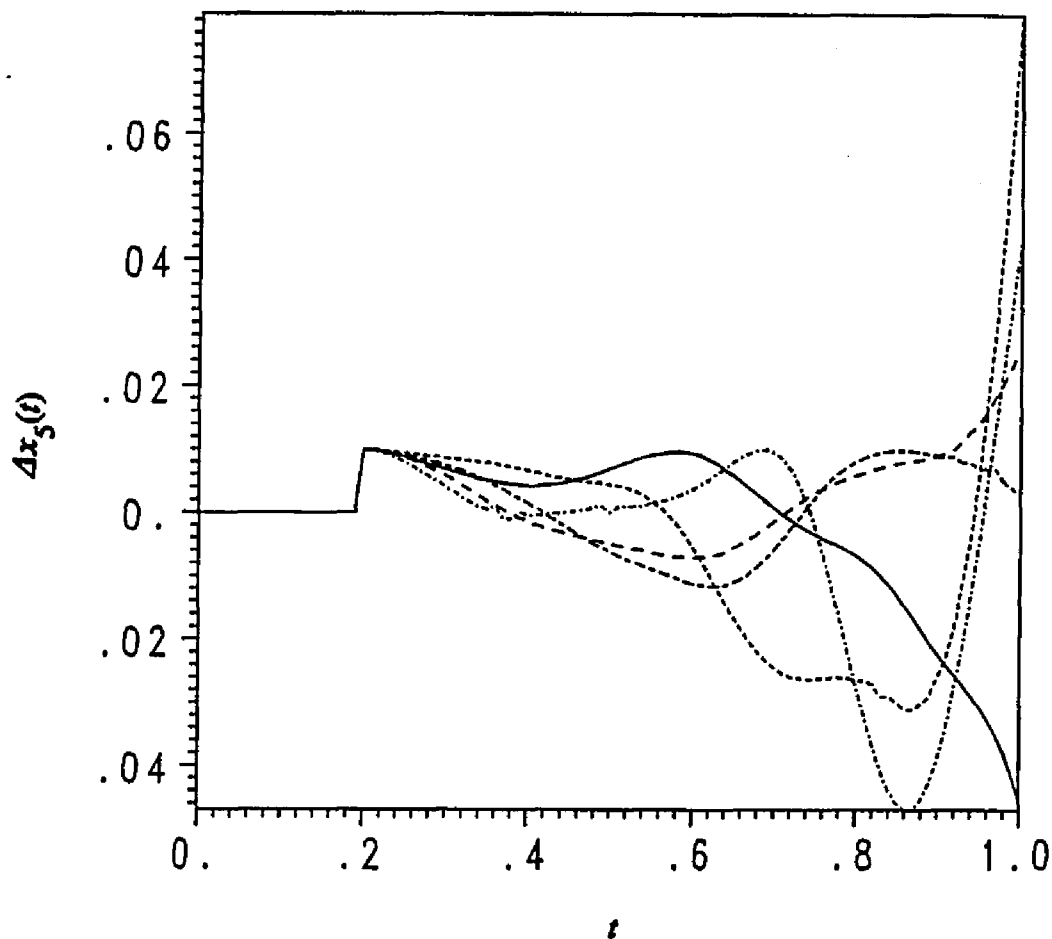


Figure B2. The function $\Delta x_5(t)$ calculated numerically for five realizations of a Betchov system with $N = 96$; in the perturbed systems, variable x_5 was perturbed by $\varepsilon = 0.01$ at time $t_p = 0.2$. The way the curves spread out from each other (and average to zero at long times) indicates the sensitive dependence of the system to initial conditions.

Figure B3

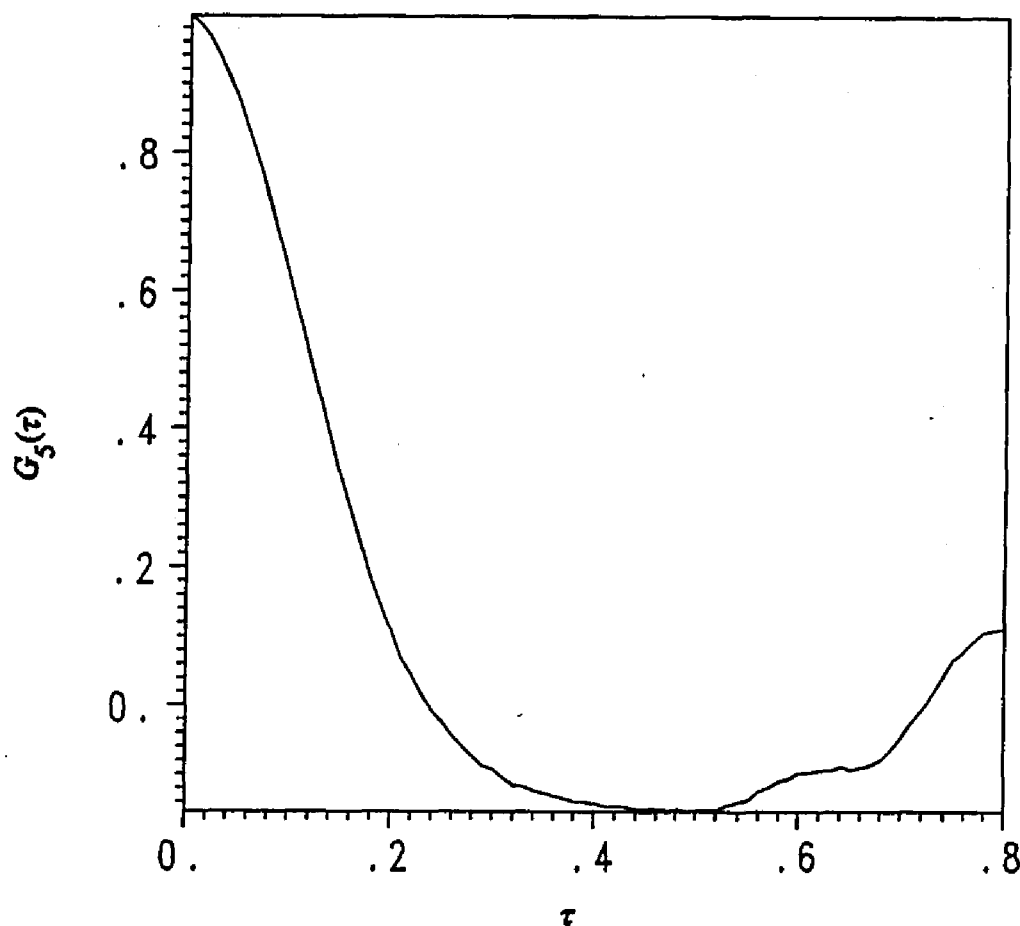


Figure B3. The single-variable regression function $G_5(\tau)$ calculated numerically for an ensemble of 128 Betchov systems with $N = 96$; in the perturbed systems variable x_5 was perturbed by $\varepsilon = 0.01$ at time $t_p = 0.2$, which corresponds to $\tau = 0$. Note the decay of the function to zero, followed by fluctuations about zero.

Now imagine that x_5 is perturbed by a continuous perturbing function $f(t)$ instead of just pulsed at t_p . That is

$$\frac{dx_5}{dt} = \sum_{j,k=1}^N C_{5jk} x_j x_k + f(t) . \quad (\text{B3})$$

Formally, one can solve this equation for $x_5(t)$:

$$x_5(t) = \mathcal{R}_5(t) + \int_{-\infty}^t G_5(t-s) f(s) ds . \quad (\text{B4})$$

In a linear system, $\mathcal{R}_5(t)$ would be $x_5^u(t)$ and $G_5(t)$ a Green's function. In a nonlinear system, $\mathcal{R}_5(t)$ is "closely related" ¹⁹ to $x_5^u(t)$; it contains the effects of the initial conditions and the unpredictable effects of $f(t)$ (unpredictable in the sense that the same $f(t)$ yields radically different effects when applied to systems with different initial conditions). The integral contains the effects of f that can be predicted via the regression function.

Consider now the ensemble averaged effect of f :

$$\langle f(t+\tau) x_5(t) \rangle = \langle f(t+\tau) \mathcal{R}_5(t) \rangle + \int_{-\infty}^t G_5(t-s) \langle f(t+\tau) f(s) \rangle ds . \quad (\text{B5})$$

The first term on the righthand side of Eq. (B5) is assumed to be zero because an average over unpredictable (fluctuating) effects is zero for the Betchov system. Then

$$\begin{aligned}
\langle f(t+\tau) x_5(t) \rangle &= \int_{-\infty}^t G_5(t-s) \langle f(t+\tau) f(s) \rangle ds \\
&= \int_{-\infty}^t G_5(t-s) h(t+\tau-s) ds
\end{aligned} \tag{B6}$$

where

$$h(\tilde{\tau}) = \langle f(\tilde{t}) f(\tilde{t}+\tilde{\tau}) \rangle .$$

(In Eq. (B6) $\tilde{t} = s$ and $\tilde{t}+\tilde{\tau} = t+\tau$.)

So far, these manipulations are purely formal. In preparation for developing the approximations of the DIA, consider now a specific single triple moment of Betchov-system variables: $\langle x_6(t+\tau) x_2(t) x_9(t) \rangle$. The first assumption of the DIA is that *this moment is zero if $\{6,2,9\}$ is not a triplet of coupled variable indices* (that is, if $C_{629} = C_{296} = C_{962} = 0$). This causes neglect of indirect effects by keeping only the direct effects of triplet interactions. Betchov argues¹⁹ that even with the worst possible choice of random couplings, the ratio of indirect-interaction (i.e., indirect-coupling with $C_{629} = 0$) contributions to this triple moment to the direct-interaction triplet moment is $O(1/N)$.

To calculate the effects of the direct interactions, imagine first that $\{2,9,6\}$ is not a coupled triplet. In this case, the moment $\langle x_6(t+\tau) x_2(t) x_9(t) \rangle$ is zero. Now "switch on" only the coupling coefficient C_{296} , leaving $C_{962} = 0 = C_{629}$; this adds one term to the righthand side of the ODE for x_2 , namely $C_{296} x_9 x_6$:

$$\frac{dx_2}{dt} = \sum_{j,k=1}^N C_{2jk} x_j x_k + C_{296} x_9(t) x_6(t) . \quad (\text{B7})$$

Here Σ'' indicates summation over all couplings to x_2 except C_{296} . This single term plays the role that $f(t)$ played in Eq. (B3) for x_5 . Replacing $f(t)$ with this term and replacing x_5 with x_2 in Eq. (B4) yields

$$x_2(t) = \mathcal{X}_2(t) + \int_{-\infty}^t G_2(t-s) C_{296} x_9(s) x_6(s) ds .$$

So

$$\begin{aligned} \langle x_6(t+\tau) x_2(t) x_9(t) \rangle &= \langle x_6(t+\tau) \mathcal{X}_2(t) x_9(t) \rangle + \\ &\int_{-\infty}^t G_2(t-s) C_{296} \langle x_9(t) x_9(s) x_6(t+\tau) x_6(s) \rangle ds . \quad (\text{B8}) \end{aligned}$$

If $\mathcal{X}_2(t)$ is equal to the "unperturbed" $x_2^u(t)$ (the solution in which C_{296} is not "switched on," then the first term on the righthand side of Eq. (B8) is zero. Since $\mathcal{X}_2(t)$ is a fluctuating quantity closely related to $x_2^u(t)$, the DIA assumes that the first term on the righthand side of Eq. (B8) is zero. Then

$$\langle x_6(t+\tau) x_2(t) x_9(t) \rangle = \int_{-\infty}^t G_2(t-s) C_{296} \langle x_9(t) x_9(s) x_6(t+\tau) x_6(s) \rangle ds . \quad (\text{B9})$$

The second major assumption of the DIA is that the quadruple moment in Eq. (B9) can be replaced with a product of two double moments:

$$\langle x_9(t) x_9(s) x_6(t+\tau) x_6(s) \rangle = \langle x_9(t) x_9(s) \rangle \langle x_6(t+\tau) x_6(s) \rangle .$$

Why is this legitimate here when it failed in the cumulant-discard approximation in Appendix A? The reason is that the quadruple moment in Eq. (B9) is multiplied by a regression function which decays to zero as its argument becomes large. Since the cumulant-discard approximation fails at large time separations, where the regression function is zero, it is acceptable for use in Eq. (B9). So

$$\begin{aligned} \langle x_6(t+\tau) x_2(t) x_9(t) \rangle &= \int_{-\infty}^t G_2(t-s) C_{296} \langle x_9(t) x_9(s) \rangle \langle x_6(t+\tau) x_6(s) \rangle ds \\ &= C_{296} \int_{-\infty}^t G_2(t-s) H_9(t-s) H_6(t+\tau-s) ds . \end{aligned} \quad (\text{B10})$$

Next, switch off the coupling C_{296} and switch on the coupling C_{629} . This adds one term to the righthand side of the ODE for x_6 , namely $C_{629} x_2 x_9$:

$$\frac{dx_6(t+\tau)}{dt} = \sum_{j,k=1}^N C_{6jk} x_j(t+\tau) x_k(t+\tau) + C_{629} x_2(t+\tau) x_9(t+\tau) ,$$

where Σ'' is defined as in Eq. (B7). Following the previous example, then,

$$\begin{aligned}
\langle x_6(t+\tau) x_2(t) x_9(t) \rangle &= \int_{-\infty}^{t+\tau} G_2(t+\tau-s) C_{629} \langle x_2(t) x_2(s) x_9(t) x_9(s) \rangle ds \\
&= \int_{-\infty}^{t+\tau} G_2(t+\tau-s) C_{629} \langle x_2(t) x_2(s) \rangle \langle x_9(t) x_9(s) \rangle ds \\
&= C_{629} \int_{-\infty}^{t+\tau} G_2(t+\tau-s) H_2(t-s) H_9(t-s) ds \quad . \quad (B11)
\end{aligned}$$

Next, switch off the coupling C_{629} and switch on the coupling C_{962} . This adds one term to the righthand side of the ODE for x_9 , namely $C_{962} x_6 x_2$:

$$\frac{dx_9}{dt} = \sum_{j,k=1}^N C_{9jk} x_j(t) x_k(t) + C_{962} x_6(t) x_2(t) \quad ,$$

where Σ'' is defined as in Eq. (B7). Following the previous two examples, then,

$$\begin{aligned}
\langle x_6(t+\tau) x_2(t) x_9(t) \rangle &= \int_{-\infty}^t G_9(t-s) C_{962} \langle x_6(t+\tau) x_6(s) x_2(t) x_2(s) \rangle ds \\
&= \int_{-\infty}^t G_9(t-s) C_{962} \langle x_6(t+\tau) x_6(s) \rangle \langle x_2(t) x_2(s) \rangle ds \\
&= C_{962} \int_{-\infty}^t G_9(t-s) H_6(t+\tau-s) H_2(t-s) ds \quad . \quad (B12)
\end{aligned}$$

Now invoke the isotropy of the Betchov system:

$$H_i(\tau) = H(\tau) = \frac{1}{N} \sum_{j=1}^N H_j(\tau) \quad \forall i \quad (\text{B13})$$

and

$$G_i(\tau) = G(\tau) = \frac{1}{N} \sum_{j=1}^N G_j(\tau) \quad \forall i \quad (\text{B14})$$

With the use of these, Equations (B10), (B11), and (B12) become

$$\langle x_6(t+\tau) x_2(t) x_9(t) \rangle = C_{296} \int_{-\infty}^t G(t-s) H(t-s) H(t+\tau-s) ds \quad , \quad (\text{B15})$$

$$\langle x_6(t+\tau) x_2(t) x_9(t) \rangle = C_{629} \int_{-\infty}^{t+\tau} G(t+\tau-s) H^2(t-s) ds \quad , \quad (\text{B16})$$

and

$$\langle x_6(t+\tau) x_2(t) x_9(t) \rangle = C_{962} \int_{-\infty}^t G(t-s) H(t+\tau-s) H(t-s) ds \quad . \quad (\text{B17})$$

These three expressions are the values of $\langle x_6(t+\tau) x_2(t) x_9(t) \rangle$ which come from the three *independent* direct interactions C_{296} , C_{629} , and C_{962} .

Now make the third major assumption of the DIA (a "linearity"

assumption): With the triplet $\{6,2,9\}$ in the system, $\langle x_6(t+\tau) x_2(t) x_9(t) \rangle$ is the sum of the expressions in Eq. (B15), Eq. (B16), and Eq. (B17). This is simple, and any calculation without this assumption is terribly complicated. Because of the time-stationarity of the Betchov system the lefthand sides of Eq. (B15), Eq. (B16), and Eq. (B17) are t -independent. Therefore one is free to choose $t = 0$ on the righthand sides. Doing this, and adding the three righthand sides yields

$$\begin{aligned} \langle x_6(t+\tau) x_2(t) x_9(t) \rangle &= C_{629} \int_{-\infty}^{\tau} G(\tau-s) H^2(-s) ds \\ &+ [C_{296} + C_{962}] \int_{-\infty}^0 G(-s) H(\tau-s) H(-s) ds . \quad (\text{B18}) \end{aligned}$$

Now use the cyclic property of the coupling coefficients,

$$C_{296} + C_{962} + C_{629} = 0 ,$$

and the symmetry of the autocorrelation function,^{19,†}

$$H(-\tau) = H(\tau) .$$

Using these and splitting the first integral in Eq. (B18) into two parts yields

[†] The symmetry of H is required because of statistical stationarity.

$$\begin{aligned}
\langle x_6(t+\tau) x_2(t) x_9(t) \rangle &= C_{629} \left\{ \int_{-\infty}^0 G(\tau-s) H^2(s) ds + \int_0^{\tau} G(\tau-s) H^2(s) ds \right\} \\
&\quad - C_{629} \int_{-\infty}^0 G(-s) H(\tau-s) H(s) ds \\
&= C_{629} \int_0^{\tau} G(\tau-s) H^2(s) ds \\
&\quad + C_{629} \int_{-\infty}^0 H(s) [G(\tau-s) H(s) - G(-s) H(\tau-s)] ds .
\end{aligned}$$

Now, following the pattern set for $\langle x_6(t+\tau) x_2(t) x_9(t) \rangle$, make the same approximation for $\langle x_i(t+\tau) x_j(t) x_k(t) \rangle$ for all triplets $\{i,j,k\}$ in the system. Now plug the results of this into Eq. (B1), then use the properties of the coupling coefficients [refer to Appendix A, Eq. (A12)]:

$$\begin{aligned}
\frac{dH(\tau)}{d\tau} &= -\frac{1}{N} \sum_{j,k=1}^N C_{ijk} \langle x_i(t+\tau) x_j(t) x_k(t) \rangle \\
&= -\frac{1}{N} \left[\sum_{j,k=1}^N C_{ijk}^2 \right] \left\{ \int_0^{\tau} G(\tau-s) H^2(s) ds + \right. \\
&\quad \left. \int_{-\infty}^0 H(s) [G(\tau-s) H(s) - G(-s) H(\tau-s)] ds \right\} \\
&= -\frac{1}{N} (3M) \left\{ \int_0^{\tau} G(\tau-s) H^2(s) ds + \right. \\
&\quad \left. \int_{-\infty}^0 H(s) [G(\tau-s) H(s) - G(-s) H(\tau-s)] ds \right\} . \quad (B19)
\end{aligned}$$

This is an integro-differential equation for $H_{\text{DIA}}(\tau)$ which can be solved if the regression function $G(\tau)$ is known.

The second part of the DIA is the derivation of an equation for G which forms with Eq. (B19) a closed set of equations for H_{DIA} and G . To begin this derivation, consider once again pulsing x_5 in a Betchov system with a pulse of strength ε at time t_p . As before [Eq. (B2)], Δx_5 is the change in $x_5(t)$ resulting from the perturbation. Now consider also the changes in all other variables δx_j ($j \neq 5$) resulting from direct and indirect interactions with x_5 . An important assumption is that the changes δx_j are *smaller* than Δx_5 .

A long time after t_p , δx_j and Δx_5 both become large. Energy conservation forces the system to stay on the surface of an N -dimensional sphere¹⁹, but δx_j and Δx_5 both eventually become of the order of the radius of that sphere. A measure of the divergence of the perturbed solutions Δx_j is the function K :

$$K(\tau) = \left[\frac{1}{N} \sum_{i=1}^N G_i^2(\tau) \right]^{1/2} ; \tau = t - t_p .$$

Note that calculation of $K(\tau)$ requires running the ensemble of Betchov systems N times, perturbing a different variable x_j each run. The observed behavior is that K grows exponentially, but follows G for a short time; it follows G for longer times as N increases. This is seen in Fig. B4.

Figure B4

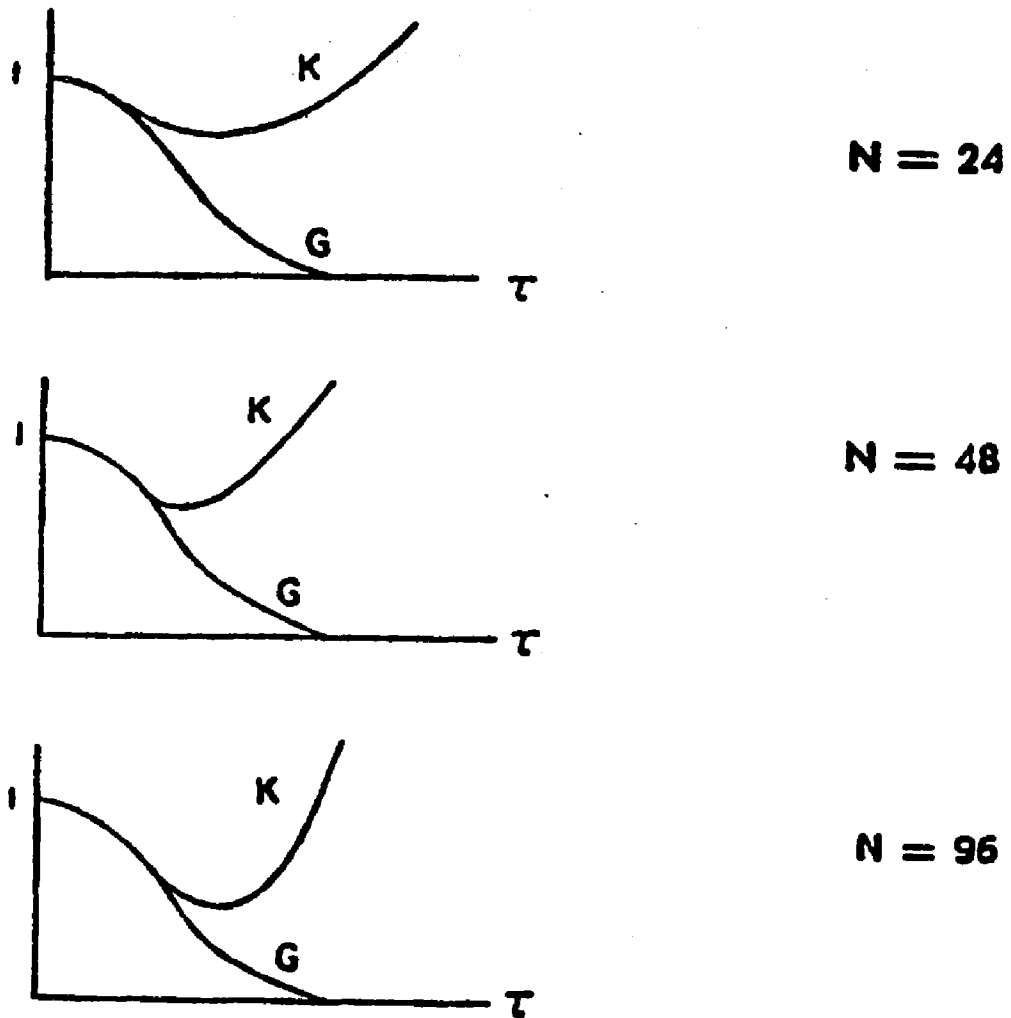


Figure B4. The functions $K(\tau)$ and $G(\tau)$ for three Betchov systems with increasing N ; the τ axes are scaled so that the curves can be compared easily. Note that $K(\tau)$ follows $G(\tau)$ for an increasing fraction of the decay time of G as N is increased. This figure is from a paper by Betchov.²⁰

Now proceed with the derivation of the equation for G by linearizing the solution of the Betchov system about the unperturbed solution. With

$$x_5^p(t) = x_5^u(t) + \Delta x_5(t) \quad (\text{B20})$$

and

$$x_j^p(t) = x_j^u(t) + \delta x_j(t) \quad \text{for } j \neq 5 ,$$

the linearized equations are derived as follows:

$$\begin{aligned} \frac{d}{dt} [x_5 + \Delta x_5] &= \sum_{j,k} C_{5jk} [(x_j^u + \delta x_j)(x_k^u + \delta x_k)] \\ &= \sum_{j,k} C_{5jk} [x_j^u x_k^u + x_j^u \delta x_k + \delta x_j x_k^u + \delta x_j \delta x_k] \\ \frac{d}{dt} \Delta x_5 &= \sum_{j,k} C_{5jk} [x_j^u \delta x_k + \delta x_j x_k^u] \end{aligned} \quad (\text{B21})$$

and

$$\begin{aligned} \frac{d}{dt} [x_j^u + \delta x_j] &= \sum_p C_{jp5} [(x_p^u + \delta x_p)(x_5^u + \Delta x_5)] \\ &\quad + \sum_q C_{j5q} [(x_q^u + \delta x_q)(x_5^u + \Delta x_5)] \\ &\quad + \sum_{p,q \neq 5} C_{jpq} [(x_q^u + \delta x_q)(x_q^u + \Delta x_q)] \quad ; \quad \forall j \neq 5 \end{aligned}$$

$$\begin{aligned}
&= \sum_p C_{jp5} \left[x_p^u x_5^u + x_5^u \delta x_p + \Delta x_5 x_p^u + \delta x_p \Delta x_5 \right] \\
&\quad + \sum_q C_{j5q} \left[x_5^u x_q^u + x_5^u \delta x_q + \Delta x_5 x_q^u + \Delta x_5 \delta x_q \right] \\
&\quad + \sum_{p,q \neq 5} C_{j pq} \left[x_p^u x_q^u + x_p^u \delta x_q + \delta x_p x_q^u + \delta x_p \Delta x_q \right] \\
&\hspace{20em} \forall j \neq 5 \\
\frac{d}{dt} \delta x_j &= \sum_p C_{jp5} \left[x_5^u \delta x_p + \Delta x_5 x_p^u \right] + \sum_q C_{j5q} \left[x_5^u \delta x_q + \Delta x_5 x_q^u \right] \\
&\quad + \sum_{p,q \neq 5} C_{j pq} \left[x_p^u \delta x_q + \delta x_p x_q^u \right] ; \forall j \neq 5 .(B22)
\end{aligned}$$

In this derivation, any double-small terms of the form $\delta x_i \Delta x_j$ or $\delta x_i \delta x_j$ have been neglected. Next, neglect the terms

$$\sum_p C_{jp5} x_5^u \delta x_p \quad \text{and} \quad \sum_q C_{j5q} x_5^u \delta x_q$$

because $|\Delta x_5| \gg |\delta x_j|$ and because the terms in these sums tend to cancel each other out. Also neglect

$$\sum_{p,q \neq 5} C_{j pq} \left[x_p^u \delta x_q + \delta x_p x_q^u \right]$$

purely because its terms tend to cancel each other out.¹⁹ (Because there are many more terms in this sum than in the previous two neglected sums, this is plausible.) With these terms removed, Eq. (B22) becomes

$$\frac{d}{dt} \delta x_j = \sum_p C_{jp5} \Delta x_5 x_p^u + \sum_q C_{j5q} \Delta x_5 x_q^u ; \forall j \neq k . \quad (B23)$$

Now use the regression function to approximate δx_j in Eq. (B23):

$$\delta x_j(t) = \sum_p C_{jp5} \int_{t_p}^t G(t-s) \Delta x_5(s) x_p^u(s) ds + \sum_q C_{j5q} \int_{t_p}^t G(t-s) \Delta x_5(s) x_q^u(s) ds .$$

Plug this result for δx_j (and the corresponding one for δx_k) into Eq. (B21):

$$\begin{aligned} \frac{d}{dt} \Delta x_5 = & \sum_{j,k} C_{5jk} \left\{ \left[\sum_p C_{kp5} \int_{t_p}^t G(t-s) x_j^u(t) \Delta x_5(s) x_p^u(s) ds \right. \right. \\ & \left. \left. + \sum_q C_{k5q} \int_{t_p}^t G(t-s) x_j^u(t) \Delta x_5(s) x_q^u(s) ds \right] \right. \\ & \left. + \left[\sum_p C_{jp5} \int_{t_p}^t G(t-s) x_k^u(t) \Delta x_5(s) x_p^u(s) ds \right. \right. \\ & \left. \left. + \sum_q C_{j5q} \int_{t_p}^t G(t-s) x_k^u(t) \Delta x_5(s) x_q^u(s) ds \right] \right\} . \end{aligned}$$

Because of the sum over j and k , the two terms in square brackets can be combined into one:

$$\begin{aligned} \frac{d}{dt} \Delta x_5 = & \sum_{j,k} C_{5jk} \left\{ 2 \left[\sum_p C_{jp5} \int_{t_p}^t G(t-s) x_k^u(t) \Delta x_5(s) x_p^u(s) ds \right. \right. \\ & \left. \left. + \sum_q C_{j5q} \int_{t_p}^t G(t-s) x_k^u(t) \Delta x_5(s) x_p^u(s) ds \right] \right\} . \quad (\text{B24}) \end{aligned}$$

Now divide both sides of Eq. (B24) by ε , ensemble average, and simplify:

$$\begin{aligned} \frac{d}{dt} G_5(t) = & 2 \sum_{j,k} C_{5jk} \left\{ \sum_p [C_{jp5} + C_{j5p}] \int_{t_p}^t G(t-s) \left\langle x_k^u \frac{\Delta x_5(s)}{\varepsilon} x_p^u(s) \right\rangle ds \right\} \\ = & 2 \sum_{j,k} C_{5jk} \left\{ \sum_p [C_{jp5} + C_{j5p}] \int_{t_p}^t G(t-s) \left\langle \frac{\Delta x_5(s)}{\varepsilon} \right\rangle \left\langle x_k^u(t) x_p^u(s) \right\rangle ds \right\} . \quad (\text{B25}) \end{aligned}$$

It is legitimate to bring $\langle \Delta x_5(s)/\varepsilon \rangle$ outside the triple moment because it can always be expressed as the sum of a fluctuating, zero-mean part plus a nonzero-mean part; the triple moment of the fluctuating part with $x_k^u(t)$ and $x_p^u(s)$ (which are also fluctuating, zero-mean quantities) is zero. The nonzero mean part of $\Delta x_5(s)/\varepsilon$ is just $G_5(s)$.

Using the definition of $G_5(s)$ and the isotropy of the Betchov system as manifested in Eq. (B13) and

$$\langle x_k x_p \rangle = H_k \delta_{kp} = H \delta_{kp} ,$$

Eq. (B39) simplifies to

$$\frac{d}{dt} G_5(t) = 2 \sum_{j,k} C_{5jk} \left\{ \left[C_{jp5} + C_{j5p} \right] \int_{t_p}^t G(t-s) G_5(s) H_{\text{DIA}}(t-s) \delta_{kp} ds \right\} .$$

Now let $\tau \equiv t - t_p$; the equation for $G_5(\tau)$ is

$$\frac{d}{d\tau} G_5(\tau) = 2 \sum_{j,k} C_{5jk} \left\{ \left[C_{jk5} + C_{j5k} \right] \int_0^\tau G(\tau-s) G_5(s) H_{\text{DIA}}(\tau-s) ds \right\} .$$

Next, repeat the procedure begun at Eq. (B20) to construct equations for $G_i(\tau)$ for all $i \neq 5$. Add the resulting equations and divide by N ; also use the symmetry relation Eq. (B14) and the properties of the couplings:

$$\begin{aligned} \frac{1}{N} \sum_{i=1}^N G_i(\tau) &= \frac{1}{N} \sum_{i=1}^N \left\{ 2 \sum_{j,k} C_{ijk} \left[\left[C_{jki} + C_{jik} \right] \int_0^\tau G(\tau-s) G_i(s) H_{\text{DIA}}(\tau-s) ds \right] \right\} \\ &= \frac{2}{N} \left[\sum_{i,j,k} C_{ijk} C_{jki} + \sum_{i,j,k} C_{ijk} C_{jik} \right] \left[\int_0^\tau G(\tau-s) G(s) H_{\text{DIA}}(\tau-s) ds \right] \\ &= \frac{2}{N} \left[-\frac{3}{2} M + 0 \right] \left[\int_0^\tau G(\tau-s) G(s) H_{\text{DIA}}(\tau-s) ds \right] \\ \frac{d}{d\tau} G(\tau) &= -\frac{3M}{N} \int_0^\tau G(\tau-s) G(s) H_{\text{DIA}}(\tau-s) ds . \end{aligned} \quad (\text{B26})$$

This equation, together with Eq. (B19), form a closed set of equations for $G(\tau)$ and $H_{\text{DIA}}(\tau)$, to be solved with the initial conditions $H_{\text{DIA}}(0) = 1 = G(0)$. If one chooses $G(\tau) = H_{\text{DIA}}(\tau)$ and uses the knowledge that $H_{\text{DIA}}(\tau) = H_{\text{DIA}}(-\tau)$, the second integral in Eq. (B19)

vanishes, leaving

$$\begin{aligned}
 \frac{d}{d\tau} H_{\text{DIA}}(\tau) &= -\frac{3M}{N} \int_0^{\tau} H_{\text{DIA}}(\tau-s) H_{\text{DIA}}^2(s) ds \\
 &= \frac{3M}{N} \int_{\tau}^0 H_{\text{DIA}}(\tau-s') H_{\text{DIA}}^2(s') ds' \\
 &\quad \text{(with } s' = \tau - s ; ds' = -ds) \\
 &= -\frac{3M}{N} \int_0^{\tau} H_{\text{DIA}}(\tau-s') H_{\text{DIA}}^2(s') ds' \\
 \frac{d}{d\tau} H_{\text{DIA}}(\tau) &= -\frac{3M}{N} \int_0^{\tau} H_{\text{DIA}}(\tau-s) H_{\text{DIA}}^2(s) ds \quad . \quad (\text{B27})
 \end{aligned}$$

Now Eq. (B26) has become

$$\begin{aligned}
 \frac{d}{d\tau} H_{\text{DIA}}(\tau) &= -\frac{3M}{N} \int_0^{\tau} H_{\text{DIA}}(\tau-s) H_{\text{DIA}}(s) H_{\text{DIA}}(\tau-s) ds \\
 &= -\frac{3M}{N} \int_0^{\tau} H_{\text{DIA}}(\tau-s) H_{\text{DIA}}^2(s) ds \quad . \quad (\text{B28})
 \end{aligned}$$

This is identical to Eq. (B27). The result of the choice $G = H$ is this single integro-differential equation for $H_{\text{DIA}}(\tau)$. Certainly the solution for this is a solution for $H_{\text{DIA}}(\tau)$, and it is almost certainly the unique solution.¹⁹

B. Numerical solution: code

c DIABET "DIA solution to model of BETchov" (10/6/87)

c Written by George Vahala.

```
dimension h(0:3000)
call dropfile(0)
call link("unit6=tty,unit7=(autoc,create,text)//")
```

c ntot is the number of timesteps.

```
ntot = 3000
```

```
write(6,*) 'Enter the value of N and the value of tmax:'
```

```
read(6,*) xn,tmax
```

c xi3m is the number of couplings.

```
xi3m = xn**2/2.25
```

```
tscale = 1.0/(sqrt((3.0*xi3m)/(1.0*xn)))
```

c del is the scaled timestep:

```
del = tmax/(ntot*tscale)
```

c Initial value for autocorrelation function, h:

```
h(0) = 1.
```

```
del3 = 3./(del*del)
```

```
del8 = 8.*del3/9.
```

```
del3p = 1. + del3
```

```
del8p = 1. + del8
```

```
a1 = (1. + 2.*del3/3.)**2 + 3.*del8
```

```
h(1) = .5*(sqrt(a1) - (1. + 2.*del3/3.))
```

```
a2 = del3p**2 - 4.*(4.*h(1)*h(1) - del3)*h(1)
```

```
h(2) = .5*(sqrt(a2) - del3p)
```

```
do 4 m=3,ntot
```

```
  if (mod(m,2).eq.0) go to 1
```

```
  sumo=0.
```

```
  do 5 i=1,m-1
```

```
    sumo=sumo+3.*h(m-i)*h(i)*h(i)
```

```
5  continue
```

```
  do 6 ii=3,m-3,3
```

```
    sumo=sumo-h(m-ii)*h(ii)*h(ii)
```

```
6  continue
```

```
  a5 = del8p**2 - 4.*(sumo - del8*h(m-1))
```

```
  h(m) = .5*(sqrt(a5) - del8p)
```

```
  go to 4
```

```
1  sume=0.
```

```
  do 8 j=1,(m-1),2
```

```
    sume=sume +4.*h(m-j)*h(j)*h(j)
```

```
8  continue
```

```
  do 9 jj=2,(m-2),2
```

```
        sume=sume + 2.*h(m-1)*h(m)*h(m)
9      continue
        a6 = del3p**2 - 4.*(sume - del3*h(m-1))
        h(m) = .5*(sqrt(a6) - del3p)
4      continue
```

c Output at most 101 time-values for h to file autoc; output
c at most 30 values to the screen:

```
        idum = 101
        write(7,*) idum
        write(6,10) (m*del*tscale,h(m),m=0,ntot,100)
        write(7,10) (m*del*tscale,h(m),m=0,ntot,30)
10      format(2f14.6)
        call exit
        end
```

APPENDIX C: CODE FOR CDS SOLUTION OF THE BETCHOV SYSTEM

```
c DSBC1 ("Decimation-Scheme Betchov solver using Constraint set 1")
c (CDS/full Betchov solver) (11/5/88)
```

```
real t,t0,tfinal,tdel,ttemp
integer itime,cmax,nsteps,shstep,ntmax
real h
integer r,s,n,c
common/parms/h,r,s,n,c
real xx(32,36,512),xsav(32,512),k1(32,512),k2(32,512),xx0(32,512)
common/vars/xx,xsav,k1,k2,xx0
real q(36,16384),qstar(36,16384),qmean(32),qsmean(32)
common/forces/q,qstar,qmean,qsmean
```

```
call dropfile(0)
call link('unit6=tty,unit5=(parms,text),
$ unit69=(htau,create,text),
$ unit77=(dout,create,text),unit66=(dsplot,create,text),
$ unit67=(qplot,create,text),unit68=(qsplot,create,text)')

```

```
c Initialize the constants and variables (and print initial output):
```

```
call initia(nsteps,cmax,t0,tfinal,shstep,tdel,ttemp)
c = 3
```

```
c (Maximum total number of constraints is equal to cmax)
```

```
c The time-loop:
```

```
do 5 itime=1,nsteps
t = t0 + itime*h
write(6,*) 't = ',t, ' c = ',c
```

```
c Save x1,x2,... from being overwritten during the Runge-Kutta:
```

```
do 43 i=1,s
do 45 j=1,r
xsav(i,j) = xx(i,1,j)
45 continue
43 continue
```

```
c The actual Runge-Kutta process:
```

```
c First stage:
```

```
call diffeq(k1)
do 7 i=1,s
do 8 j=1,r
xx(i,1,j) = xsav(i,j) + k1(i,j)
8 continue
7 continue
```

```
c Evaluate q(t+h):
```

```
if (n .ne. s) call stforc(itime)
```

```
c Second stage:
```

```

        call diffeq(k2)
        do 9 i=1,s
            do 10 j=1,r
                xx(i,1,j) = xsav(i,j) + 0.5*(k1(i,j) + k2(i,j))
10         continue
9         continue

```

c Output:

```

        if (amod(t,ttemp) .lt. 1.e-6) call out2(t,tdel,cmax,t0)

```

c Update time-history stored:

```

        if (n .ne. s) then
            call stintp
            if ((mod(itime,shstep) .eq. 0).or.(itime.lt.4)) then
                ntmax = c - 3 + 4
                do 2 k=ntmax,2,-1
                    do 4 i=1,s
                        do 6 j=1,r
                            q(k,(j+r*(i-1))) = q((k-1),(j+r*(i-1)))
                            qstar(k,(j+r*(i-1))) = qstar((k-1),(j+r*(i-1)))
                            xx(i,k,j) = xx(i,(k-1),j)
6                            continue
4                            continue
2                            continue

```

c Update the number of constraints to enforce:

```

        if (c .lt. cmax) c = c + 1
        endif
        endif
5    continue

```

```

        call exit
        end

```

c DIFFEQ ("DIFFERential EQUations")

c This subroutine contains the information in the set of ordinary

c differential equations. It evaluates the time derivatives of all

c realizations of the set of dynamical variables.

c Note: hxdxt(i,j) is h*(time derivative of jth realization of xi).

```

subroutine diffeq(hxdxt)
real hxdxt(32,512)
real h
integer r,s,n,c
common/parms/h,r,s,n,c
real xx(32,36,512),xsav(32,512),k1(32,512),k2(32,512),xx0(32,512)
common/vars/xx,xsav,k1,k2,xx0
real q(36,16384),qstar(36,16384),qmean(32),qsmean(32)
common/forces/q,qstar,qmean,qsmean
real cof(5462),wt
integer index(5462),m,m2
common/couple/cof,index,wt,m,m2

```

c Initialize

```

      do 1 i=1,s
        do 4 j=1,r
          hxdxt(i,j) = 0.0
4       continue
1       continue

c h times the deterministic part of the derivatives:
      do 2 k=1,(3*m)
        mm = index(k)/m2 + 1
        kk = (index(k) - (mm-1)*m2)/m + 1
        jj = index(k) - (mm-1)*m2 - (kk-1)*m
        do 5 j=1,r
          hxdxt(jj,j) = hxdxt(jj,j) + h*cof(k)*xx(mm,1,j)*xx(kk,1,j)
5       continue
2       continue

c For DAS, apply h times the stochastic forcing, q:
      if (n .ne. s) then
        do 3 i=1,s
          do 6 j=1,r
            hxdxt(i,j) = hxdxt(i,j) + h*q(1,(j+(i-1)*r))
6         continue
3       continue
      endif

      return
      end

c INITIA ("INITIALizations")
c This subroutine initializes the variables and constants.

      subroutine initia(nsteps,cmax,t0,tfinal,shstep,tdel,ttemp)
      real t0,tfinal,rnorm,qvar(32),qnorm(32),tdel,ttemp
      integer cmax,nsteps,shstep,outstp,seed
      real h
      integer r,s,n,c
      common/parms/h,r,s,n,c
      real xx(32,36,512),xsav(32,512),k1(32,512),k2(32,512),xx0(32,512)
      common/vars/xx,xsav,k1,k2,xx0
      real q(36,16384),qstar(36,16384),qmean(32),qsmean(32)
      common/forces/q,qstar,qmean,qsmean
      real cof(5462),wt
      integer index(5462),m,m2
      common/couple/cof,index,wt,m,m2

c Read in the relevant parameters:
      read(5,*) n,s,cmax,r,nsteps,t0,tfinal,shstep,seed

c Generate the coupling coefficients:
      call coefic(seed)

c Calculate the stepsize from t0, tfinal, and nsteps:
      h = (tfinal - t0)/(1.0*nsteps)

```



```

c The weighting for the statistical interpolation:
  wt = sqrt(1.0*(n - s)/(1.0*s))

c Initialize xx by choosing random values from a Gaussian
c distribution with zero mean and unit variance. Use the Slatec
c function RGAUSS (see Document writeup Slatecv3).
  do 2 i=1,r
    do 3 j=1,s,1
      xx(j,1,i) = rgauss(0.0,1.0)
    3 continue
  2 continue

c Normalize xx so that every realiz. initially has e = 0.5n**2/s**2:
  do 4 j=1,r
    rnorm = 0.0
    do 5 k=1,s
      rnorm = rnorm + xx(k,1,j)**2
    5 continue
    do 6 k=1,s
      xx(k,1,j) = sqrt(1.0*s/rnorm)*xx(k,1,j)
    6 continue
  4 continue

c For CDS, initialize stochastic forces for 1st Runge-Kutta stage of
c first timestep:
  if (n .ne. s) then
c Initialize q at random from a Gaussian distribution, and normalize so
c that <q**2> = <qstar**2>:
c Initial random q:
  do 13 i=1,r*s
    q(1,i) = rgauss(0.0,1.0)
  13 continue
c Calculate qstar and its variance; calculate norm of q:
  call stintp
  do 9 i=1,s
    qvar(i) = 0.0
    qnorm(i) = 0.0
    do 7 j=(r*(i-1)+1),(r*i),1
      qvar(i) = qvar(i) + qstar(1,j)**2/(r*1.0)
      qnorm(i) = qnorm(i) + q(1,j)**2/(r*1.0)
    7 continue
  9 continue
c Normalize q accordingly:
  do 11 i=1,s
    do 8 j=(r*(i-1)+1),(r*i),1
      q(1,j) = q(1,j)*sqrt(qvar(i))/sqrt(qnorm(i))
    8 continue
  11 continue
c Store initial x, q, and q* values for later use in unequal-t
c constraints:
  do 14 i=1,s
    do 15 j=1,r
      xx(i,2,j) = xx(i,1,j)

```

```

                q(2,(j+(i-1)*r)) = q(1,(j+(i-1)*r))
                qstar(2,(j+(i-1)*r)) = qstar(1,(j+(i-1)*r))
15      continue
14      continue
      endif

c Store initial x values in xx0 for computing autocorrelation:
      do 16 i=1,s
        do 17 j=1,r
          xx0(i,j) = xx(i,1,j)
17      continue
16      continue

c Print the chosen parameter values and the header for the summary
c output table to be printed as the program runs:

c Print the important parameters:
      write(77,*) 'n = ',n,'      s = ',s,'      r = ',r,'      cmax = ',cmax
      write(77,*) 't0 = ',t0,'      tfinal = ',tfinal,'      h = ',h
      write(77,*) 'shstep = ',shstep,'      m = ',m,'      seed = ',seed
      write(77,*)

c Print the header for the main output table:
      write(77,104)
104  format(3x,'t',6x,' <E> ',7x,' qm',9x,'qv',8x,'t-1 qq',7x,
      $      't-2 qq',6x,'t-3 qq')
      write(77,105)
105  format('_____',1x,6('_____',1x))

c Write the number of points to be plotted (outstp), r, s, n, s, cmax,
c t0, tfinal, and h to the plot data file(s):
      if (nsteps .gt. 100) then
        outstp = 101
      else
        outstp = nsteps + 1
      endif
      write(69,*) outstp
      write(66,167) outstp,r,s,n,s,cmax
      write(66,173) t0,tfinal,h
      if (n .ne. s) then
        write(67,167) outstp,r,s,n,s,cmax
        write(68,167) outstp,r,s,n,s,cmax
        write(67,173) t0,tfinal,h
        write(68,173) t0,tfinal,h
      endif
167  format(6i7)
173  format(3e12.4)

c Spacings for outputs and shiftings:
      tdel = (tfinal - t0)/20.0
      if (nsteps .gt. 100) then
        ttemp = (tfinal - t0)/100.0
      else
        ttemp = h
      endif

c Write the t=t0 data to the summary and plot files:

```

```

call out2(0.0,tdel,cmax,t0,xx0)

return
end

c COEFIC ("coupling COEFFicients")
c Generates s**2/2.25 coupling coefficient triplets for Betchov system
c of s variables. (For full-system run, N=S).

subroutine coefic(seed)
integer jj,kk,mm,icount,sp1,jj0,kk0,mm0,seed
real sqrt6m,ra,rb,rc
logical uniq3
real h
integer r,s,n,c
common/parms/h,r,s,n,c
real cof(5462),wt
integer index(5462),m,m2
common/couple/cof,index,wt,m,m2

c Constants and initalizations:
m = s**2/2.25
m2 = m**2
sp1 = s + 1
sqrt6m = 1.0/sqrt(6.0)
icount = 0

c Perform a specified number of calls to random number generators
c before beginning coefficient generation. This provides for running
c the same system with different sets of random couplings:
do 9 i=1,seed,1
dummy1 = rand(0.0)
dummy2 = rgauss(0.0,1.0)
9 continue

c Keep looping (up to one million times) until a complete set of unique
c couplings is found:
do 1 i=1,1000000
uniq3 = .true.
jj = sp1*rand(0.0)
if ((jj .ne. 0) .and. (jj .le. s)) then
kk = sp1*rand(0.0)
if ((kk .ne. 0) .and. (kk .le. s) .and. (kk .ne. jj)) then
mm = sp1*rand(0.0)
if ((mm .ne. 0) .and. (mm .le. s) .and.
$ (mm .ne. kk) .and. (mm .ne. jj)) then
c Test for uniqueness of triplet just generated:
do 2 j=1,icount,1
mm0 = index(j)/m2 + 1
kk0 = (index(j)-(mm0-1)*m2)/m + 1
jj0 = (index(j)-(mm0-1)*m2-(kk0-1)*m)
if ((mm.eq.mm0).or.(mm.eq.kk0).or.(mm.eq.jj0)) then
if ((kk.eq.mm0).or.(kk.eq.kk0).or.(kk.eq.jj0)) then
if ((jj.eq.mm0).or.(jj.eq.kk0).or.(jj.eq.jj0)) then

```

```

                uniq3 = .false.
            endif
        endif
    endif
    2      continue
c If unique, set up coupling coefficients:
    if (uniq3) then
        index(icount+1) = jj + (kk-1)*m + (mm-1)*m2
        index(icount+2) = kk + (mm-1)*m + (jj-1)*m2
        index(icount+3) = mm + (jj-1)*m + (kk-1)*m2
        ra = rgauss(0.0,1.0)
        rb = rgauss(0.0,1.0)
        rc = rgauss(0.0,1.0)
        cof(icount+1) = (2.0*ra-rb-rc)*sqrt6m
        cof(icount+2) = (2.0*rb-rc-ra)*sqrt6m
        cof(icount+3) = (2.0*rc-ra-rb)*sqrt6m
        icount = icount + 3
c If m triplets generated, return:
        if ((icount/3) .ge. m) return
    endif
endif
endif
1  continue

write(77,*) 'Could not get unique set of coefics, million tries.'
call exit

return
end

c OUT2 ("OUTput of 2 types: summary and detailed")
c This subroutine writes out the variables (and q and qstar for CDS)
c for all realizations at all chosen timesteps (at most 100 times
c outputted). It also writes out summary information at a few
c spaced-out timesteps.

subroutine out2(t,tdel,cmax,t0)
real t,tdel,t0,c(512),qq(36),energy
integer cmax,ntimes
real h
integer r,s,n,c
common/parms/h,r,s,n,c
real xx(32,36,512),xsav(32,512),k1(32,512),k2(32,512),xx0(32,512)
common/vars/xx,xsav,k1,k2,xx0
real q(36,16384),qstar(36,16384),qmean(32),qsmean(32)
common/forces/q,qstar,qmean,qsmean

c Evaluate the energy; output all realizations of all variables:
c Also calculate newest qstar; output q(1) & qstar(1) for CDS runs:
sr = 1.0*s*r
c Energy:
do 1 i=1,r

```

```

        e(i) = 0.0
        do 2 j=1,s
            e(i) = e(i) + 0.5*(1.0*n/(1.0*s))*xx(j,1,i)**2
2       continue
1       continue
c Output; format allows two extra numbers--use e(j):
        do 3 j=1,r
            write(66,100) (xx(i,1,j),i=1,s),e(j),e(j)
3       continue
c For CDS runs:
        if (n .ne. s) then
c Get newest qstar:
            call stintp
            do 5 j=1,r
                write(67,100) (q(1,(j+(i-1)*r)),i=1,s),e(j),e(j)
                write(68,100) (qstar(1,(j+(i-1)*r)),i=1,s),e(j),e(j)
5         continue
            endif
100      format(5e12.4)
c Calculate system-averaged autocorrelation function and output it:
        htau = 0.0
        do 19 i=1,s
            do 20 j=1,r
                htau = htau + xx(i,1,j)*xx0(i,j)/sr
20         continue
19        continue
        write(69,*) t,htau

c At spaced-out timesteps, check constraints and output summary
c information to the file 'dout':
        if (amod(t,tdel) .lt. 1.e-6) then
c Evaluate <E>; check <q>, <(q-<q>)**2> and <qq'> constraints:
        energy = 0.0
        do 12 j=1,r
            energy = energy + e(j)/(1.0*r)
12        continue
c For CDS, check the <q> and <(q-<q>)**2> constraints:
        if (n .ne. s) then
            qq(1) = 0.0
            qq(2) = 0.0
            do 11 i=1,s
                do 4 j=1,r
                    qq(1) = qq(1) + (q(1,(j+(i-1)*r)) - qstar(1,(j+(i-1)*r)))/sr
                    qq(2) = qq(2) + ((q(1,(j+(i-1)*r)) - qmean(i))**2 -
                    (qstar(1,(j+(i-1)*r)) - qsmean(i))**2)/sr
2         continue
4         continue
11        continue
c Check the <q(t)*q(t')> constraints:
        ntimes = c - 3
        do 6 k=1,ntimes,1
            qq(k+2) = 0.0
            do 7 j=1,r*s
                qq(k+2) = qq(k+2) +

```

```

      $          (q(1,j)*q((k+1),j) - qstar(1,j)*qstar((k+1),j))/sr
7      continue
6      continue
      endif
c Output the summary information and constraint checks:
      write(77,111) t,energy,qq(1),qq(2),qq(3),qq(4),qq(5)
111    format(f6.3,1x,6(e11.3,1x))
      endif

      return
      end

c*****
c STFORC ("STochastic FORCe evaluation")
c This subroutine evaluates q at time t by solving for q iteratively
c via the iterative stochastic Newton-Raphson constraint-equation
c method of section 5 of Kraichnan's chapter in the book:

      subroutine stforc(itime)
      real cnvchk,alpha(36),dqnp1(16384),wks1(36)
      integer itime,ia,ifail,iterat
      real h
      integer r,s,n,c
      common/parms/h,r,s,n,c
      real xx(32,36,512),xsav(32,512),k1(32,512),k2(32,512),xx0(32,512)
      common/vars/xx,xsav,k1,k2,xx0
      real q(36,16384),qstar(36,16384),qmean(32),qsmean(32)
      common/forces/q,qstar,qmean,qsmean
      real fmat(36,16384),v(36,36),f(36)
      common/mats/fmat,v,f
      data ia/36/

c Choose the initial random qn to start the iteration:
      do 11 i=1,r*s
          q(1,i) = rgauss(0.0,1.0)
11    continue

c Initializations:
      niters = 45

c The iterative loop:
      do 1 iterat=1,niters

c Evaluate qstar(t+h), based on current iterate of q(t+h):
          call tplush
c Set up the righthand side of the matrix problem, identical to the
c righthand side of equation 5.2 in Kraichnan's paper:
          call fsetup
c Set up the f-matrix:
          call fmset
c Use the f-matrix to generate the v-matrix:
          call vsetup
c Solve the least-squares problem for the current iteration; i.e.,

```

```

c solve the v-matrix problem  $v * \alpha = f$  using NAG routine F04ATF:
  ifail = 1
  call f04arf(v,ia,f,c,alpha,wks1,ifail)
  if (ifail .ne. 0) then
    write(6,*) 'matsol F04ATF ended with IFAIL = ',ifail
    write(77,*) 'matsol F04ATF ended with IFAIL = ',ifail
  endif
c Update q and set up convergence check:
  cnvchk = 0.0
  do 7 i=1,s
    do 8 j=1,r
      dqnp1(j+(i-1)*r) = 0.0
      do 9 k=1,c
        dqnp1(j+(i-1)*r) = dqnp1(j+(i-1)*r) +
          $                               alpha(k)*fmat(k,(j+(i-1)*r))
      9   continue
      q(1,(j+(i-1)*r)) = q(1,(j+(i-1)*r)) + dqnp1(j+(i-1)*r)
      cnvchk = cnvchk + abs(dqnp1(j+(i-1)*r))
    8   continue
  7   continue

c Test for convergence:
  if (cnvchk .le. (r*s*1.0e-8)) then
c Warn about possible zero solution:
  if (cnvchk .eq. 0.0) write(77,*) 'cnvchk = 0.0'
c If converged, wind up and return to main routine:
c Restore the proper value of xx for use in getting k2 in main:
  do 4 i=1,s
    do 6 j=1,r
      xx(i,1,j) = xsav(i,j) + k1(i,j)
    6   continue
  4   continue
  return
endif
1 continue

c Convergence not achieved for q:
  write(77,*) 'q nonconvergence at itime =',itime
  write(6,*) 'q nonconvergence at itime =',itime
  call exit

  return
end

c TPLUSH ("T PLUS H")
c This subroutine calculates  $xx(t+h)$  using the ODE's and the current
c iterate of  $q(t+h)$ . Then stintp is called to calculate  $qstar(t+h)$ 
c using these  $xx(t+h)$  values.

  subroutine tplash
  real h
  integer r,s,n,c
  common/parms/h,r,s,n,c

```

```

real xx(32,36,512),xsav(32,512),k1(32,512),k2(32,512),xx0(32,512)
common/vars/xx,xsav,k1,k2,xx0
real q(36,16384),qstar(36,16384),qmean(32),qsmean(32)
common/forces/q,qstar,qmean,qsmean

```

```

c Initialize xx = xx(end of 1st Runge-Kutta stage)
  do 1 i=1,s
    do 2 j=1,r
      xx(i,1,j) = xsav(i,j) + k1(i,j)
    2 continue
  1 continue

c Using ODE's, evaluate xx(t+h) based on current iterate of q:
  call diffeq(k2)
  do 3 i=1,s
    do 4 j=1,r
      xx(i,1,j) = xsav(i,j) + 0.5*(k1(i,j) + k2(i,j))
    4 continue
  3 continue

c Now evaluate qstar(t+h) using these new xx(t+h) values
  call stintp

  return
end

```

c FSETUP ("F SETUP")

c This subroutine sets up the righthand side of the matrix problem,
c which is identical to the righthand side of equation (12) in
c the dissertation.

```

subroutine fsetup
integer ntimes
real h
integer r,s,n,c
common/parms/h,r,s,n,c
real xx(32,36,512),xsav(32,512),k1(32,512),k2(32,512),xx0(32,512)
common/vars/xx,xsav,k1,k2,xx0
real q(36,16384),qstar(36,16384),qmean(32),qsmean(32)
common/forces/q,qstar,qmean,qsmean
real fmat(36,16384),v(36,36),f(36)
common/mats/fmat,v,f

```

c Initialize:

```

  do 1 i=1,c
    f(i) = 0.0
  1 continue

```

c The constraints are coded explicitly here:

```

  do 2 j=1,r
    do 3 i=1,s

```

c The <E> constraint:

```

    f(1) = f(1) - (xx(i,1,j)**2 - xsav(i,j)**2)

```


c The $\langle q - qstar \rangle$ constraint (force mean):
 $f(2) = f(2) - (q(1,(j+(i-1)*r)) - qstar(1,(j+(i-1)*r)))$
c The $\langle (q - \langle q \rangle)^2 - (qstar - \langle qstar \rangle)^2 \rangle$ constraint (force variance):
 $f(3) = f(3) - ((q(1,(j+(i-1)*r)) - qmean(i))^{**2} -$
 $\$ (qstar(1,(j+(i-1)*r)) - qsmean(i))^{**2})$
3 continue
2 continue

c The ntimes $\langle q*q(t') - qstar*qstar(t') \rangle$ constraints:
c (ntimes is the # of unequal times to constrain against)
ntimes = c - 3
do 4 k=1,ntimes,1
do 5 i=1,s
do 6 j=1,r
 $f(3+k) = f(3+k) -$
 $\$ (q(1,(j+(i-1)*r))*q((k+1),(j+(i-1)*r)) -$
 $\$ qstar(1,(j+(i-1)*r))*qstar((k+1),(j+(i-1)*r)))$
6 continue
5 continue
4 continue
return
end

c FMSET ("FMat SETup")

c This subroutine sets up the s*rxr fprime matrix, whose c rows are
c the q-derivatives of the c constraint functions at all r qn-values
c for each of the s q's.

```
subroutine fmset
integer ntimes
real h
integer r,s,n,c
common/parms/h,r,s,n,c
real xx(32,36,512),xsav(32,512),k1(32,512),k2(32,512),xx0(32,512)
common/vars/xx,xsav,k1,k2,xx0
real q(36,16384),qstar(36,16384),qmean(32),qsmean(32)
common/forces/q,qstar,qmean,qsmean
real fmat(36,16384),v(36,36),f(36)
common/mats/fmat,v,f
```

c Initialize:

```
do 1 i=1,c
do 2 j=1,r*s
fmat(i,j) = 0.0
2 continue
1 continue
```

c The partial derivatives of the constraints with respect to the unknown
c (here qn(t)) are coded explicitly here:

```
do 3 i=1,s
do 4 j=1,r
```

c Row 1: the $\langle E \rangle$ constraint:

```

      fmat(1,(j+(i-1)*r)) = h*xx(i,1,j)
c Row 2: c The <q - qstar> constraint (force mean):
      fmat(2,(j+(i-1)*r)) = 1.0
c Row 3: the variance constraint:
      fmat(3,(j+(i-1)*r)) = 2.0*(q(1,(j+(i-1)*r)) - qmean(i))
  4   continue
  3   continue

c Rows 4 through 4+ntimes: the <qn*q(t') - qstar*qstar(t')>
c constraints (ntimes is the # of unequal times to constrain against):
      ntimes = c - 3
      do 5 k=1,ntimes,1
        do 6 i=1,s
          do 7 j=1,r
            fmat((3+k),(j+(i-1)*r)) = q((k+1),(j+(i-1)*r))
  7     continue
  6     continue
  5     continue

      return
      end

c VSETUP ("V SETUP")
c This subroutine sets up the v-matrix. It is a square (c x c)
c matrix whose elements are the dot products of the rows of the fmat
c matrix. The matrix problem v * alpha = f yields the least squares
c solution of the underdetermined problem fmat * dqn = f. (alpha is
c a c dimensional vector, dqn is r-dimensional, and f is the c
c dimensional righthand side of the matrix problem, found in fsetup:

      subroutine vsetup
      real h
      integer r,s,n,c
      common/parms/h,r,s,n,c
      real fmat(36,16384),v(36,36),f(36)
      common/mats/fmat,v,f

c Initialize:
      do 1 i=1,c
        do 2 j=1,c
          v(i,j) = 0.0
  2     continue
  1     continue
c Calculate the dot products of fmat's rows; note that v is symmetric:
      do 3 i=1,c
        do 4 j=i,c
          do 5 k=1,r*s
            v(i,j) = v(i,j) + fmat(i,k)*fmat(j,k)
  5     continue
          v(j,i) = v(i,j)
  4     continue
  3     continue

```

```

return
end

```

```

c STINTP ("STatistical INTerPolation")
c Calculate the summation to which q should be stastically similar
c (called qstar).

```

```

subroutine stintp
integer mm,kk,jj
real h
integer r,s,n,c
common/parms/h,r,s,n,c
real xx(32,36,512),xsav(32,512),k1(32,512),k2(32,512),xx0(32,512)
common/vars/xx,xsav,k1,k2,xx0
real q(36,16384),qstar(36,16384),qmean(32),qsmean(32)
common/forces/q,qstar,qmean,qsmean
real cof(5462),wt
integer index(5462),m,m2
common/couple/cof,index,wt,m,m2

```

```

c Initialize:

```

```

do 1 j=1,r*s
qstar(1,j)=0.0
1 continue

```

```

c Calculate qstar:

```

```

do 4 k=1,(3*m)
mm = index(k)/m2 + 1
kk = (index(k) - (mm-1)*m2)/m + 1
jj = index(k) - (mm-1)*m2 - (kk-1)*m
do 5 j=1,r
qstar(1,(j+(jj-1)*r)) = qstar(1,(j+(jj-1)*r)) +
$ cof(k)*xx(mm,1,j)*xx(kk,1,j)
5 continue
4 continue

```

```

c Weight qstar appropriately (statistical interpolation weighting).

```

```

c Also calculate means of q's and qstars now.

```

```

do 6 i=1,s
qmean(i) = 0.0
qsmean(i) = 0.0
do 7 j=1,r
qstar(1,(j+(i-1)*r)) = wt*qstar(1,(j+(i-1)*r))
qmean(i) = qmean(i) + q(1,(j+(i-1)*r))
qsmean(i) = qsmean(i) + qstar(1,(j+(i-1)*r))
7 continue
qmean(i) = qmean(i)/(1.0*r)
qsmean(i) = qsmean(i)/(1.0*r)
6 continue

```

```

return
end

```

APPENDIX D: MULTIDIMENSIONAL NEWTON-RAPHSON PROCEDURE

For a function of N variables $f(x_1, x_2, x_3, \dots, x_N) = f(\mathbf{x})$ which has a zero at \mathbf{z} ($f(\mathbf{z}) = 0$), a first-degree Taylor polynomial expanded about a guess \mathbf{x}_0 is

$$f(\mathbf{x}) = f(\mathbf{x}_0) +$$

$$\left[(\mathbf{x} - \mathbf{x}_0) \cdot \nabla \right] f(\mathbf{x}_0) + \frac{1}{3} \sum_{i,j=1}^3 \left[x_i - x_{0i} \right] \left[x_j - x_{0j} \right] \frac{\partial^2 f[\xi(\mathbf{x})]}{\partial x_i \partial x_j} . \quad (\text{D1})$$

Here $\xi(\mathbf{x})$ is a point in N -space such that the N -dimensional distance between \mathbf{x} and \mathbf{z} is less than the the distance between ξ and \mathbf{z} , provided that $(\mathbf{x} - \mathbf{x}_0)$ points toward the $(N - 1)$ -dimensional surface of zeroes of f on which \mathbf{z} lies. Neglecting the third term in the righthand side of Eq. (D1) and setting $\mathbf{x} = \mathbf{z}$ yields

$$\begin{aligned} 0 &\approx f(\mathbf{x}_0) + \left[(\mathbf{z} - \mathbf{x}_0) \cdot \nabla \right] f(\mathbf{x}_0) \\ &\approx f(\mathbf{x}_0) + \sum_{i=1}^N \left[z_i - x_{0i} \right] \frac{\partial}{\partial x_i} f(\mathbf{x}_0) . \end{aligned} \quad (\text{D2})$$

This is an underdetermined equation for (z_1, z_2, \dots, z_N) .

Equation (D2) is enough to determine one component of \mathbf{z} , such as z_1 , in terms of the other $(N-1)$ components (z_2, z_3, \dots, z_N) . A determined set of N equations can be constructed by requiring, in addition to Eq. (D2), that the square of the magnitude of $(\mathbf{z} - \mathbf{x}_0)$ be minimized with respect to variations in \mathbf{x}_0 .

$$\frac{\partial}{\partial x_{0i}} \left\{ \sum_{j=1}^N [z_j - x_{0j}]^2 \right\} = 0 \quad \text{for } i=2,3,\dots,N .$$

This suggests a sequence of sets of equations for increasingly accurate approximations to a value of \mathbf{x} which satisfies $f(\mathbf{x}) = 0$:

$$0 = f(\mathbf{x}_0) + \sum_{i=1}^N [x_{1i} - x_{0i}] \frac{\partial}{\partial x_i} f(\mathbf{x}_0)$$

and

$$\frac{\partial}{\partial x_{0i}} \left\{ \sum_{j=1}^N [x_{1j} - x_{0j}]^2 \right\} = 0 \quad \text{for } i=2,3,\dots,N ;$$

$$0 = f(\mathbf{x}_1) + \sum_{i=1}^N [x_{2i} - x_{1i}] \frac{\partial}{\partial x_i} f(\mathbf{x}_1)$$

and

$$\frac{\partial}{\partial x_{1i}} \left\{ \sum_{j=1}^N [x_{2j} - x_{1j}]^2 \right\} = 0 \quad \text{for } j=2,3,\dots,N ;$$

⋮

$$0 = f(\mathbf{x}_n) + \sum_{i=1}^N [x_{(n+1)i} - x_{ni}] \frac{\partial}{\partial x_i} f(\mathbf{x}_n)$$

and

$$\frac{\partial}{\partial x_{ni}} \left\{ \sum_{j=1}^N [x_{(n+1)j} - x_{nj}]^2 \right\} = 0 \quad \text{for } j=2,3,\dots,N . \quad (D3)$$

This yields a point \mathbf{x}_n which satisfies $f(\mathbf{x}_n) = 0$ to any desired accuracy; the procedure is stopped when $|\mathbf{x}_{n+1} - \mathbf{x}_n|$ is as small as desired. This procedure has no control over where on the

$(N-1)$ -dimensional surface on which $f(\mathbf{x}) = 0$ the \mathbf{x}_n 's converge.

An entirely equivalent way to formulate this least-squares solution procedure is to require at each iteration that $(\mathbf{x}_{n+1} - \mathbf{x}_n)$ is parallel to the gradient of f at \mathbf{x}_n . The sequence $\{(\mathbf{x}_1 - \mathbf{x}_0), (\mathbf{x}_2 - \mathbf{x}_1), \dots, (\mathbf{x}_{n+1} - \mathbf{x}_n)\}$ moves along the gradient from the initial guess \mathbf{x}_0 toward the surface on which $f(\mathbf{x}) = 0$. (This assumes that ∇f is monotonic in magnitude between the initial guess \mathbf{x}_0 and the surface on which z lies.) That this is equivalent to the least-squares minimization conditions can be seen as follows:

Denote the difference $(\mathbf{x}_1 - \mathbf{x}_0)$ by $\delta\mathbf{x}_1$. This vector can be resolved into components perpendicular and parallel to ∇f ,

$$\delta\mathbf{x}_1 = \delta\mathbf{x}_{1\parallel} + \delta\mathbf{x}_{1\perp}.$$

$\delta\mathbf{x}_{1\perp}$ is arbitrary, and $\delta\mathbf{x}_{1\parallel}$ is determined by the first line of Eq. (D04). Since

$$[\delta\mathbf{x}_1]^2 = [\delta\mathbf{x}_{1\parallel}]^2 + [\delta\mathbf{x}_{1\perp}]^2,$$

the minimization of $(\delta\mathbf{x}_1)^2$ implies that

$$(\delta\mathbf{x}_{1\perp})^2 = 0.$$

The same reasoning applies to all iterates in the sequence in Eq. (D04), using

$$\delta\mathbf{x}_{n+1} = \mathbf{x}_{n+1} - \mathbf{x}_n.$$

References

- ¹G.K. Batchelor, *An Introduction to Fluid Dynamics*, Cambridge University Press, Cambridge, 1983, p. 214.
- ²J.F. Douglas, J.M. Gasiorek, and J.A. Swatfield, *Fluid Mechanics, 2nd Edition*, (Pittman Publishing Limited, London, 1985), p. 100.
- ³V. Yakhot and S.A. Orszag, *J. Sci. Comput.* **1**, 3 (1986).
- ⁴L.D. Landau and E.M. Lifshitz, *Fluid Mechanics*, (Pergamon, London, 1959), §33.
- ⁵S. Kida and Y. Murakami, *Phys Fluids* **30**, 2030 (1987).
- ⁶M. Rogers and P. Moin, *J. Fluid. Mech.* **176**, 33 (1987).
- ⁷S.A. Orszag, in *Fluid Dynamics*, edited by R. Balian and L.L. Peube (Gordon & Breach, New York, 1977), p. 235.
- ⁸D. Forster, D. Nelson, and M. Stephen, *Phys. Rev. A* **16**, 732 (1977).
- ⁹J.P. Fournier and U. Frisch, *Phys. Rev. A* **28**, 1000 (1983).
- ¹⁰Y. Zhou and G. Vahala, *Phys. Lett. A* **124**, 355 (1987).
- ¹¹Y. Zhou, G. Vahala, and M. Hossain, *Phys. Rev. A* **37**, 2590 (1988).
- ¹²R.H. Kraichnan, *Phys. Fluids* **30**, 2400 (1987).
- ¹³R.H. Kraichnan, *Phys. Rev.* **109**, 1407 (1958).
- ¹⁴R.H. Kraichnan, *J. Fluid Mech.* **5**, 497 (1959).
- ¹⁵R.H. Kraichnan, *Phys. Fluids* **7**, 1030 (1964).
- ¹⁶R.H. Kraichnan, *Phys. Fluids* **7**, 1723 (1964).
- ¹⁷R. H. Kraichnan, in *Theoretical Approaches to Turbulence*, edited by D. L. Dwoyer, M. Y. Hussaini, and R. G. Voigt (Springer-Verlag, New York, 1985), p. 215.
- ¹⁸R.H. Kraichnan paper, "Some Recent Progress in Statistical Turbulence Theory," submitted to AIAA Progress Series: Proceedings of the Fifth Beer-Sheva International Seminar on MHD Flows and Turbulence, Jerusalem, March 1987.
- ¹⁹R. Betchov, in *Dynamics of Fluids and Plasmas*, edited by S.I. Pai (Academic, New York, 1966), p. 215.
- ²⁰R. Betchov, *Phys. Fluids* **10** pt. II (Supplement), S17 (1967).

- ²¹Philip J. Davis and Ivan Polonsky, in *Handbook of Mathematical Functions*, edited by M. Abramowitz and I.A. Stegun (Dover, New York, 1972), p. 875.
- ²²R.H. Kraichnan, *J. Math. Phys.* **2**, 124 (1961).
- ²³R.H. Kraichnan, "Reduced Descriptions of Hydrodynamic Turbulence," preprint (LA-UR-88-1008).
- ²⁴R.H. Kraichnan and Raj Panda, *Phys. Fluids* **31**, 2395 (1988).
- ²⁵C.E. Seyler, Jr., Y. Salu, D. Montgomery, and G. Knorr, *Phys. Fluids* **18**, 803 (1975).
- ²⁶G.J. Hartke and V.M. Canuto, *Phys. Fluids* **31**, 1034 (1988).
- ²⁷J.A. Krommes, *Phys. Fluids* **25**, 1393 (1982).
- ²⁸R.E. Waltz, *Phys. Fluids* **26**, 169 (1983).
- ²⁹J.C. Hill, R.C. Sanderson, and J.R. Herring, in *Advances in Turbulence*, Proceedings of the First European Turbulence Conference, Lyon, France, 1986, ed. by G. Compte-Bellot and J. Mathieu (Springer-Verlag, Berlin, West Germany, 1987), p. 184.

VITA**Timothy Joe Williams**

Born in Cabool, Missouri on December 6, 1959. Graduated from Bayside High School in Virginia Beach, Virginia, June 1978; B.S. in Physics and Mathematics at Carnegie-Mellon University, May 1982; M.S. in Physics at the College of William and Mary, May 1984. Ph.D. candidate in Physics at the College of William Mary — degree will be completed after approval of this dissertation.